

University of Kentucky

UKnowledge

Theses and Dissertations--Physiology

Physiology


2023

The Influence of APOE Genotype on Lipid Droplet Dynamics

Cassi Friday

University of Kentucky, cassi.friday@uky.edu

Author ORCID Identifier:

 <https://orcid.org/0000-0001-9712-316X>

Digital Object Identifier: <https://doi.org/10.13023/etd.2023.031>

[Right click to open a feedback form in a new tab to let us know how this document benefits you.](#)

Recommended Citation

Friday, Cassi, "The Influence of APOE Genotype on Lipid Droplet Dynamics" (2023). *Theses and Dissertations--Physiology*. 61.

https://uknowledge.uky.edu/physiology_etds/61

This Doctoral Dissertation is brought to you for free and open access by the Physiology at UKnowledge. It has been accepted for inclusion in Theses and Dissertations--Physiology by an authorized administrator of UKnowledge. For more information, please contact UKnowledge@lsv.uky.edu.

STUDENT AGREEMENT:

I represent that my thesis or dissertation and abstract are my original work. Proper attribution has been given to all outside sources. I understand that I am solely responsible for obtaining any needed copyright permissions. I have obtained needed written permission statement(s) from the owner(s) of each third-party copyrighted matter to be included in my work, allowing electronic distribution (if such use is not permitted by the fair use doctrine) which will be submitted to UKnowledge as Additional File.

I hereby grant to The University of Kentucky and its agents the irrevocable, non-exclusive, and royalty-free license to archive and make accessible my work in whole or in part in all forms of media, now or hereafter known. I agree that the document mentioned above may be made available immediately for worldwide access unless an embargo applies.

I retain all other ownership rights to the copyright of my work. I also retain the right to use in future works (such as articles or books) all or part of my work. I understand that I am free to register the copyright to my work.

REVIEW, APPROVAL AND ACCEPTANCE

The document mentioned above has been reviewed and accepted by the student's advisor, on behalf of the advisory committee, and by the Director of Graduate Studies (DGS), on behalf of the program; we verify that this is the final, approved version of the student's thesis including all changes required by the advisory committee. The undersigned agree to abide by the statements above.

Cassi Friday, Student

Dr. Lance A. Johnson, Major Professor

Dr. Lance A. Johnson, Director of Graduate Studies

The Influence of *APOE* Genotype on Lipid Droplet Dynamics

DISSERTATION

A dissertation submitted in partial fulfillment of the
requirements for the degree of Doctor of Philosophy in the
College of Medicine
at the University of Kentucky

By

Cassi M. Friday (Binkley)

Lexington, Kentucky

Director: Dr. Lance A. Johnson, Professor of Physiology

Lexington, Kentucky

2022

Copyright © Cassi Friday 2022
<https://orcid.org/0000-0001-9712-316X>

ABSTRACT OF DISSERTATION

The Influence of *APOE* Genotype on Lipid Droplet Dynamics

Excess lipid droplet (LD) accumulation is associated with several pathological states, including neurodegenerative disorders such as Alzheimer's disease (AD). However, the mechanism(s) by which changes in LD composition and dynamics may contribute to the pathophysiology of AD remains unclear. Apolipoprotein E (ApoE) is a droplet-related protein with a common variant (ApoE4) that confers the largest increase in genetic risk for late-onset AD. Interestingly, ApoE4 is associated with both increased neuroinflammation and excess LD accumulation. This dissertation work seeks to quantitatively profile the lipid and protein composition of LDs between the 'neutral' ApoE3 and 'risk' ApoE4 isoforms, in order to gain insight into potential LD-driven contributions to AD pathogenesis.

Targeted replacement mice expressing human ApoE3 or ApoE4 were injected with saline (control) or LPS (inflammatory stimulus) and after 24 hours, hepatic lipid droplets were isolated and droplet proteomes and lipidomes were analyzed. Quantitative proteomics showed that LD fractions from E4 mice are enriched for proteins involved in innate immunity, while E3 LDs are enriched for proteins involved in lipid β -oxidation. Lipidomics revealed a shift in the distribution of glycerophospholipids in E4 LDs with an increase in multiple phosphatidylcholine (PC) species. There was also substantial overlap between LD proteins and AD-proteomes of human whole brain tissue. To translate these findings to the brain, primary microglia from the same strain of mice were exposed to exogenous lipid, inflammatory stimulation, necroptotic N2A cells (nN2A), or a combination of treatments to evaluate lipid droplet accumulation and impact on cell function. Microglia from ApoE4 mice accumulated more LDs at baseline, with exogenous OA, LPS stimulation, and nN2As as a percentage of E3 control across multiple experiments. E4 microglia also secreted significantly more cytokines (TNF, IL-1 β , IL-10) than E3 microglia in the control, oleic acid, and nN2A treatment conditions. Interestingly, droplet inhibitors for ACAT and DGAT both decreased droplet accumulation in cells, but did not ameliorate the cytokine response. Finally, we have established a biobank of *APOE* genotyped peripheral blood mononuclear cells (PBMCs) from research participants. These easily accessible immune cells will serve as a highly translational model to understand LD dynamics as it relates to ApoE and AD risk.

In summary, E4 cells accumulate more LDs compared to E3 under all conditions tested, while the proteomic profile of E4 LDs support the hypothesis that E4 expression increases inflammation under basal conditions. This increased LD formation in non-aged, non-diseased E4 cells may suggest preclinical dysfunction associated with the highest risk *APOE* genotype, and a better understanding of LD dynamics within these cells and their functional implications may provide novel targets to improve E4-related outcomes.

KEYWORDS: Apolipoprotein E, Alzheimer's disease, Lipid Droplets, Inflammation,
Liver, Microglia

Cassi M. Friday
(Name of Student)

12/08/2022

Date

The Influence of *APOE* Genotype on Lipid Droplet Dynamics

By
Cassi Friday

Lance A. Johnson, PhD

Director of Dissertation

Lance A. Johnson, PhD

Director of Graduate Studies

12/08/2022

Date

DEDICATION

To Memaw
Blanche Lois Merrilees Nair
September 8, 1926 – February 4, 2011

Your mind may have left before your body due to Alzheimer's disease, but your many lessons, humor, faith, applesauce cookies, and love of a good blazer live on through one of your biggest fans.

ACKNOWLEDGMENTS

I would like to give my biggest ‘thank you’ to Dr. Lance Johnson - my mentor not only for this dissertation research, but for all general life endeavors. You took a chance on me as a returning PhD student, you challenged and encouraged me along the way, and you gave me the flexibility I needed as a parent. Thank you so much for rebuilding my confidence as a scientist and sharing your contagious passion for research and science communication with me. Thank you for sharing the same weakness as an over-committer to all opportunities and things and for being my check-point before I obligated myself to anything new – it was great to have you as a decision filter the last couple of years. Also, thank you for entertaining my anxious opposition to your chill procrastination. Finally, thank you for encouraging me to pursue a job that isn’t related to your work. I think this speaks volumes about you as a mentor and I will always appreciate you for being excited for me above all else. You are brilliant and I can’t wait to follow your journey through the illusive and exclusive ranks of the illuminati.

Thank you so much to my committee members. Your expertise, feedback, questions, and advice have been invaluable. Dr. Josh Morganti, thank you for the support you’ve shown since we first met – doing blood draws, PBMC prep, and talking through techniques with you was so helpful and I have loved collaborating with your lab. Dr. Jamie Sturgill, thank you for your mentorship in careers, parenting, and life. I’m amazed by the work you do and the passion and energy you devote to it – I loved shadowing you and learning about it all. Dr. Sarah D’Orazio, thank you for your insight and for the tough questions. You are impressively smart and I have learned so much from your guidance. Also, thank you for the opportunity to get out of the lab for science fair judging - it could

not have come at a better time to give me a boost of excitement through a middle schooler's eyes. Dr. Ryan Temel, thank you for contributing knowledge about lipids and metabolism and your great advice on study design. You are practical and I have learned a lot by listening to your feedback about how not to overcomplicate things. Collectively, thank you all for believing in me and getting me to this point – I'll always be grateful.

A huge thank you to Tanya Graf. Had you not been the amazing human and friend you are, we would not have kept in touch when I left in 2015 and I would have likely not returned. Thank you for working with Dr. Ken Campbell to have me reinstated to the graduate school and the suggestion to talk with Lance (and thank you Dr. Campbell for your mentorship, support, and advice throughout my journey!). Tanya, thank you for always having an open door, for your prayers, and for cheering me on. Every time I stepped in your office and spilled my guts, I was always met with love and reassurance. You're the best!

Thank you to the past and present members of the Johnson Lab for your help with projects that complete this dissertation and for your comradery (and often debauchery (Lesley)). You make being in lab so much fun and working with mice tolerable – something I never thought I would say! A special thanks to the students I have had the chance to mentor or act as 'lab mom' to – you are all so smart and I know you will do great things! I will be following you and cheering you on from wherever I go. My door is always open - please call, come visit, and reach out any time for any reason.

Because my PhD journey began in another lab over ten years ago, I would be remiss if I did not thank my previous committee and mentor for laying a foundation of knowledge and skills to build on. Thank you, Dr. Brandon Fornwalt, for growing my

interest in clinical research, for introducing me to every person you knew, building my networking and presentation skills, and for a great first-half of my degree. Thank you to Dr. Jody Clasey and Dr. Karen Esser for the incredible outreach opportunities with kids in Eastern Kentucky and for your help with my project. Also, thank you Dr. Moriel Vandsburger and Dr. Dennis Bruemmer for being on my first committee, allowing me to rotate in your lab, and supporting me through tough decisions. Thank you also to Dr. Speck – I learned an incredible amount from you through the teaching certification and you planted a seed for education and teaching physiology that grew into several fun opportunities down the line.

Thank you to the kids who bravely volunteered for my first study. It is not an easy task to complete a 45-minute MRI, but every single one rocked it! Your enthusiasm and curiosity drove me forward and made a lasting impact on my motivation to do research. Also, thank you to the hundreds of volunteers for my current study. Without your altruism and interest in research, the science community would truly be at a loss.

Thank you to my friends and my family for your constant encouragement, prayers, Starbucks gift cards, and cheers. I am blessed beyond measure to have sisters and friends to check in on me, offer help, and send me goodies. I did not intend to finish a PhD during a pandemic with three kids at home and a husband serving overseas, but here we are and I couldn't do it without your help and inspiration. To my parents – Mom and Dad – thank you for raising me in the country, for instilling a farmer's work ethic, for keeping me humble, and for giving me everything you could when you had little. You have never missed an opportunity to tell me you are proud of me and those words always keep me

going. I love you so incredibly much and owe you big for shaping me into the person I am today.

To my forever boyfriend and our sweet wildlings. Anthony, I love you and I am so glad to have met you at the beginning of this journey over a decade ago. Who knew it would have unfolded like this? You have been my biggest advocate, my loudest encourager, and my most practical advisor. You mean the world to me and the sacrifices we have shared and endured for the betterment of one another and our family make me love you even more. Eleanor Lucille, you are by far my biggest cheerleader and you have been a constant source of light when I am overwhelmed with everything. Your optimism is infectious and you have carried me more than you know. Theodore Gregory Isaac, your terrible twos extended into your threes and fours and I thought we would never survive all of this together, but you keep me on my toes, give me endless reasons to be thankful for you, and you always make me laugh. Graham Radley, thank you for always being happy, chill, and hilarious – you bring me so much joy and so little sleep. I love you all so much!

A lengthier acknowledgements section than I intended, but I have so many people to thank for believing in me. However, none of this would be possible without my belief in a gracious God that has kept me grounded and at peace during the chaos of life and the many ups and down of this ride.

And whatever you do, whether in word or deed, do it all in the name of the Lord Jesus, giving thanks to God the Father through him. -Colossians 3:17

TABLE OF CONTENTS

ACKNOWLEDGMENTS.....	iii
LIST OF TABLES	x
LIST OF FIGURES.....	xi
CHAPTER 1. <i>APOE</i> , Alzheimer’s disease, and lipid droplets	1
1.1 <i>Alzheimer’s Disease – the sixth leading cause of death and the most financially burdensome disease in America.....</i>	1
1.2 <i>Apolipoprotein E – A lipid transport protein implicated in Alzheimer’s disease.....</i>	3
1.3 <i>The genetic prevalence of APOE and how isoform differences translate to variable disease risk ...</i>	5
1.4 <i>ApoE is found on the surface of lipid droplets</i>	9
1.5 <i>Lipid droplet biogenesis and cellular function: the good</i>	10
1.6 <i>Lipid droplets and cellular function: the bad.....</i>	14
1.7 <i>ApoE and lipid droplets across the liver, brain, and blood axis</i>	15
1.8 <i>Summary and Impact</i>	19
CHAPTER 2. <i>APOE4</i> alters the lipid droplet proteome and modulates droplet dynamics in the liver	21
2.1 <i>Introduction.....</i>	21
2.2 <i>Methods.....</i>	24
2.2.1 <i>Mouse Model.....</i>	24
2.2.2 <i>Lipid Droplet Enrichment.....</i>	24
2.2.3 <i>Proteomic and Lipidome Analyses</i>	25
2.2.4 <i>Oil Red O.....</i>	27
2.2.5 <i>WGCNA.....</i>	29
2.2.6 <i>Western Blotting.....</i>	30
2.3 <i>Results.....</i>	31
2.3.1 <i>LD-enriched fractions show greater droplet accumulation in cells expressing ApoE4 and after inflammation with LPS.....</i>	31
2.3.2 <i>E4- and LPS-stimulated LDs show increases in phosphatidylcholine composition.</i>	31
2.3.3 <i>E4 droplets are enriched for immune-associated proteins.</i>	32
2.3.4 <i>Proteins implicated in human E4 carriers and Alzheimer’s disease proteomics studies are largely LD-enriched.....</i>	33
2.3.5 <i>Proteins changed in Alzheimer’s disease associated with metabolism and microglial activation, overlap with LD-resident proteins and include disease associated microglia genes.</i>	34
2.4 <i>Discussion</i>	35
CHAPTER 3. Lipid droplets in microglia are modulated by <i>APOE</i> genotype	53
3.1 <i>Introduction.....</i>	53
3.2 <i>Methods.....</i>	56
3.2.1 <i>Cell Culture</i>	56

3.2.2	Lipid Droplet Imaging	57
3.2.3	Cytokine Analysis	58
3.2.4	Western Blots	58
3.3	<i>Results</i>	60
3.3.1	E4 expressing microglia accumulate more LDs at baseline, with exogenous lipid sources, and with pro-inflammatory stimuli.	60
3.3.2	DGAT1 and ACAT1 inhibitors attenuate LD accumulation in primary microglia.	60
3.3.3	E4 microglia secrete more TNF, IL-1 β , and IL-10.	61
3.3.4	Immunohistochemistry (IHC) identified proteins of interest from liver LD analyses in primary microglia and on the droplet surface in primary microglia cells.	62
3.3.5	Human brain tissue shows increase in Plin5 associated with dementia status in E4 carriers.	62
3.4	<i>Discussion</i>	63
CHAPTER 4. Lipid droplets in macrophages – a study initiation to investigate <i>APOE</i> modulation		75
4.1	<i>Introduction</i>	75
4.2	<i>Methods</i>	81
4.2.1	Recruitment	81
4.2.2	Saliva Kits	83
4.2.3	DNA Extraction	83
4.2.4	Genotyping	84
4.2.5	Venipuncture	84
4.2.6	PBMC Isolation	85
4.2.7	Freeze & Thaw	85
4.2.8	Culture	86
4.2.9	Treatment	86
4.2.10	Imaging	87
4.3	<i>Preliminary Results</i>	87
4.3.1	Study enrollment to date includes over 250 volunteers.	87
4.3.2	Protocol optimization yields adequate cell numbers after freeze and thaw.	88
CHAPTER 5. Discussion		95
5.1	<i>Summary of Dissertation</i>	95
5.2	<i>Lipid Droplet Inhibition</i>	100
5.3	<i>The role of phosphatidylcholine (and other molecules) in LD biophysics</i>	104
5.4	<i>Droplet size, content, and droplet proteins</i>	105
5.5	<i>Lipid Droplets and Immunometabolism</i>	107
5.6	<i>E4 lipid droplets may drive changes in immunometabolism, increase risk for AD onset, and exacerbate existing AD pathology</i>	111
5.7	<i>What do we do about it?</i>	112
APPENDIX		116
REFERENCES		119
VITA		129

LIST OF TABLES

Table 1: Top Ten Hub Proteins of Modules 1-12	40
Table 2: Enrollment and Demographics	89
Table 3: List of Medicines within Exclusion Criteria.....	90

LIST OF FIGURES

Figure 1: Lipid droplet isolation from mouse liver tissue successfully targeted the droplet fraction revealing increased droplets in E4 and inflamed liver tissue.	41
Figure 2: The lipidome of E4 droplets at baseline is similar to LPS-treated droplet lipidomes.....	42
Figure 3: E4 LDs experience a blunted composition change after exposure to inflammation compared to E3 droplets.....	45
Figure 4: Differentially expressed proteins and reveal enriched immune pathways on E4 LDs and metabolic pathways on E3 LDs.....	46
Figure 5: Weighted gene co-expression network analysis (WGCNA) shows module trait relationships and p values between genotype and treatment comparisons.	47
Figure 6: Incipient AD protein signature has significant overlap with LD proteins.	49
Figure 7: Human AD brain proteomes have overlap with LD proteins highlighting microglial activation and metabolism.....	50
Figure 8: AD brain proteome shows similar trends as LD proteome with respect to E3 and E4 pathways.	52
Figure 9: Primary mouse microglia expressing human E4 accumulate more LDs than E3.	68
Figure 10: ACAT inhibitor reduced LD accumulation in all bud OA-treated conditions.....	69
Figure 11: DGAT1 inhibitor reduced droplet formation in all conditions except nN2A treatment.	70
Figure 12: E4 expressing primary microglia secrete more cytokines at baseline compared to E3, but do not respond as robustly to LPS.....	71
Figure 13: Heat map of cytokines show differences between genotypes in each treatment.	72
Figure 14: IHC to identify liver droplet proteins on primary microglia LDs.	73
Figure 15: Western blots of human brain tissue show hypothesized increased in Plin5 with E4 genotype and dementia, but shows variable expression of Plin2.....	74
Figure 16: Study Design	91
Figure 17: E4 microglia express increased levels of glycolytic genes.	92
Figure 18: To date, study enrollment very closely mirrors the predicted genotype frequency of the general population.	93
Figure 19: PBMC optimization procedures.	94

CHAPTER 1. *APOE*, ALZHEIMER'S DISEASE, AND LIPID DROPLETS

1.1 Alzheimer's Disease – the sixth leading cause of death and the most financially burdensome disease in America

Alzheimer's disease (AD) is the most common cause of dementia, a mental state characterized by memory loss and cognitive decline that interferes with daily life. Dementia can occur in multiple disease states, but between 60 and 80% of people with dementia have AD [1]. AD is an age-related disease with risk increasing as age increases. These age-related cases of AD are known as late-onset AD (LOAD). Conversely, a subset of about 5% of AD patients have genetic mutations that cause early dementia characterized as symptom onset before the age of 65, referred to as early-onset (familial) AD. Currently, in the United States, approximately 6 million people are living with this disease [2].

Due to the age advancement of the baby boomer generation born in the two decades after World War II and the steady increase in life expectancy, our country is poised to see a tripling of AD cases in the next 20-30 years. Not only will this be a tremendous burden on our healthcare system (that already sustains a \$300+ billion cost due to AD [3]), but the implications will expand to the job market and broader economy as family members bear the burden to become caregivers to their loved ones. The Alzheimer's Association reported more than 11 million caregivers in 2021 who provided a cumulative 16 billion hours of unpaid care, valued at \$272 billion.

These statistics warrant an unprecedented urgency to treat and cure AD. Unfortunately, the last few decades of clinical trials have yielded poor results toward treating, slowing progression, and preventing AD. In general, the end pathology is characterized similarly for all patients – the brain becomes burdened with amyloid beta plaques and tau

neurofibrillary tangles. Due to the accumulation of tau within neurons, one hypothesis of AD manifestation is disruption of the communication and metabolic pathways of cells in the brain, causing neurons to eventually lose their function and die [4]. Both plaque accumulation and neuronal death cause inflammation – a response facilitated by the brain’s innate immune cell-type, microglia. In AD, microglia work to clear away the plaque build-up, a function that is lost over time with age or disease progression. However, they still secrete pro-inflammatory signals that further the cycle of inflammation, damage, death, and more inflammation [5].

In the AD brain, the above-described pathologies generally begin in regions that support memory, like the entorhinal cortex and hippocampus. As AD progresses, other areas of the brain become affected and patients see a worsening in memory and deficits in language and reasoning skills [6]. Eventually, AD pathology burdens the brain and the afflicted person succumbs to the effects of functional loss, typically from the inability to swallow properly, which leads to aspirational pneumonia or malnutrition. AD also poses a huge risk to the safety of patients it affects due to their loss of social behavior skills and awareness of danger. Many view AD as a slow and cruel thief of one’s self and the burden of care is often placed on family members, creating a much larger societal implication than just the burden of AD healthcare alone.

There are many ways AD can develop and all are impacted by genetics, lifestyle choices, and environment. Though the end pathology is fundamentally the same, the mechanism of AD onset is variable and should be treated as such. Thus, our approach to understanding AD treatment or prevention should focus on the etiology of the disease, rather than the end manifestations. One way the field is turning to this approach is by

investigating the genetic risk factors for AD and understanding if individuals with increased genetic risk should be evaluated separately for treatment efficacy or progression of disease. Genome-wide association studies (GWAS) are one method researchers use to understand genetic risk factors for AD, and dozens of genes linked to an increase in AD risk have emerged from these studies. The vast majority of GWAS genes that are relatively common in the population (20-50%) present a low risk for the development of AD. However, the most common gene with a strong risk is the E4 allele of apolipoprotein E (*APOE4*) [7, 8] The largest genetic risk factor for LOAD is the presence of *APOE4*, a risk factor found in about 25% of the population. Carrying one copy of E4 leads to about 3 times the risk for AD. About 2% of the population carries two copies of E4, which increases their risk of AD up to 15x with a much earlier onset [9]. The E4 variant of apolipoprotein E (ApoE) has become a focus within the AD research field due to its large risk profile as well as its many implications on systemic lipid transport and metabolism.

1.2 Apolipoprotein E – A lipid transport protein implicated in Alzheimer’s disease

Apolipoprotein E (ApoE) is an apolipoprotein made peripherally in the liver and in the brain primarily by astrocytes. Like its name suggests, ApoE is an apolipoprotein that is localized to the surface of circulating lipoprotein particles. Through binding to its requisite receptors, ApoE aids in the docking and internalization of lipoproteins to the cell surface, thus facilitating lipid transport between cells [10]. In the brain, ApoE is the primary transport mechanism of cholesterol-rich lipoprotein particles between glia and also to neurons, a requirement for synaptic transmission and neuronal membrane integrity [11].

Though most of the body's ApoE is produced by the liver and astrocytes, other cells conditionally make ApoE during times of stress. For example, when activated, peripheral macrophages and central microglia also produce ApoE [12]. A point of interest in ApoE production is the distinction of two separate pools of protein; the periphery and the central nervous system. This fact was not known until the 1990s when liver transplant patients were found to have the majority of the donor's ApoE isoform in their plasma, but their original isoform in the brain did not change. This observation tells us that the majority of the peripheral ApoE is made in the liver and does not cross the blood brain barrier (BBB) [13]. Though these peripheral and central pools of ApoE are distinct from one another, there are clues they may still influence one another through downstream effects, a concept discussed in Chapter 2. Regardless of the cell type secreting ApoE, the protein acts as a ligand for the low density lipoprotein receptor (LDLR) family, which includes LDLR, LDLR-related protein 1 (LRP1), very-low-density lipoprotein receptor (VLDLR), and ApoE receptor 2 (ApoER2). The distribution of these receptors varies in the brain and throughout the body [14]. LDLRs work by way of receptor-mediated endocytosis and subsequent cellular signaling. In the brain, astrocytes express LDLR and LRP, microglia express VLDLR and LRP, and neurons express the four primary LDLR family members: LDLR, LRP, ApoER2, and VLDLR [15].

The general structure of ApoE, a 34-kDa protein, is a tetramer formation with an N- and C- terminal domain with a hinge region between. The N-terminal side of the protein has a receptor binding region and the C-terminal side has a lipid binding region. We do not have a full understanding of the structure of ApoE because it is only in a tetramer at low concentrations, but at the concentration necessary for NMR and crystallography, ApoE

forms aggregates with one another, precluding its structural recapitulation from this technology [16].

In order to function effectively to move cholesterol, particularly HDL-like particles in the brain, ApoE must become lipidated by the ATP binding cassette subfamily A member 1 (ABCA1). ApoE forms a subcomplex with ABCA1 via protein-protein interactions and all three isoforms have similar binding abilities to ABCA1 [17]. The initiation of this lipidation is typically triggered by liver X receptors (LXRs) and retinoid X receptors (RXRs), nuclear receptors that upregulate transcription of *ABCA1* and *APOE*. Adequate lipidation is essential for the receptor binding capacity of ApoE and successful cholesterol transport [18] due to the structural change upon lipidation that fully reveals the receptor binding domain on the protein [19].

1.3 The genetic prevalence of *APOE* and how isoform differences translate to variable disease risk

In the human population, there are three common isoforms of ApoE which differ by amino acids at positions 112 and 158, flanking the receptor binding domain. In the E2 isoform, both 112 and 158 positions have a cysteine residue. The E3 structural variant maintains cysteine at 112 and replaces the 158 position with an arginine. The E4 isoform has arginine residues in both positions. Though the protein remains functional in all isoform types, the replacement of a small, uncharged cysteine with a larger, positively charged arginine has implications for interactions with various lipids, receptor binding affinities, and other potential unknown effects [10].

Researchers have learned about ApoE's structure and isoform-dependent binding abilities through measurements of lipoproteins in the blood. For example, when ApoE3 is added to plasma, it preferentially binds HDL and ApoE4 has a greater binding affinity to VLDL. ApoE2 can bind to lipoproteins, but it has trouble binding to LDLR to clear the lipids. ApoE4 has a stronger ability to bind lipids because the positive arginine residues destabilize its structure and allow it to unfold more readily for binding access [10, 14, 20]. These binding preference differences implicate ApoE isoforms in various diseases, described in the next section.

In the brain, ApoE4 is expressed in lower levels compared to the other isoforms, one potential contribution to the dysregulation of cholesterol transport, but ApoE4 is also more poorly lipidated [21] (despite its ability to strongly bind lipids). Evidence of poor ApoE4 lipidation is derived from nondenaturing gel electrophoresis experiments in multiple models and cell types that show lower molecular weight (i.e. smaller) lipid complexes with ApoE4 compared to the other isoforms ($E3 < E2$) [22-25]. A promising therapeutic approach is to increase the lipidation of ApoE4 to open the receptor binding domain and hopefully increase E4's transport function. Alternatively, structural correctors or anti-ApoE4 immunotherapy to remove nonlipidated E4 have also been proposed as potential solutions that have seen success in mouse models, but none have been tested in clinical trials [26, 27].

ApoE prevalence varies slightly within ethnic or local ancestry groups, but generally, the worldwide frequency of the isoforms is $E2 = 8.4\%$, $E3 = 77.9\%$, and $E4 = 13.7\%$ [9]. Overall, the distribution of possible *APOE* genotypes is: $E2/E2 = 1\%$; $E2/E3 = 12\%$; $E2/E4 = 3\%$; $E3/E3 = 58\%$; $E3/E4 = 24\%$; $E4/E4 = 2\%$ [28]. Some populations have a prevalence

of the AD risk allele E4 up to 30% and the predicted prevalence of E4 in the United States is between 20 and 30% [29-31]. Studies looking at the prevalence of *APOE* genotypes in AD patients show the magnitude in E4-related risk, as at least 40-60% of AD patients carry an E4 allele. The age of onset of AD symptoms is also lower with carriage of an E4 allele in a dose-dependent manner. One copy of E4 is associated with about eight years earlier onset of symptoms compared to neutral risk E3 individuals, and two copies is associated with an onset 16 years sooner than a non-E4 carrier [9, 30, 32]. The true allelic frequency of E4 in the AD population is difficult to define, as many E4 carriers have decreased life spans, therefore skewing the higher E4 prevalence to the younger age distribution of the AD population.

Just as there are notable ranges in the *APOE* variant frequency due to global differences in prevalence, there are also notable ranges in E4's risk for AD. The most striking risk statistics are seen in Caucasian populations, also the most frequently studied in the literature. However, some African American and Hispanic populations confer a reduced odds ratio for AD development despite carriage of the E4 allele, compared to the general population as a whole. Researchers are beginning to study populations with reduced AD incidence and recently have identified a single nucleotide polymorphism (SNP) upstream of *APOE* on chromosome 19 that is associated with a reduction in AD odds ratio in a population of African ancestry [33]. More research is necessary to understand how these loci provide protection in the presence of *APOE4*, but their continued identification is important.

It is also noteworthy to report on other *APOE* variants and associated mutations which help guide research and understanding in the AD field. For example, the Christchurch

mutation of *APOE* is a mutation at R136S, which provides protection from early-onset AD in carriers of mutant *PSEN1*, an early-onset AD gene. This mutation was first noted in Christchurch New Zealand in 1987 [34], but has become infamous through a Colombian family with a *PSEN1* mutation. One woman carrying the mutation did not develop cognitive impairment until her 70s, unlike hundreds of her family members who experienced early cognitive decline well before their 60s. In addition to carrying the Christchurch mutation, her brain showed regional differences in hyperphosphorylated tau distribution compared to the normal AD pathology, with more tau in the occipital cortex as opposed to the frontal cortex [35].

Like the Christchurch mutation, the Jacksonville variant (V236E) is co-inherited with E3 and reduces AD risk more than 50%. A new variant in the E4 allele (R251G) has a mutation in the lipid binding region that reduces the risk of E4 by 60%. As genome wide association studies are employed in larger populations, we can begin to understand more about the prevalence and impact of these mutations and use them to inform research about the structure and function of ApoE4 as it associates with AD risk [36] and other diseases.

Though this dissertation research focuses on ApoE's influence on AD, it is worthwhile to mention the risk ApoE isoforms confer for other diseases. Outside the central nervous system, peripheral ApoE also traffics cholesterol and lipids, making it an important modulator of the cardiovascular system. Both E4 and E2 carriers have risk for unfavorable lipid profiles and cardiovascular disease, with E4 conferring an increased risk for hypercholesterolemia and E2 conferring an increased risk for type III hyperlipoproteinemia. Plasma concentrations of ApoE isoforms vary, with ApoE2 found in the highest concentration followed by E3 and E4 [37]. E2 is found in high concentrations

presumably due to its decreased binding affinity to LDLR family receptors, therefore clearance of its resident lipoproteins from the blood is not as effective. This, combined with its preference for HDL binding, contributes to the risk E2 carriers have of cardiovascular disease from aberrant lipid accumulation in the blood, as whatever lipoproteins E2 can clear via its receptors are preferentially HDL, leaving behind higher LDL levels [38]. E4 binds preferentially to VLDL and E4 carriers typically present with increased plasma cholesterol levels independent of a normal BMI [39], but the effect is exaggerated in the presence of obesity.

1.4 ApoE is found on the surface of lipid droplets

One lipid phenotype associated with both E4 and E2 carriers in disease is an accumulation of lipid droplets (LD), cellular storage organelles for neutral lipids. Though LD deposition can occur in cells with any of the ApoE isoforms, there is an increased LD accumulation in E2 expressing macrophages as they accumulate LDs (“foamy macrophages”) in atherosclerosis pathology [40], and an increased accumulation in E4 glial cells within the brain [41]. ApoE is a protein found on the droplet surface, as evidenced from several LD proteome studies [42-46], however the presence of ApoE is simply an observation and no research to-date has been published on the protein’s role on or influence over LDs. Furthermore, no studies have shown if there are different implications for *APOE* genotypes in LD biology. The connection of ApoE as a droplet protein itself, ApoE’s role in lipid trafficking and metabolism, and *APOE4*’s role as the largest genetic risk factor for LOAD beg for further investigation into LD dynamics between *APOE* genotypes. Perhaps the most convincing motive to study LDs in the context of AD risk is that the first

description of AD by Dr. Alois Alzheimer himself in 1906 highlighted lipid inclusions in glia which is widely recognized as LD accumulation [47].

1.5 Lipid droplet biogenesis and cellular function: the good

LDs are ubiquitous storage organelles which are conserved across many species and expressed in multiple cell types [48-50]. Although historically presumed to be innocuous and inert lipid storage depots, recent studies highlight the dynamic nature of LDs in terms of their formation, turnover, and composition across a number of homeostatic and pathological conditions. It is well documented that several diseases are associated with excessive LDs, including but not limited to obesity, atherosclerosis, cancer, type 2 diabetes, and relevant to this body of work - AD [51]. Evidence suggests these organelles may be active participants in disease mitigation, progression, or both [52].

LD formation in eukaryotic cells occurs in the endoplasmic reticulum (ER). In order to form a LD, first, neutral lipids must be synthesized to be incorporated within them. Two common pathways in which this occurs are the acetylation of diacylglycerol (DAG) to triacylglycerol (TAG) via diglyceride acyltransferase (DGAT) enzymes, or the esterification of cholesterol into a cholesteryl ester by acyl-CoA cholesterol acyltransferase (ACAT). As concentrations of neutral lipids increase, they coalesce together between the leaflets of the ER bilayer. This coalescence is also known as the formation of an oil lens. Expansion of this lens gives rise to 'budding' or the separation of the lipid droplet from the ER [49]. Researchers are unclear on which, if any, proteins are involved in the scission process of the LD bud from the ER membrane, but once there is significant enough

accumulation of neutral lipids in the bud to increase the contact angle between the bud and the ER, the bud can leave the membrane into the cytosol [53].

From there, LDs can increase their size by fusing with other droplets or taking in more neutral lipid. Proteins are then targeted to the LD surface and universally include perilipins (Plin) and lipid metabolism proteins. Other protein types recruited to the LD surface are variable and have not been consistently studied. The recruitment of proteins occurs in the ER leaflet and from the cytosol (Class I and Class II proteins, respectively) [49]. Profiling the LD proteome is not a trivial task due to the varying amounts of LD accumulation in different tissue and cell types and the possibility of contaminating proteins in the sample. However, quantitative proteomics in LDs has been done by a handful of groups in cell lines and mouse liver tissue [43-46, 54]. Most groups use density gradient centrifugation to obtain the LD-enriched buoyant fraction which contains LD proteins, but may also contain contaminant or transiently-associated LD proteins. Notably, the Olzmann lab developed a highly sensitive method to quantify the LD proteome in osteosarcoma and immortal hepatic cell lines using APEX2-PLIN2, an engineered ascorbate peroxidase [55]. APEX2 catalyzes the oxidation of biotin-phenol to a radical in the presence of hydrogen peroxide and this biotin-phenol reacts with electron-rich amino acids on neighboring proteins to allow them to become biotinylated. A streptavidin isolation is used to separate labeled LD proteins with a high specificity. From this high-confidence LD proteome classification, each cell line shared common LD proteins with one another, but also contained proteins that were exclusively found on their own LDs. This highlights the diversity of the droplet proteome and though this method identifies bona-fide LD proteins within the droplet surface, it may not capture important transiently associated proteins. As mentioned above, LD isolation is

methodologically challenging, in part due to the large volume of material required for accurate quantification of the LD proteome. Despite this highly sensitive assay, Olzmann's lab still used 18 15-cm plates for each cell line studied. This size cell culture plate holds 20 million cells at confluency, therefore over 350 million cells were used to isolate LDs induced with oleic acid using their method.

LD function is widely variable depending on the cell type and condition in which they are found. Some of the observed roles of LDs include storage of excess lipids (adipocytes during calorie excess) for energy, buffering cells against peroxidated lipids or free fatty acids, protein storage, and liberation of signaling precursors. Plin5, a perilipin on the LD surface, recruits mitochondria to the LD through its C-terminal region, forming a cross-bridge between the organelles. Researchers believe Plin5 is an essential regulator of the hydrolysis of fatty acids from LDs to be released for beta-oxidation in the mitochondria [56, 57]. Plin5 can achieve this function with or without a physical linkage to the mitochondria, as demonstrated with the addition of a truncated Plin5 in the paper by Kien et al. Regardless, Plin5 contributes to the use of LDs in an energy-generating capacity through hydrolysis of its contents to beta-oxidation [57].

Bosch et al. profiled the LD proteome in liver tissue from mice infected with *Escherichia coli* (*E. coli*) or stimulated with lipopolysaccharide (LPS). When liver cells are inflamed through a pathogenic (*E. coli*) or inflammatory (LPS) stimuli *in vitro*, researchers observed a downregulation of Plin5 and the uncoupling of the physical and functional linkage between Plin5 and the mitochondria. This uncoupling occurred alongside decreased fatty acid metabolism and increased physical LD contacts with bacteria invading the cell in their hepatocyte model of *E. coli* infection. This versatility

offers evidence of the dynamic nature of LDs and their flexibility to meet the cell's specific needs [54]. In the context of LD-bacteria interactions, they observed an upregulation in Plin2 as Plin5 decreased. Other groups have also associated Plin2 with immune responses in macrophages [58, 59], fibroblasts [60], in various cancers [61], and microglia in the brain [62, 63].

Additionally, in the case of pathogen vs. host relationships, LDs are hijacked by pathogens as energy pools to replicate and survive during infection. From this type of interaction, LDs have also been observed to 'fight back' as a hub for innate immunity, releasing lipids from their core to become lipid mediators of inflammation [64-66]. This and the above-mentioned association of LD proteins with inflammation offers the question 'does inflammation drive LD accumulation or does the presence of LDs increase inflammation?' Technically, both are true depending on the circumstance. The next section elaborates on the latter part of this question. To explain the link between inflammation and the subsequent accumulation of LDs, several papers have observed an increase in LDs after inflammatory activation of cells as a way to store mediators of inflammatory signaling [67-70]. Lipids released from droplets that are not utilized in oxidative phosphorylation can be used directly as signaling molecules or turned into them. Liberated LD contents serve as ligands for G protein-coupled receptors (GPCRs), Toll-like receptors (TLRs; also stimulated by LPS), peroxisome proliferator-activated receptors (PPARs), sterol regulatory element-binding proteins (SREBPs), and nuclear factor κ B (NF κ B) [71, 72]. The downstream effect of these pathways is typically the modulation of energy production, cell survival and proliferation, and inflammation. LDs also store polyunsaturated fatty acids (PUFAs), precursors for eicosanoids. Adipose triglyceride lipase (ATGL)-mediated LD

lipolysis facilitates the production of eicosanoids in addition to cleavage of membrane phospholipids by phospholipases for the same purpose [73, 74]. Eicosanoids are derivatives of arachidonic acid with hundreds of species that initiate, perpetuate, and/or resolve inflammation.

1.6 Lipid droplets and cellular function: the bad

LDs are believed to be compensatory, protecting cells from toxicity, providing energy, and acting as hubs of immunity. However, abnormal LD accumulation can become detrimental, contributing to disease pathogenesis. One of the most obvious examples of excessive LD accumulation is in obesity where LDs are formed to store excess fatty acids. Increased LD size can cause cellular remodeling and drive inflammatory infiltration of macrophages and exacerbate obesity-induced inflammation [75]. Fatty liver disease is also characterized by increased LDs in hepatocytes and may be due to impairments in lipophagy, or the breakdown of LDs through autophagic turnover [76].

In atherosclerosis, the hallmark pathology is the presence of foamy, or LD-laden macrophages in the arterial wall. LDs are primarily composed of esterified and stored cholesterol in this instance and this buildup in the arterial wall causes a pathologic narrowing, increasing susceptibility to stroke and heart attack [77]. Additionally, cardiomyocytes can accumulate LDs in a state known as cardiac steatosis due to increased delivery of metabolic substrates to the heart and is typically associated with obesity, type II diabetes, or hyperlipidemia. Researchers have investigated the effect of lipid overload on the heart in animal models and cardiotoxicity from excess lipid caused cardiomyopathy and in some cases, sudden death. This suggests there is a ceiling to how much lipid

accumulation cells of the heart can handle, and decreased LD capacity in the presence of lipid overload leads to cellular dysfunction [78].

In the brain, LD accumulation is described in the context of aging in microglia, leading to a dysfunctional state characterized by increased cytokine release, increased reactive oxygen species (ROS), and impaired phagocytosis [62]. LDs are present in several disease states other than AD, including Parkinson's disease, Huntington's disease, and Multiple Sclerosis (MS). A pathologic hallmark of Parkinson's disease is the accumulation of α -synuclein in the form of Lewy bodies. This protein can be found on LD surfaces and similar to Plin structural proteins, it can slow lipolysis [79]. A recent paper validated previous findings implicating LD pathology in Parkinson's disease by observing α -synuclein-LD interactions in *Drosophila* that provided protection of α -synuclein from proteolytic digestion and lipolysis. Researchers hypothesized that LDs harboring α -synuclein proteins promoted protein misfolding and initiation toward disease pathogenesis [80]. In mouse models of Huntington's disease, excessive LD accumulation is observed in multiple cell types due to presumed deficits in the macroautophagy of lipids [81]. In MS, microglia accumulate LDs as they phagocytize myelin fragments during demyelination. However, excessive LD accumulation causes MS microglia to resemble lipid-laden microglia in aging, leading to deficits in phagocytosis and increased inflammation [82].

1.7 ApoE and lipid droplets across the liver, brain, and blood axis

Not much is known about the role of ApoE as a LD protein. Structurally, ApoE is similar to Plin3, another LD surface protein [83], but there are currently no studies investigating ApoE's direct influence on the droplet's contribution within the cell.

However, there are a few studies observing LD accumulation in various cell types based on *APOE* genotype.

In the liver, ApoE4 expressing hepatocytes have been observed to accumulate significantly more LDs compared to E3 in a targeted replacement mouse model of diabetic dyslipidemia [84]. Interestingly, Johnson et al. found a concomitant reduction in fatty acid oxidation in primary hepatocytes from the same E4 mice with increased droplets. Additional background on liver-specific ApoE is found in Chapter 2.

Consistent with the previously cited study, Farmer et al found an increase in LDs in primary astrocytes from targeted replacement mice expressing human ApoE4 compared to ApoE3 [41]. These cells also exhibited a decrease in fatty acid oxidation in favor of an increase in glycolysis. Notably, E4 astrocytes had smaller individual LDs than E3, despite having a larger total accumulation. Qi et al studied the neuron-astrocyte coupling of fatty acid metabolism in the context of *APOE* genotype and also found E4 astrocytes to accumulate more LDs, experience a lower capacity for fatty acid oxidation, and an increased use of glucose compared to E3 astrocytes [85]. They further described the origin of LDs in astrocytes as primarily from *de novo* fatty acid synthesis and decreased fatty acid degradation. The consequence of this droplet phenotype in astrocytes prevented E4 from accepting fatty acids from neurons in a co-culture to shield them from toxicity and from achieving normal metabolic and synaptic support. In addition to the E4 expressing astrocytes accumulating more LDs, ApoE is responsible for some of the fatty acid transport from neurons to glia through its lipid binding domain [86, 87]. This suggests two potentially compounding avenues for dysfunction – the accumulation of lipids in E4 cells and the lipid binding and transport deficits of the E4 isoform.

Sienski et al found isogenic induced pluripotent stem cell (iPSC) astrocytes expressing E3 or E4 had significant differences in droplet accumulation with E4 cells displaying more LDs with increased expression of Plin2 [88]. They also observed a trend toward increased droplets in E4 microglia iPSCs. Recently, this finding was verified in both iPSC microglia and primary microglia from targeted replacement human ApoE mice [89, 90]. Along with the increase in LDs in E4 microglia, Machlovi et al. observed an altered morphology and increased cytokine production, and Victor et al. observed a blunted capacity of E4-microglia-like iPSCs to communicate with neurons alongside an increase in lipid metabolism and inflammatory transcription factors. This falls in line with previous research from their group showing upregulation of inflammation-related genes in E4 microglia [91]. These studies are expanded upon in Chapter 3 to further compare LDs in microglia to our own results.

To date, there are no direct studies investigating LD dynamics in the context of *APOE* in peripheral blood mononuclear cells (PBMCs), particularly monocyte-derived-macrophages (MDMs) from human subjects. In 2014, Gale et al. describe an increase in lipid rafts in monocytes of E4 carriers with an increase in inflammatory cytokines after ex vivo stimulation of TLR. The increase in lipid rafts is postulated to be due to the decreased ability of ApoE4 to facilitate cholesterol efflux [92]. Although this group did not describe LD formation in cells, it is possible based on the increased lipid raft formation and decreased cholesterol efflux, there could be increased LD accumulation in E4 monocytes and macrophages. Another paper in 2012 looked at the effect of mouse ApoE on neutral lipid accumulation in the context of hyperlipidemia and atherosclerosis. They found the presence of ApoE in the plasma, compared to the mouse model with no plasma ApoE, was

responsible for reducing lipid accumulation in circulating monocytes and reducing atherosclerotic lesions. The presence of ApoE also reduced monocyte activation and circulating leukocyte levels in the mice [93]. Although mice do not have different isoforms of ApoE like humans (the reason we use targeted replacement mice expressing the humanized *APOE* alleles), it is possible that with increased ApoE amounts in the plasma, we could see reduced LD accumulation in the circulating monocytes. By this reasoning, as E4 is the least concentrated ApoE isoform found in the blood of humans, we would hypothesize that E4 carriers accumulate more LDs in their circulating blood cells. Chapter 4 details work done to initiate and execute a human research study to answer this hypothesis by characterizing LDs in E3 vs E4 MDMs.

Despite the physical separation of the peripheral and central pools of ApoE in normal physiology, there is a clearly established liver-brain-blood axis that links the two systems in terms of inflammation, insulin signaling, metabolism, and amyloid beta [94-96]. The linkage of the liver and brain occurs via the blood where signals and proteins are transported and either cross the blood brain barrier (BBB) or influence factors that can cross to each organ. The interplay between these systems, their responsibility for producing the vast majority of the body's ApoE, and their ability to accumulate LDs provides justification to study LD dynamics between genotypes in these specific tissues. Although several researchers observe a greater LD accumulation in E4 expressing liver and glial cells, there is still no information about the composition of E4-associated LDs, their protein makeup, or their contribution within the cell. Due to the indication that LD composition influences their function, it is imperative to elucidate LD differences between *APOE* genotypes.

1.8 Summary and Impact

Therapies to prevent, delay progression, and cure AD are lacking, but the scientific community is covering a wide breadth of potential therapeutic targets to decrease the burden of this disease. One current area of interest is understanding how different *APOE* variants present risk for AD, contribute to pathology, and respond to treatment. A person carrying an E4 allele has increased disease risk for AD and animal models implicate E4 in various loss of function and toxic gain of function effects within the brain. The differences between E3 and E4 carriers suggests the etiology for AD pathogenesis is different among *APOE* carriers and should be approached as such in the pursuit of meaningful therapeutics.

A common feature observed in E4 expressing cells is an increase in LDs, cellular organelles that accumulate in glial cells with aging and in neurodegenerative diseases like AD. E4 expressing cells throughout the body accumulate more LDs than from individuals expressing E3 (neutral risk to AD), but there are no studies determining if LDs between genotypes are characteristically different and if those differences affect the function of the cell or contribute to disease risk.

This dissertation work begins to answer these questions by quantitatively profiling LDs from E3 and E4 expressing cells in various conditions to understand lipid and protein composition changes and their role in cellular function. Chapter 2 describes LD dynamics in the liver of mice expressing human ApoE3 and ApoE4. In the liver, E4 droplets have an increase in the abundance of surface proteins involved in innate immunity compared to E3 droplets that have more surface proteins involved in metabolism. This reflects a broader cellular phenotype observed in microglia, described in Chapter 3, where E4 cells have an increased cytokine secretion and an altered metabolism (E4 glycolytic and inflamed; E3

oxidative). It was also found that E4 LDs have a blunted response to an inflammatory challenge compared to E3, perhaps because they are already in an inflamed state. LD inhibition did not ameliorate inflammation, but did provide critical evidence on LDs as a delicately balanced necessity for properly functioning glia. The final work of this dissertation, detailed in Chapter 4, set up a long-term biobank of *APOE* genotyped PBMCs and plasma to understand the functional differences of LDs in the circulation of human subjects. This created a store of easily accessible cells to study the direct impact of LD accumulation and to target various ways to shift LD dynamics to have a more favorable contribution within the cell.

CHAPTER 2. *APOE4* ALTERS THE LIPID DROPLET PROTEOME AND MODULATES DROPLET DYNAMICS IN THE LIVER

2.1 Introduction

The liver is a primary site for lipoprotein uptake and it relies heavily on ApoE to transport and clear these lipid storage molecules. A brief summary of the types of lipoproteins and how ApoE works to transport them is imperative for understanding how ApoE isoforms impact health: The three major classes of lipoproteins are chylomicrons, very low density lipoproteins (VLDL), and high density lipoproteins (HDL). Chylomicrons are synthesized in the small intestine and carry absorbed dietary lipids into the plasma. As chylomicrons release fatty acids for delivery to various tissues, the chylomicron remnants, with ApoE now acquired on their surface, are trafficked back to the liver for breakdown. VLDL is synthesized in the liver with surface ApoE proteins attached. The primary job of VLDL is to transport endogenously made lipid and cholesterol and serve as a precursor to LDL; a process that occurs when its cholesterol content becomes greater than its triglyceride content. LDL is taken into various tissues via an LDL receptor when the cells have a need for cholesterol. HDL is also made in the liver and is the highest density lipoprotein responsible for carrying lipids and cholesterol from peripheral tissues and the blood back to the liver for clearance [97]. This action dubs HDL as ‘good cholesterol’ while LDL is labeled ‘bad cholesterol’ for its contribution to atherosclerosis.

Lipoproteins release their triglyceride contents through the action of lipoprotein lipase (LPL) which hydrolyzes triglycerides into free fatty acids that can be used within tissues [98]. LPL activity has been shown to modulate LDs in cardiomyocytes [99], microglia [100], hepatocytes [101], and macrophages [102]. An overexpression of LPL is

associated with an increase in peroxisome proliferator activated receptor α (PPAR α), which is the main regulator of fatty acid oxidation. With increased LPL and PPAR α , cells accumulate fewer LDs, presumably because their contents are being liberated for fatty acid oxidation or their substrates are being used for energy before droplets form [101], in contrast to an LPL knockdown with increased LD accumulation that is rescued by PPAR α agonists [100]. LDs also undergo lipolysis, similar to lipoproteins, but via ATGL. ATGL also promotes activation of PPAR family members to increase oxidation of fatty acids hydrolyzed from droplets. In a way similar to LPL, overexpression of ATGL reduces hepatic LDs and increases fatty acid oxidation, while depletion causes LD buildup and reduced oxidation [103, 104]. Another way to liberate fatty acids from droplets is through autophagy, also known in LDs as lipophagy [105]. To allow this process to occur, Plin2, a LD structural protein that typically inhibits lipase activity on the droplet, is degraded by chaperone-mediated autophagy. LD size may also influence the mechanism of fatty acid release through either lipolysis or lipophagy, as ATGL seems to hydrolyze larger LDs until they become small enough for lipophagy [106]. Similar to Plin2 on the surface of LDs to inhibit lipase activity, ApoE adornment on lipoproteins also reduces hydrolytic activity of triglycerides [107, 108]. Overexpression of ApoE in the liver has shown increased VLDL secretion and reduced hydrolysis of lipoproteins [109]. When the process of VLDL secretion or hydrolysis is impaired, hepatic steatosis and increases in hepatic LDs occurs. The isoform differences of ApoE, their preferences in binding lipoproteins, their respective efficiencies at receptor-mediated clearance, and their association with differing levels of LD accumulation, necessitate the characterization of LDs from ApoE3 and ApoE4

expressing cells and could yield valuable information about lipid metabolism and clearance.

The liver's role in lipid metabolism, its large tissue volume, and its tendency to accumulate LDs make it an optimal organ system to study LD dynamics, particularly in the context of ApoE, as the liver synthesizes the majority of the body's ApoE. Studying droplet dynamics between ApoE isoforms has obvious and important implications for diseases like hepatic steatosis and non-alcoholic fatty liver disease, but has less-studied, yet highly relevant implications for the brain. In a recent, pivotal publication by Guojun Bu's laboratory, a conditional mouse model expressing humanized ApoE3 or ApoE4 *only* in the liver showed adverse pathology on the brain of E4 mice. With no ApoE protein in the brain, E4-liver-expressing mice had reduced blood brain barrier (BBB) integrity, activated glial cells, increased amyloid β , and synaptic loss [110]. More exciting yet, injections of plasma from young, E3 mice into wild-type mice improved memory, BBB leakage, and resolved reactive gliosis, whereas injections from young E4 mice failed to do so. This research provides evidence that peripheral ApoE has influence on the brain in the context of AD pathology through factors in the blood and the administration of plasma from an alternative genotype shows therapeutic promise. Although this paper did not look at LDs, plasma proteomics revealed downregulation of a module enriched for plasma lipoproteins, lipid transport, and clearance in the conditional E4 mice.

Here, we sought to develop a deeper knowledge of LD characteristics between *APOE3* and *APOE4* cells in the liver. E3 and E4 expressing LDs were analyzed for their relative accumulation at baseline and in response to stress and for their physical characteristics including size, lipid composition, and protein composition. First, we show

an increase in LD accumulation in E4 hepatocytes at baseline and with LPS treatment, with E4 LDs being smaller in individual size compared to E3. Next, we show differences in the lipid and protein profiles of E4 droplets compared to E3 at baseline and with inflammatory stimulation. The lipidome of E4 droplets is strikingly similar to LPS treated conditions in both E3 and E4 droplets and this is also reflected in the E4 proteome which emphasizes innate immunity pathways. Our results suggest that E4-expressing cells accumulate more LDs which participate in inflammatory processes within the cell and this could have broader, systemic implications due to the connections between the liver, blood, and brain in the context of AD.

2.2 Methods

2.2.1 Mouse Model

Targeted replacement mice expressing human *APOE3* and *APOE4* under the endogenous *APOE* mouse promoter were used in the following experiments [111]. All mice received standard chow food and water ad libitum and were housed under a standard light/dark cycle. Procedures concerning mice were in compliance with the University of Kentucky's Institutional Animal Care and Use Committee.

2.2.2 Lipid Droplet Enrichment

Twelve-month-old female mice were used to determine LD dynamics at baseline and upon inflammatory stimulation between E3 and E4 genotypes. Mice were injected with saline or lipopolysaccharide (LPS; isolated from *E. coli*; Sigma L2880) at 5mg/kg (n = 5 per group). There were no group differences in body weight. After 24 hours, mice were

humanely euthanized with a lethal injection of pentobarbital. Mice were perfused with saline and 400g of liver tissue was removed for lipid droplet enrichment. Sections were taken from the median and left lobes of the liver for LD isolation, The caudate lobe was taken for extra frozen tissue (Liquid nitrogen), and the right lobe was collected for histology. On ice, liver tissue was minced and bathed in homogenization buffer from the LD Isolation Kit from Cell Biolabs Inc. (product No MET-5011). Homogenate was collected into a 2mL vial and 600ul of density gradient separation buffer from the LD kit was gently layered on top. Samples were spun at 13,500 RCF for 3 hours. A layer of lipid known as a fat-pad gathered at the top of the vial after centrifugation and this buoyant layer is enriched with lipid droplets. The top 270µl of liquid was removed, along with the fat pad aspirated in the pipette with the liquid, and placed into a new tube. Two liver sections per mouse were processed this way and flash frozen in liquid nitrogen to send for proteomics and lipidomics at BGI Genomics. An additional section of liver was centrifuged and the top 270µl was added to 1mL of ice-cold acetone for protein precipitation and later western blot analysis.

2.2.3 Proteomic and Lipidome Analyses

Proteomics: After lipid droplet enrichment via density gradient centrifugation, the top 270ul and ‘fat pad’ containing lipid droplets was removed and placed into a microcentrifuge tube. Tubes were frozen in liquid nitrogen and placed in a -80C freezer prior to shipment to BGI Global for quantitative TMT proteomics analysis using methods and normalization procedures previously described [112]. Briefly, two normalization procedures were applied for a 30-plex experiment (3 TMT experiments with 10 channels

each). First, within each 10-channel TMT run, the grand total reporter ion intensity for each channel was multiplied by scaling factors globally to adjust the channel intensity to the average total intensity across all ten channels in order to correct for sample loading and reaction efficiency differences. Secondly, common, pooled internal standards were utilized to normalize reporter ion intensities between the three TMT experiments.

Proteomics analysis revealed 6,192 results. Proteins were accepted if they contained more than two unique peptides and were within the false discovery rate of 5%. A final 4,267 proteins were included and analyzed. These final proteins are considered as both LD-resident proteins and LD- interacting proteins. To determine which proteins may be true LD resident proteins, the accepted 4,267 were referenced against 6 known lipid droplet proteomes from liver cells and mouse and rat liver tissue [43-46, 54, 55]. Upon cross-referencing our database with the six others, 2092 overlapping proteins were identified and considered as LD-resident proteins.

Both the full list from the proteomic analysis and the overlapping list of proteins were analyzed in the same ways. Abundance averages were calculated within groups and multiple group t-tests were performed on the entire dataset. Significantly differentiated proteins were plugged into the open source gene ontology analysis site, Enrichr, to understand protein interactions within biological processes. Volcano plots were made for each condition in the entire data set and the overlapping data set.

Our full database was also compared against proteomes from papers investigating differences in the brain, Alzheimer's disease, and microglia [62, 113-115]. We analyzed overlapping proteins from our database with these papers and further investigated their contribution to our hypothesis.

Lipidomics: After LD enrichment via density gradient centrifugation, the top 270 μ l and fat pad containing LDs was removed and placed into an Eppendorf tube. Tubes were frozen in liquid nitrogen and placed in a -80°C freezer. Samples were packaged and sent to BGI global.

Nontargeted lipidomics analysis was performed using LC-MS/MS. High resolution mass spectrometer Q Exactive (Thermo Fisher Scientific, USA) was used for data acquisition in positive-ion and negative-ion mode respectively to improve the lipid coverage. The data were processed by LipidSearch 4.1 and BGI's statistical software package, metaX.

Lipidome analysis revealed 321 unique lipid metabolites. An outlier analysis was performed in Prism Graphpad and revealed 176 statistical outliers among the 20 samples and 321 metabolites (2.7% outliers from original data). Metabolite abundance averages were calculated within groups and multiple group t-tests were performed on the entire data set. Volcano plots were made for each condition in the data set and also by lipid class.

2.2.4 Oil Red O

Additional liver sections from mice treated with LPS or saline were stained with Oil Red O and Hematoxylin to quantify LD accumulation. Dissected liver specimens were fixed in 4% PFA for 24 hours then sunk in 30% sucrose + 0.05% sodium azide before being fixed in optimal cutting temperature (OCT) compound (Thermo Fisher; 23-730-571) Free-floating sections were cut at 10 μ M and washed 3x for 5 minutes with PBS prior to staining. Sections were placed in 100% propylene glycol for 5 minutes then incubated in pre-heated Oil Red O (Abcam #150678) for 6 minutes at 60°C. After staining, sections were placed

in 85% propylene glycol for 1 minute, rinsed with 2 changes of distilled water, and counterstained with Hematoxylin. Sections were mounted with ProLong Gold upon air drying. Liver sections were imaged on the Zeiss Axio Scan Z1 and 3 areas from each sample were randomly selected for droplet analysis. Total lipid droplet area was assessed using an automated algorithm which removed white (blank) background from the images and separated the colors to highlight the red-stained droplets. Individual droplet area was evaluated using ImageJ based on circularity of the droplets.

Total area percentage: For total lipid droplet area calculation, the images were loaded in a BGR format using the OpenCV module in Python. A Gaussian filter with a kernel value of 5 was applied to the images in order to reduce the noise of the pixels. The now blue lipid droplets were thresholded by performing color detection of the range of red (corresponding to the other tissue), using the cv2.inRange function and defining the boundaries in the RGB color space. The lower limit of the color was set as [60, 20, 2], and the upper limit, as [126, 255, 255]. A binary mask was then imposed on top of the original image, producing a new one where the values of the pixels within the defined color range become 0 (black). Upon counting the non-black pixels, that number was then multiplied by 100 and divided by the total amount of pixels conforming the image.

Individual area: For individual lipid droplet area calculation, the segmented images were imported into ImageJ and subsequently turned into 8 bit grayscale images using the command Image>Type>8 bit (black and white). A new mask was imposed on top of the image using the command Image>Adjust>Threshold, setting the lower limit as 0 and the upper limit as 20 to re-cover the black pixels in the image. Upon inverting the colors of the image using the command Edit>Invert, the droplets were quantified and measured using

the command Analyze>Analyze particles; the pixel size was set to 0-100 and circularity was set to 0 (1 being a perfect circle). Configurations were set to display the resulting outlines as new images. Perimeter and area measurements were selected and found under the menu Analyze>Set measurements.

2.2.5 WGCNA

Weighted gene co-expression network analysis (WGCNA) (v1.70-3) [116] was used to identify modules and build unsigned co-expression networks, to include negative and positive correlations. WGCNA constructs a gene co-expression matrix, using hierarchical clustering in combination with the Pearson correlation coefficient to cluster genes into groups of closely co-expressed genes termed modules, and then uses singular value decomposition (SVD) values as module eigengenes (MEs) to determine the similarity between gene modules or calculate association each module with sample traits (ex. *APOE* genotype and treatment). The gene names from the full 4,267 proteins quantified in the LD proteome were selected to identify gene modules and network construction. Soft power of 6 was chosen by the WGCNA function `pickSoftThreshold`. Next the function `TOMsimilarityFromExpr` was used to calculate the TOM (Topological Overlap Matrix) similarity matrix via setting `power = 6`, `networkType = "signed"`. The distance matrix was generated by subtracting the values from the similarity adjacency matrix by one. The function `flashClust` (v.1.01) was used to cluster genes based on the distance matrix, and the function `cutreeDynamic` was utilized to identify gene modules by setting `deepSplit = 3`. Cytoscape (v.3.8.2) was applied for the gene-gene network visualization.

2.2.6 Western Blotting

Protein from the lipid droplet enriched fraction was precipitated with acetone and resuspended in radioimmunoprecipitation assay buffer (RIPA; Sigma-Aldrich R0278-500mL) with 1mM protease inhibitor (Sigma-Aldrich 4693124001). The sample was diluted with 10 μ l deionized water and 2x Laemmli Sample Buffer (Bio-Rad Laboratories, Hercules, CA, USA). The samples were heated at 96.5° Celsius for 10 minutes, after which they were chilled on ice for 5 minutes before loading into the gel. Twenty μ l of the protein sample was loaded on 4-20% Criterion TGX Gels (Bio-Rad Laboratories, Hercules, CA, USA) and ran at 180V. Gels were transferred onto 0.2 μ m nitrocellulose membrane (Bio-Rad Laboratories, Hercules, CA, USA) using the Trans-Blot Turbo Transfer System (Bio-Rad Laboratories, Hercules, CA, USA). After transfer, membranes were blocked for 30 minutes in 1% casein solution while gently rocking back and forth. The membranes were incubated overnight at 4°C in 1:1000 Plin-2 primary antibody solution (Novus Biologicals, Centennial, CO, USA). After incubation, the membranes were washed with PBS-T (0.05% Tween-20), three times for five minutes each wash. The membranes were then incubated for one hour at room temperature, while protected from light, in 1:5000 Goat α -rabbit IR 700 secondary antibody solution. (Bio-Rad Laboratories, Hercules, CA, USA). They were then washed with PBS-T, three times for five minutes each, and then with PBS two times for five minutes each. Membranes were imaged using a ChemiDoc XRS Imaging System (Bio-Rad Laboratories, Hercules, CA, USA).

2.3 Results

2.3.1 LD-enriched fractions show greater lipid droplet accumulation in cells expressing ApoE4 and after stimulation with LPS.

Here, we confirm previous observations in the liver that LD accumulation is dependent on *APOE* genotype and inflammatory state, and we seek to further investigate the composition and implication of LDs across *APOE* genotypes with a comprehensive analysis of the LD proteome and lipidome. We first studied the abundant and easily accessible LDs from the liver of human E3 and E4 expressing mice to quantify ApoE isoform-specific changes in LD composition (Figure 1a). Mice were injected intraperitoneally with LPS (5mg/kg) or saline (control) and liver tissue was harvested after 24 hours. LDs were enriched via density gradient centrifugation where the buoyant, lipid-rich fractions at the top of the centrifuge tube were collected for western blot verification of lipid droplet surface protein Plin2 (Figure 1b). The next two sequential fractions did not contain Plin2, confirming LD enrichment within the top ‘LD-enriched’ fraction used for downstream analyses (Figure 1a). Consistent with previous studies [84], there is increased lipid content in the E4 liver, with oil red o staining showing an appreciable increase in positive staining in E4 liver tissue at baseline. Both E3 and E4 liver tissue increased lipid content after LPS stimulation (Figure 1c-d).

2.3.2 E4- and LPS-stimulated LDs show increases in phosphatidylcholine composition.

As anticipated, the bulk of lipid content in LD enriched fractions was composed of glycerolipid, with >90% as TAGs in the inner core of the LD (Figure 2a). The other lipid species highlighted in Figure 2a are largely glycerophospholipid species that make up the

outer LD monolayer. When looking at the distribution of glycerophospholipids, there was a noticeable increase in the distribution of PC in saline E4 droplet fractions compared to E3 saline droplets (Figure 2a). This closely mirrors the lipid class distribution in both E3 and E4 LPS-treated conditions and the lipid distributions in each group correlated with histograms of LD size. Similarly, volcano plots of differentially abundant metabolites reveal an increase in glycerophospholipids in E4 saline LDs compared to E3 saline LDs (Figure 2b-e). Additionally, E3 droplets increase their PC content when stimulated with LPS (Figure 2d), but a similar response was not observed in E4 droplets, as their PC lipid distribution remained the same (Figure 2e). Further breakdown of individual PC species and the respective changes between genotypes and conditions are described in Figure 3. These results suggest E4 droplets do not respond to inflammation as robustly as E3 droplets because they either do not have the capacity to shift, or based on their similar lipid profile to LPS droplets, they are already in a heightened inflammatory state, or a combination of both.

2.3.3 E4 droplets are enriched for immune-associated proteins.

Quantitative proteomic analyses revealed 4,267 LD-enriched proteins. Due to the nature of the LD enrichment, some proteins that transiently associate with LDs may have been included in the analysis. To determine which proteins in our LD-enriched fractions were ‘LD resident’ proteins commonly found on other LDs, we cross referenced with other known LD proteomes to identify proteins that are consistently and/or exclusively expressed on the LD surface (as others in the literature do). Overlapping LD proteomes included those from liver cell lines and liver tissue (Figure 4d) [43-46, 54, 55]. A total of 2,092 ‘LD resident’ proteins were identified in our dataset which overlap with the aforementioned LD

proteomes. Due to the unique nature of analyzing proteomes between *APOE* genotypes, we chose to conduct analyses on the full LD proteome, as to not exclude important interactions of proteins in each genotype, or previously undocumented proteins specific to our LDs. To further support this decision, the proximity labeling strategy used by the Olzmann lab identified unique LD proteins (i.e. non-overlapping) between the osteosarcoma LDs and the hepatic LDs. However, Figure 4e and f show the overall trends in protein networks and pathway contributions are similar between the full list and the overlapping list featured in Figure 4a-c. In Figure 4, differentially expressed proteins between baseline (saline injected) E3 and E4 LDs were plotted (Figure 4a). Proteins enriched on E3 LDs include metabolic proteins like *Por*, *Echdc2*, and *Acaa1a*. Proteins enriched on E4 LDs included known immune modulators such as *Stat5a*, *Ighg3*, and *Gsk3b* (Figure 4a). Immune-related genes enriched in the droplet proteome are presented as black dots in Figure 4a and 4d. Gene ontology revealed proteins increased on E4 LDs are implicated in innate immunity and proteins increased on E3 LDs are involved in beta-oxidation. Further, a weighted gene co-expression network analysis (WGCNA) of the LD proteome revealed a significant downregulation of lipid-related metabolic and synthetic pathways, including fatty acid β -oxidation, on E4 droplets (Figure 5a-c). The top ten hub genes between treatment groups and genotype are available in Table 1.

2.3.4 Proteins implicated in human E4 carriers and Alzheimer's disease proteomics studies are largely LD-enriched.

A unique protein signature (Figure 6a) highly expressed in young E4 carrier brains, but reduced in AD brains was observed by Roberts et al. - a signature referred to as “incipient AD (iAD) proteins” [117]. Intriguingly, 15 out of 25 (60%) of these AD-

predictive proteins are highlighted in our LD proteome (Figure 6b). Of interest, Stat3 and Snx4 show significant increases upon inflammation in E4 LDs. Stat3 is a transducer of several cytokines and its inhibition reduces neuroinflammation and cognitive impairment in mouse models of AD [118]. Another study noted Stat3 may act as a transcription factor for β -APP cleaving enzyme 1 (BACE1), the important enzyme for amyloid β production [119]. Interestingly, Snx4 is also implicated in BACE1-related AD pathology, as it prevents trafficking of BACE1 to the endosome for degradation, therefore increasing its half-life and ability to cleave APP [120]. Figure 6c shows a proposed feed-forward mechanism where inflammation and cytokines increase transcription of Stat3 and further release of cytokines. These cytokines also act to increase transcription of Stat3 in neurons where it increases expression of BACE1. When Snx4 is also increased, this prevents BACE1 trafficking to the endosome, allowing it to continue cleaving APP and increase amyloid beta.

2.3.5 Proteins changed in Alzheimer's disease associated with metabolism and microglial activation, overlap with LD-resident proteins and include disease associated microglia genes.

Proteomic analyses from human brain samples in previously reported literature reveal a module of differentially expressed proteins in the AD brain specifically related to microglial metabolism (M4) [113]. In this research, Johnson et al characterized the top 30 most differentially expressed microglial transcripts that correspond to the metabolic module in microglia. This list has almost all (27 of 30, Figure 7a) LD proteins and is largely involved in the anti-inflammatory activation of microglia (Figure 7b). Proteins of significant difference in the LD proteome determined by a two-way ANOVA are highlighted in Figure 7c. Notably, disease associated microglia (DAM) [115] genes Fabp5,

Tspo, and Spp1 are included along with the binding protein for DAM gene Lgals3 (Lgals3bp). Together, this highlights an interesting connection of LDs to the microglial immune response and metabolism in AD. This paper did not analyze data based on *APOE* genotypes, however, a study from the same group in 2018 identified differentially expressed proteins in E4-AD brain tissue [114]. Again, there is substantial overlap between proteomes, with 1,823 of our LD proteins with 4,196 of their brain proteome (43%), including 512 proteins upregulated in our E4-LDs (Figure 8a). Gene ontology from this overlap (Up in Dai et al E4-AD brains and Up in Friday et al E4-LDs) shows significant immune-related functions (Figure 8b). A similar comparison of proteins with increased expression in E3 AD brains compared to E3 LDs highlight RNA splicing and fatty acid beta-oxidation as their primary function (Figure 8c).

2.4 Discussion

Expression of ApoE4 is associated with an increase in LD accumulation compared to ApoE3 expressing cells across multiple cell-types and organ systems. However, a characterization of LDs and their contribution in an *APOE* genotype-dependent way has not been previously described. Here we show LDs from E4 cells have a different lipid and protein profile than E3 droplets, and that the E4 droplet composition is similar to the profile of LDs from inflamed cells. Livers from E4-expressing mice accumulate more LDs that are smaller in size, with a similar size distribution as LPS-treated LDs. Interestingly, the LD protein profile featured significant overlap with several recently published proteomes implicated in AD, suggesting there could be a broad impact of LDs beyond the cell in which they reside, the LD's composition could be reflective of the larger environment outside their host cell, or both.

The first description of the AD brain by Dr. Alois Alzheimer himself highlighted lipid inclusions in glia, a description now widely recognized as a characterization of LD accumulation [47]. It is also now recognized that rather than droplets inertly sequestering lipid, these interesting organelles seem to play a much more active role within the cell, contributing to metabolic regulatory mechanisms and the immune response. Multiple studies, including our own, show a disproportionate accumulation of LDs in E4 expressing cells compared to E3 in a variety of cell types including fibroblasts, astrocytes, microglia, and hepatocytes [41, 84, 89, 90]. What is currently unknown is if there are compositional differences between E4 and E3 droplets. Here, we observed LD dynamics in the liver, as research implicates not only brain-derived ApoE4, but also peripheral ApoE4 in AD pathogenesis [110]. Our hypothesis that LDs play a key role in disease progression led us to capture differences between *APOE* genotypes and understand the LD contribution to ApoE4-related AD risk.

In the liver, we found ApoE4 expressing mice had an increased accumulation of LDs compared to ApoE3 mice. Both genotypes increased their LD amount in response to injection with inflammatory LPS, as expected and as observed in other research studies [54]. E4-LPS LDs were the most abundant and also the smallest in individual droplet size. The increased surface-to-volume ratio of smaller droplets may provide clues to their fate within the cell, as there is evidence of larger droplets experiencing lipolysis for fatty acid liberation to contribute to β -oxidation and smaller droplets experiencing lipophagy [106].

An unbiased lipidomics analysis of LD fractions indicated that, regardless of *APOE* genotype or treatment, LDs were primarily composed of TGs, an expected finding based on LD biology [48]. However, the other lipids within the droplet core and membrane were

markedly different between genotypes and conditions. E4-LDs showed an increase in PC distribution that mirrored the lipid profile of LPS-treated droplets. This finding could be indicative of the smaller droplet size and increased surface-to-volume ratio that would require increased phospholipids in the membrane. Specifically, PC incorporation in the LD monolayer has been shown to act as a surfactant to prevent LD coalescence [121]. It could be that an increased distribution of PC in the LD membrane is important to maintain a smaller droplet size, thereby driving its LD content away from energy contribution within the cell through β -oxidation. This hypothesis is additionally bolstered by pathway analysis results from differentially expressed proteins (Up in E3 = beta oxidation; Up in E4 = immune-functions) and WGCNA networks (a module enriched for beta oxidation proteins was differentially expressed between E3 and E4 at baseline). Further, our lab previously described smaller LDs in E4 astrocytes. These small-LD E4 cells had a decrease in glucose uptake and an increase in aerobic glycolysis compared to E3 astrocytes which had increased cellular respiration and fewer, but larger LDs [41].

Proteomic analysis from LD-enriched liver fractions quantified LD-associated proteins on E3 and E4 droplets. To corroborate the increase in droplets observed in oil red o staining, LD structural proteins Plin2 and Plin5 were differentially expressed between E4 and E3 droplets. The abundance of both Plin2 and Plin5 was increased in E4 fractions, suggesting an increase in LD amount in E4 mice. Plin2 and Plin5 were also increased in LPS-LD fractions indicating an increase in droplets with inflammatory stimulation. The increase of Plin2 from baseline to LPS-treatment was 3x more than the increase of Plin5 in the same conditions, suggesting Plin2 upregulation and incorporation on LDs is more associated with inflammation compared to Plin5 – an observation made by several others

in multiple cell types and models [54, 122]. The increase in Plin2 on the LD surface on E4 droplets and LPS-treated droplets could shield LDs from lipolysis by preventing lipase access to hydrolyze lipids for energy production [106]. In addition to the increase of Plin2 on E4 droplets, the E4-LD proteome contains a higher abundance of proteins involved in innate immunity while the E3-LD proteome consists of quantitatively more proteins involved in metabolism. Likewise, WGCNA indicates E4 involvement in immune function while E3 LDs contribute to metabolic-related pathways in the cell, namely beta oxidation of fatty acids.

Despite the current LD proteome originating from mouse liver tissue, we observed a striking overlap between multiple AD proteomes from whole brain tissues in humans. For example, an intriguing observation in our data is the significant overlap with an incipient AD proteomic signature of young E4-carriers published by Roberts et al [117]. In this study, tissue from two human AD studies were analyzed for proteomic differences between cognitively normal and AD brains. The significant differentially expressed proteins from both studies were compared to significant proteins between the brains of young E4-carriers and non-E4-carriers. The overlapping proteins (n=25) between these three studies revealed an interesting upregulation in young E4 carriers and a downregulation with AD pathology present. 15 of the 25 identified proteins are LD-proteins from our database and 9 of these are LD-resident proteins also found in other LD databases. Inflammatory transcription factor, Stat3, and sorting nexin, Snx4, are particular overlapping proteins of interest based on their contribution to inflammation and amyloid beta accumulation, respectively. Both were significantly increased in E4 LPS droplets, suggesting an E4-dependent increase upon inflammation. Further investigation of how

these proteins contribute to LD-related function and AD pathology is warranted, and identification of them on microglia LDs is detailed in Chapter 3.

Another noteworthy overlap in the LD-proteome is with data from Johnson et al [113] looking at control and AD human brain tissue in a large-scale proteomic study and their overlap with significantly increased microglial genes from an AD mouse model. Thirty proteins were identified, 27 of which are LD proteins. Of these proteins, four are DAM genes identified by Krasemann et al (SPP1, TSPO, FABP5, and LGALS3) [115]. They identify these 30 proteins as contributors to microglial activation in a primarily anti-inflammatory response. This particular study did not include *APOE* genotype in its analysis, however a previous study from the Seyfried laboratory in 2018 highlighted differentially expressed proteins from E4-expressing brain tissue [114]. Similar to our results, gene ontology pathways identify several immune and inflammatory-related functions in the proteins upregulated in E4-AD brains. The overlap between our LD proteins and those upregulated in E4-AD brains further reinforces the immune and reactive oxygen species-related pathways and the overlap between proteins upregulated in E3-LDs and E3-AD brains highlight beta-oxidation. Together, these findings validate the theme of E4 carriers having increased inflammation (often associated with a decrease in aerobic metabolism in exchange for increased glycolysis) and E3 carriers having increased oxidative phosphorylation, a metabolic phenotype also seen in E3 microglia in contrast to E4-related glycolysis [123].

Table 1 Top Ten Hub Proteins of Modules 1-12

1	2	3	4	5	6	7	8	9	10	11	12
Ppp1r12a	Uck2	Rps6ka3	Cisd2	Gstt1	Glyctk	Slc27a2	Eif4a1	Nop58	Rab5a	Aco2	Pdia3
Ubr7	Wdr26	Rnf213	Cds2	Scrn2	Dpys	Ugt2b5	Ppp4c	Rpl30	Rab21	Etfa	Hspa5
2700050L 05Rik	Isy1	Zbp1	Vdac1	Col4a3bp	Akr7a5	Ugt1a1	Eif2s3x	Abcf2	Rac1	Clybl	Hsp90b1
Cast	Pole3	Sbno1	Tmem19	Akr1c13	Eno1	Mpc2	Sec13	Hnmpk	Rab3d	Mdh2	Calr
Fam86	Hspa12a	Usp25	Letm1	Aldh8a1	Ptgr2	Hsd11b1	Eif2s2	Pcbp2	Rab9	Adhfe1	Hyou1
Tubb6	Mepce	Mkl1	Sec11a	Acat2	Idh1	Stt3b	Pdlim1	Ddx5	Rab5c	Acaa2	P4hb
Dlgap4	Ccnt1	Nfkb2	Sec22b	Cacybp	Acy1	Faah	Smek1	Srsf3	Rab33b	Acad10	Prdx4
Rbm27	Rbms1	Gbp3	5730469 M10Rik	Pgls	Naprt1	Spes2	Eif4e	Ddx6	Rab1	Ivd	Txndc5
Tnip1	Gca	0610007P 22Rik	Soat2	4931406C 07Rik	Aarsd1	Tmem109	Uba3	Ncbp1	Ubxn4	Aldh2	Uggt1
Map7d1	Tsr1	Q60710	Erlin2	Nit1	Gpd11	Phb2	Ube3a	Csde1	Glipr2	Gfm2	Mttp

1: Turquoise; 2: Blue; 3: Brown; 4: Yellow; 5: Green; 6: Red; 7: Black; 8: Pink; 9: Magenta; 10: Purple; 11: GreenYellow; 12: Tan

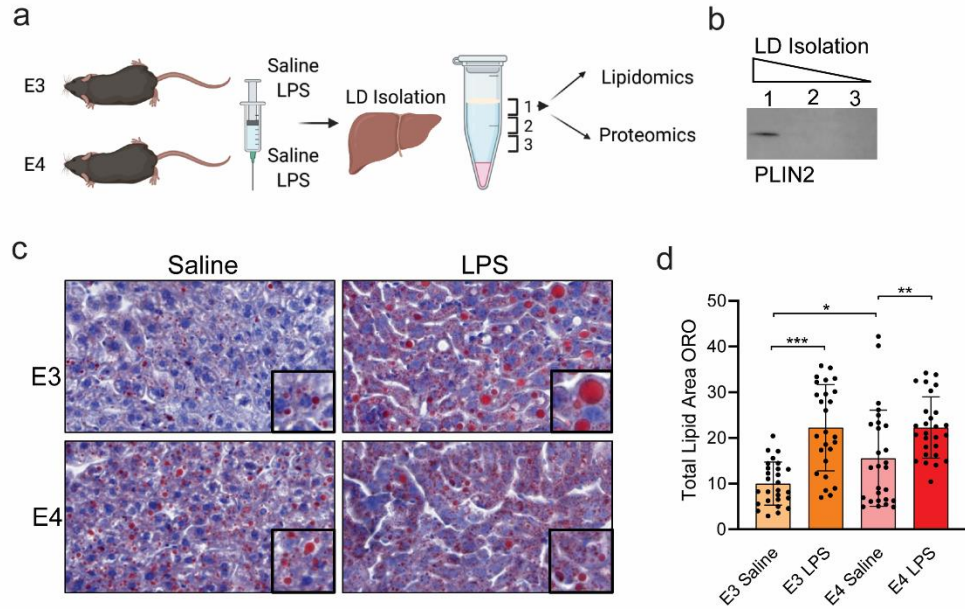


Figure 1: Lipid droplet isolation from mouse liver tissue successfully targeted the droplet fraction revealing increased droplets in E4 and inflamed liver tissue.

A) Targeted replacement mice expressing human ApoE3 or ApoE4 (n = 5/group) were either injected with saline or 5mg/kg of LPS. After 24 hours, liver tissue was homogenized for lipid droplet enrichment. B) Western blot of the top sequential liquid volumes after density gradient centrifugation showed LD marker, Plin2 in only the top fraction. This fraction was analyzed for proteomics and lipidomics. C) Oil Red O (ORO) staining of liver sections from the same mice to quantify lipid amount. D) Quantification of ORO staining represented as total lipid area.

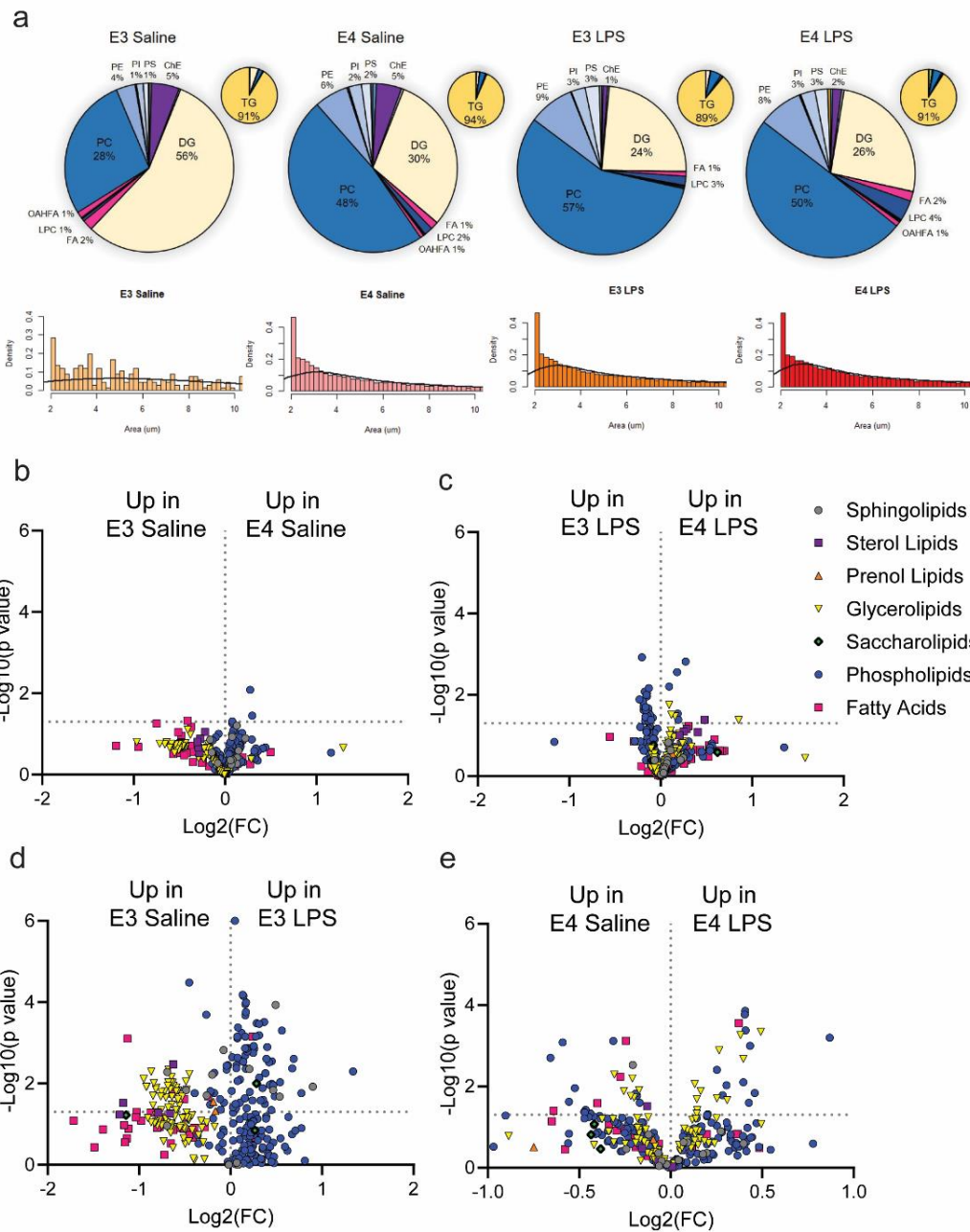


Figure 2: The lipidome of E4 droplets at baseline is similar to LPS-treated droplet lipidomes.

A) The small pie charts indicate the majority abundance of triacylglycerol in the droplet lipidome. The larger pie chart expands the remaining lipid species to observe lipid distributions between genotypes and treatments. Histograms below show the size distribution of LDs analyzed from ORO staining. LD size reflects the similar lipid distribution in the lipidomics analysis. B) Volcano plot of differentially abundant lipids by class between baseline conditions (Higher abundance in E4 saline on the right; Higher abundance in E3 saline on the left). C) Volcano plot of differentially abundant lipids by class between E3 LPS and E4 LPS treatments. D and E) Volcano plots of differentially

abundant lipids by class within the same genotype from baseline (saline injection) to LPS treatment. PC – Phosphatidylcholine; DG – Diacylglycerol; PI – Phosphatidylinositol; PE – Phosphatidylethanolamine; PS – Phosphatidylserine; ChE – Cholesterol; FA – Fatty Acid; LPC – Lysophosphatidylcholine; OAHFA – O-acyl-hydroxy Fatty Acids

Phosphatidylcholine Species

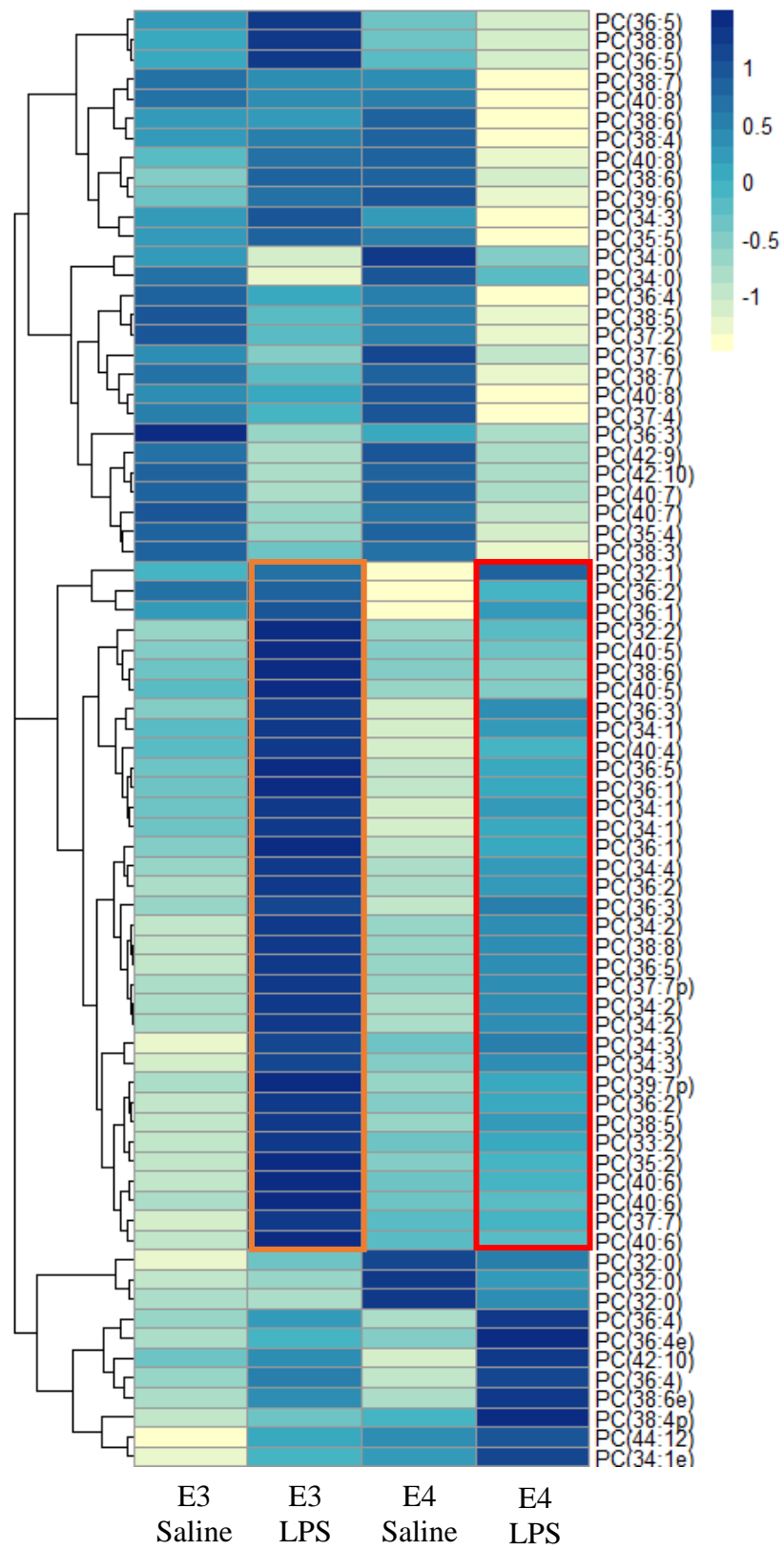


Figure 3: E4 LDs experience a blunted composition change after exposure to inflammation compared to E3 droplets.

E3 LPS LD membranes experience a change in phosphatidylcholine (PC) species after exposure to inflammation. The orange box indicates an area of significant change after LPS treatment in E3 droplets, but the same PCs (red box) have a blunted shift in expression after LPS treatment.

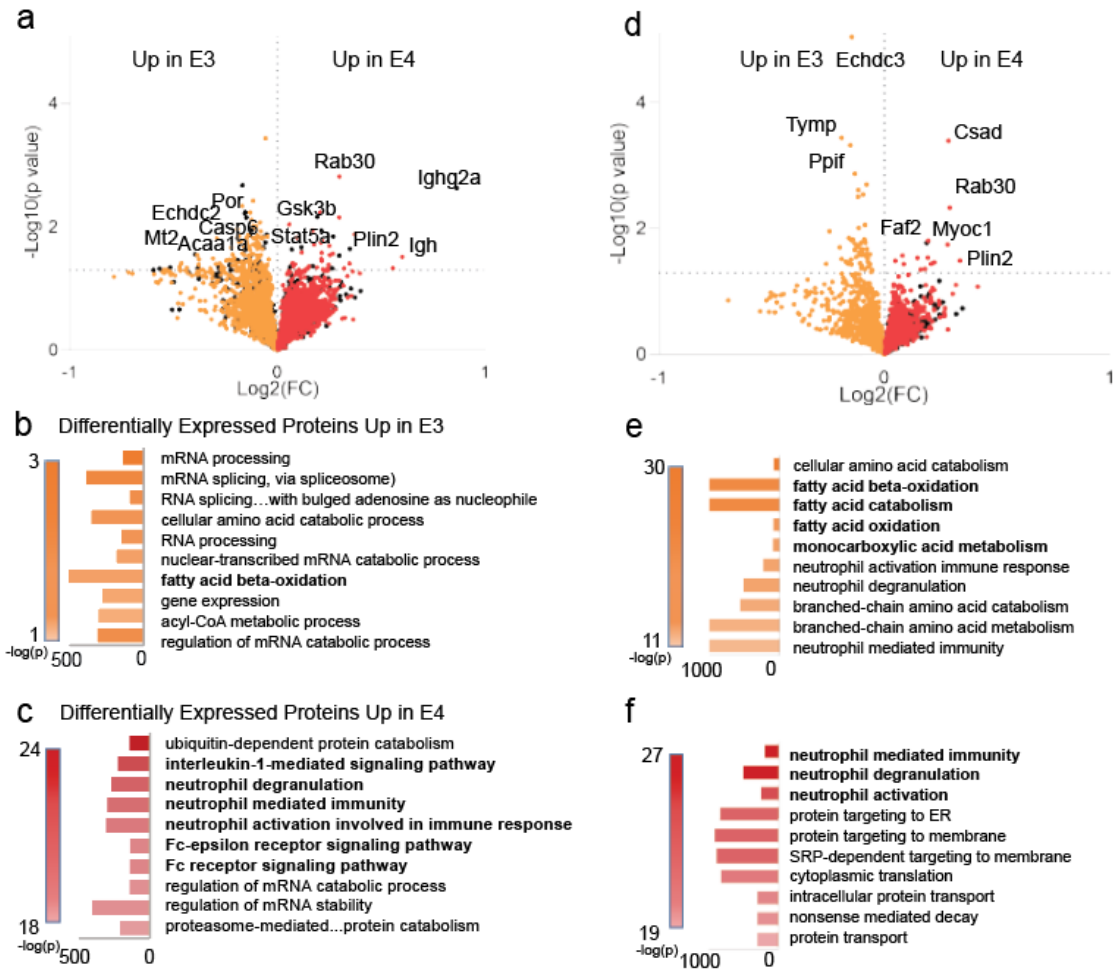


Figure 4: Differentially expressed proteins reveal enriched immune pathways on E4 LDs and metabolic pathways on E3 LDs.

A) Volcano plot of differentially expressed proteins from the entire quantified LD proteome are shown (n = 4,267). B) Gene ontology from differentially expressed proteins increased on E3 droplets compared to E4 at baseline highlight normal cell processes and fatty acid beta-oxidation. C) Gene ontology from differentially expressed proteins increased on E4 droplets compared to E3 at baseline feature several immune-related pathways. D) Volcano plot of differentially expressed proteins from overlapping proteins with established LD proteomes (n = 2,092). E) Gene ontology from the E3 overlapping, or 'resident' LD proteins maintains connection to lipid metabolism while F) gene ontology from E4 overlapping LD proteins implicates immune pathways.

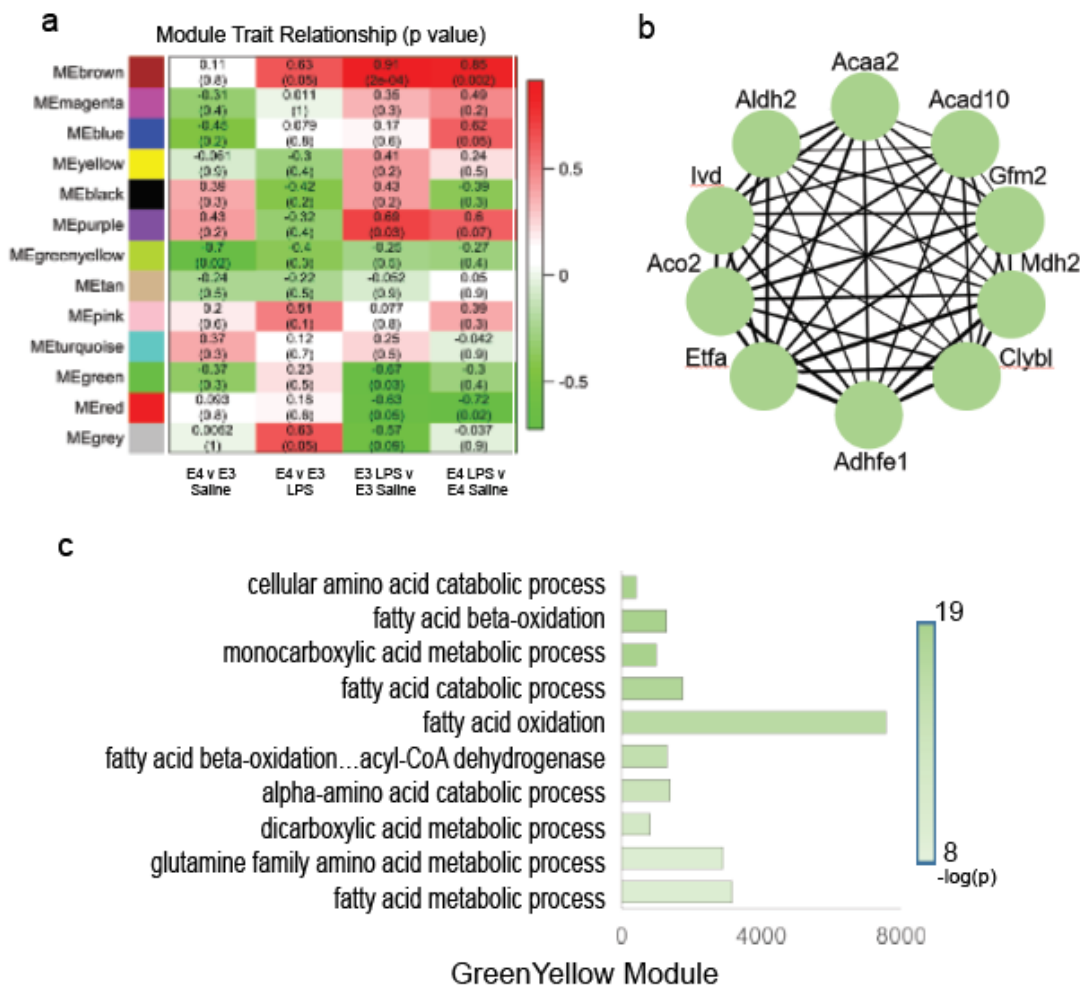


Figure 5: Weighted gene co-expression network analysis (WGCNA) shows module trait relationships and p values between genotype and treatment comparisons.

A) Network relationships and significance show large changes in modules upon stimulation in E3 LDs that is less robust in E4 droplets. B) A significantly different module (GreenYellow #11) that is increased on E3 droplets. C) Gene ontology from the GreenYellow module highlights metabolic pathways involved in fatty acid catabolism and fatty acid oxidation.

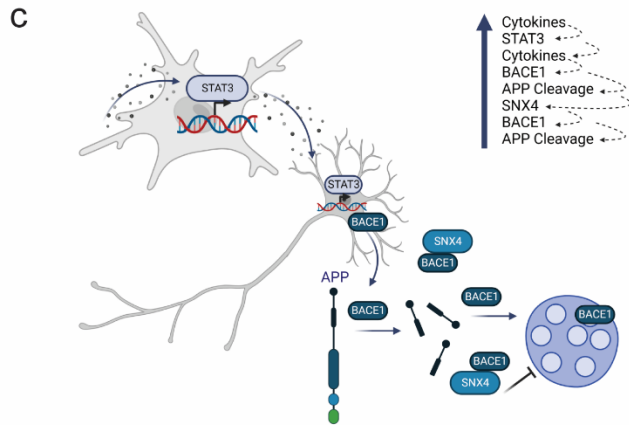
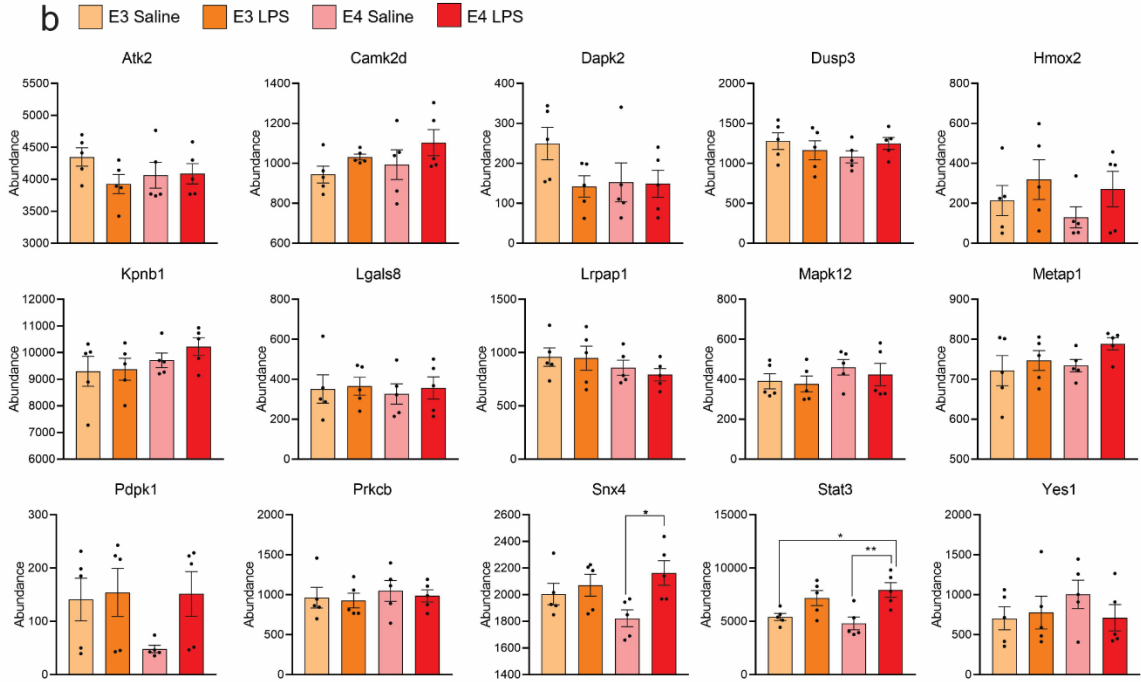


Figure 6: Incipient AD protein signature has significant overlap with LD proteins.

A) A paper looking at young E4-carrier brain proteomes and two independent cohorts (ROS and BLSA) of proteomics analyses on AD brains found a unique signature where proteins are increased in young E4-carriers compared to non-carriers, but decreased in AD brains compared to cognitively normal brains. The incipient AD signature was compared to our proteome and 60% overlap was observed. B) Individual protein abundances between genotype and treatment of overlapping incipient AD proteins are shown in bar graphs with significance displayed as result of a two-way ANOVA. C) A proposed pathway of Stat3 and Snx4 involvement in amyloid accumulation and AD.

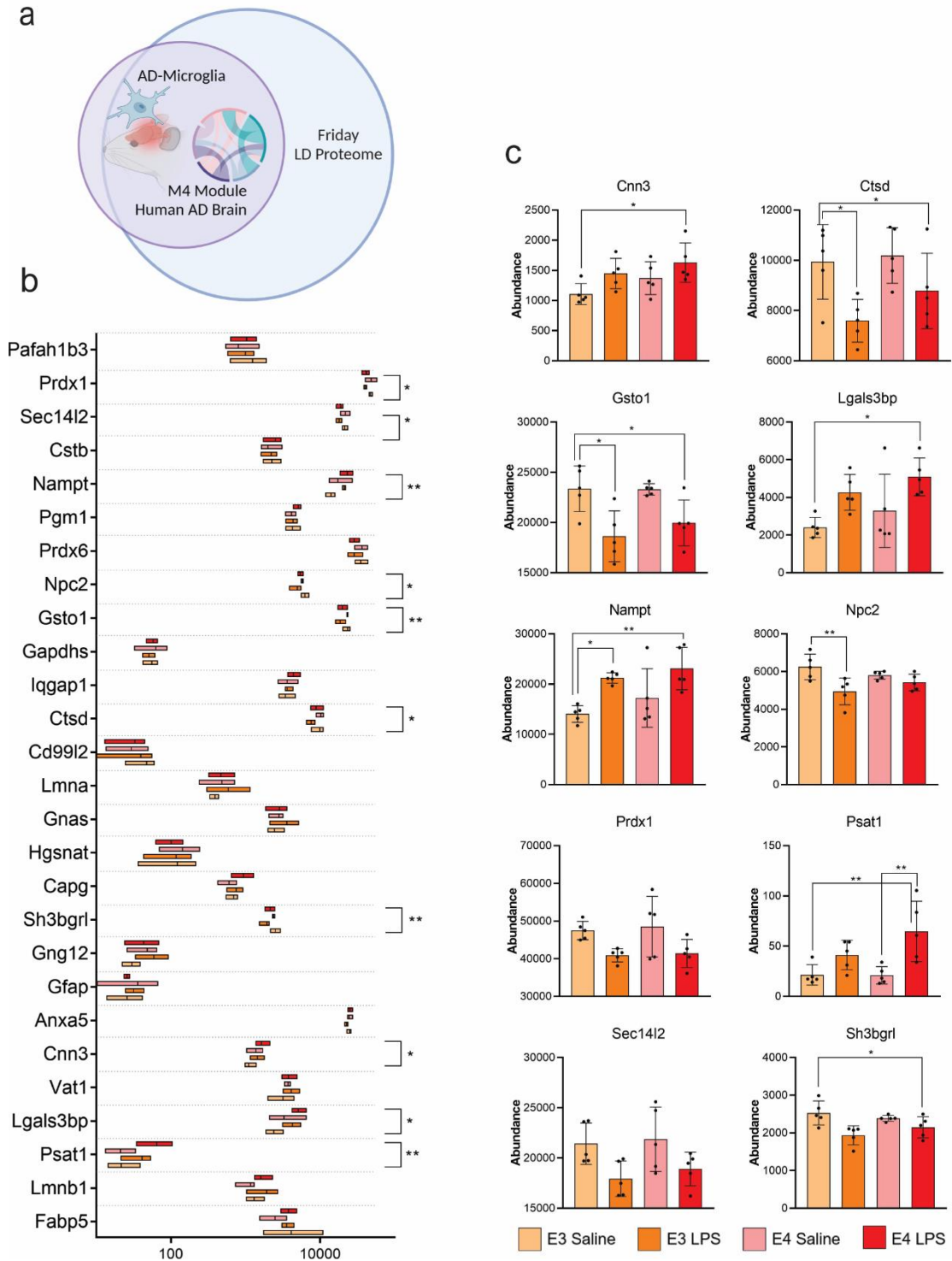


Figure 7: Human AD brain proteomes have overlap with LD proteins highlighting microglial activation and metabolism.

A) A large proteomic study of AD brains revealed a glial metabolism module, M4, which was different in AD brains. Interestingly, the top differentially expressed transcripts of microglia from a mouse-AD model overlapped with M4. This AD-glia-metabolism

signature has 90% overlap with our LD proteome. B) Box and whisker plots of the 27 overlapping proteins show several differences from two-way ANOVA analyses. C) Significant proteins are highlighted in individual bar charts.

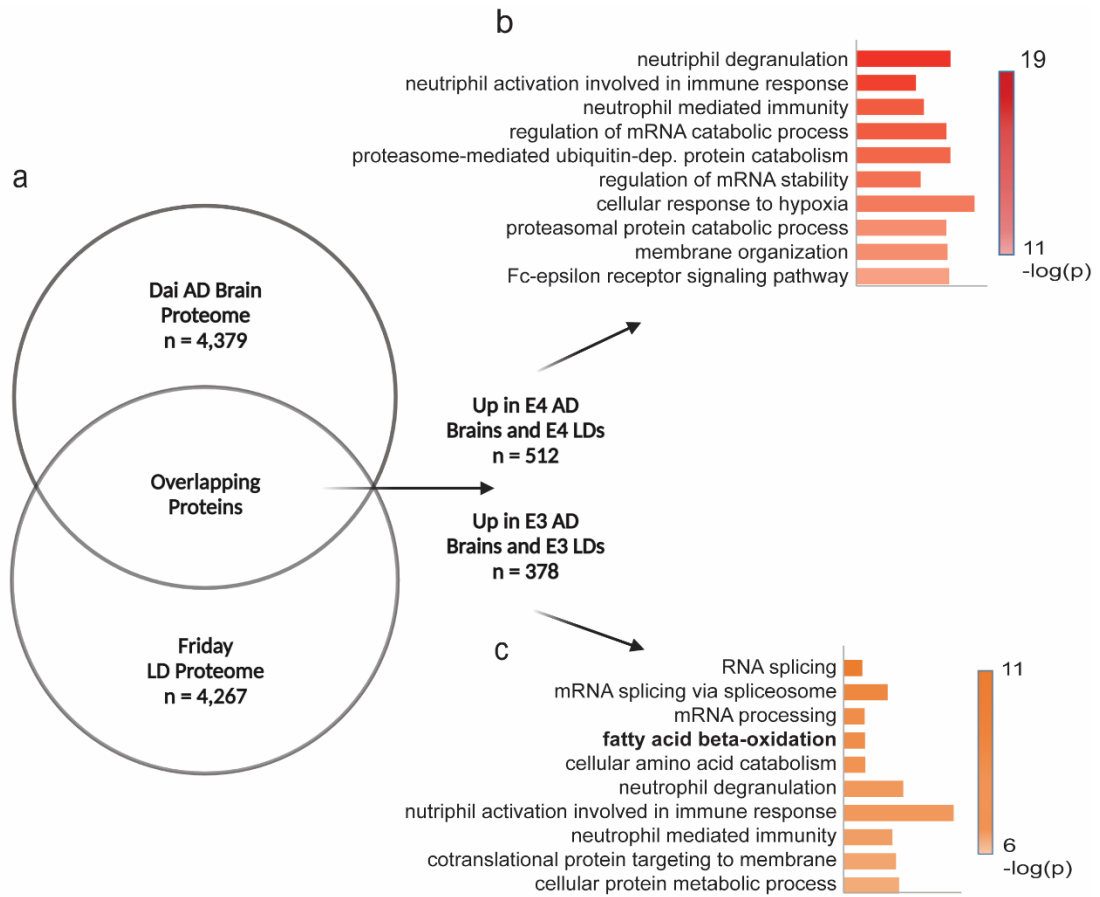


Figure 8: AD brain proteome shows similar trends as LD proteome with respect to E3 and E4 pathways.

A) Dai et al in 2018 performed quantitative proteomics on human AD brains and compared APOE genotypes. Differentially expressed proteins up in E3 v up in E4 were compared with the LD proteome to identify overlapping proteins (378 and 512, respectively). B) Gene ontology implicates immune pathways in the E4 overlap between LDs and AD brains. C) Gene ontology highlights fatty acid beta-oxidation and metabolism in the E3 overlap between LDs and AD brains.

CHAPTER 3. LIPID DROPLETS IN MICROGLIA ARE MODULATED BY *APOE* GENOTYPE

3.1 Introduction

Genome-wide association studies (GWAS) pinpoint several AD risk genes involved in the immune response and microglia function [124], particularly genes involved in microglial phagocytosis and debris processing. Deficits in these key functions could be due to an impaired ability of microglia to recognize lipids – a hypothesis to explain the decreased uptake of poorly lipidated ApoE4 and decreased lipid uptake in TREM2 mutants [125]. The strongest effect size across the AD-risk genes is attributed to the $\epsilon 4/\epsilon 4$ (E4) allele of Apolipoprotein E (*APOE*), a gene also implicated in microglial function. *APOE* is a disease-associated-microglia (DAM) gene [126] and diseased or stressed microglia upregulate production of ApoE. Similarly, a microglial phenotype known as neurodegenerative microglia (MGnD) has a distinct genetic signature also driven by increased ApoE secretion. Unlike the DAM phenotype, which is reversible in nature, the MGnD phenotype is thought to reflect a perpetual cycle of inflammation and neurodegeneration centered on abnormal microglial function [115]. Recently, a group of researchers made a microglia-specific ApoE knockout mouse and found no significant transcriptional changes to DAM genes, suggesting ApoE may not be a central driver to this phenotype. However, total ApoE protein levels maintained similar to controls when the microglia ApoE knockout model was crossed with the 5XFAD mouse model of AD, suggesting astrocytes still secreted enough ApoE, having a nonautonomous effect on microglia and the DAM signature[127].

Another recently described microglia-specific phenotype is termed lipid droplet accumulating microglia (LDAM). These lipid-laden microglia show similar functional

deficits to the MGnD and DAM microglia with increased cytokine release, increased reactive oxygen species, but differ by decreased phagocytosis. This phenotype seems to be mediated by age, as treatment with young plasma reduces LD accumulation in BV2 cells [62]. An important thing to note is that the three aforementioned studies (DAM, MGnD, and LDAM) were all performed in mice expressing murine ApoE protein and not in targeted replacement mice expressing human ApoE. Our lab has recently found aged E4 expressing microglia from mice to have ~60% overlap with MGnD genes with single cell RNA sequencing [123]. It is thought that E4 expression exacerbates each of these abnormal microglial phenotypes.

Intriguingly, ApoE is a droplet-associated protein found on the LD surface [55], and E4 expressing astrocytes [41] and E4 microglia [88-90] both accumulate more lipid droplets than neutral AD-risk $\epsilon 3/\epsilon 3$ (E3) expressing cells. Additionally, carriage of the E4 allele is associated with increased neuroinflammation [128] and metabolic disturbances within neurons and glial cells, two things potentially altered by LD accumulation and composition [85]. It is of particular interest that glial cells accumulate LDs in response to neuronal stress, age, or neurodegeneration [62, 129, 130]. LD accumulation has been thought of as both a beneficial compensatory response and a pathological feature within the brain. For example, there is compelling evidence of a synergistic relationship between neurons and astrocytes whereby fatty acids are shuttled from neurons to sequester in astrocytic LDs to protect neurons against fatty acid toxicity [130]. However, a more pathologic accumulation of LDs associated with age in microglia, causes abnormal cellular function [62]. LD accumulation with age is highly relevant in Alzheimer's disease (AD),

where even the first description of AD by Alois Alzheimer noted glia with adipose inclusions [47] and it is typically considered a disease of aging.

Though the LD lipidomics and proteomics data presented in Chapter 2 were derived from liver tissue, there are several connections and overlap to the brain which support translation of these findings to LD dynamics in microglia. LD accumulation in cells results in functional changes, with E4 cells showing increased abnormal and altered function compared to E3. Primary microglia expressing humanized ApoE4 exhibit changes in morphology and increased cytokine production associated with LD accumulation compared to E3 microglia [89]. Additionally, iPSC-microglia expressing ApoE4 also accumulate more LDs and have disrupted communication with neurons in co-cultures compared to E3 iPSCs. Communication deficits are ameliorated with LD inhibition [90]. Marshallinger et al observed increases in pro-inflammatory cytokines, ROS, and abnormal function in LDAMs, but when LDs were inhibited with Triacsin C, the authors noted normalization in ROS, but did not comment on the restoration of cytokine output after LD inhibition [62]. Though these results are promising, the restoration of homeostatic function through LD inhibition has not been studied in the context of *APOE* genotype, nor in the context of cytokine release.

In summary, this Chapter seeks to understand the impact of LDs on *APOE* genotype in microglia and their resulting impact on the function of the cells. We looked at droplet accumulation following exposure to a variety of CNS-relevant substrates, cytokine release as a measure of microglia function, and droplet inhibition. Our hypothesis was that E4 microglia will accumulate more LDs with an increased release of inflammatory cytokines, and inhibition of LD formation will reduce the cytokine response. Our findings show that

E4 microglia do in fact accumulate more LDs under all conditions, and that they secrete higher concentrations of several pro-inflammatory cytokines. However, droplet inhibition did not reduce cytokine output regardless of which synthesis pathway was inhibited. Exciting findings were the confirmation of key LD proteins from the liver proteome on microglial LDs via immunohistochemistry, increasing the translation of liver LD findings to the brain. Additionally, human brain samples indicated increased droplet accumulation (Plin5 as a marker) in E4 carriers with dementia compared to non-E4 carriers of the same cognitive and Braak stage.

3.2 Methods

3.2.1 Cell Culture

Human *APOE* expressing mice were bred and pups were taken at postnatal day P1-3 to obtain primary microglia for experiments. Littermates were pooled together to increase cell counts, but pups from the same litter were not genotyped for sex chromosomes. During dissection, forebrains were removed from mice and placed in a dissection buffer consisting of ice-cold Hanks Balanced Salt Solution (HBSS #). Under the dissection scope, meninges were carefully removed and the brain was placed in DMEM F12 media (10% FBS and 1% pen/strep). Pooled brains were cut into small pieces and digested with trypsin at 37C for 25 minutes, agitating every five minutes. Trypsin was neutralized with an equal volume of DMEM media and brains were centrifuged for 5 minutes at 400xg prior to washing with HBSS. Brain homogenate was resuspended in DMEM, triturated, and passed through a 70 micron filter. Mixed glial cells from this preparation were split into T75 flasks (1 flask per brain). Dead cells and debris were washed after day 1 in culture and media was switched

to a supplemented (containing conditioned media from fibroblast culture) DMEM: F12 media on day 7. After two weeks, microglia begin to emerge from the other glial cells. Flasks were placed on an orbital shaker for two hours to detach emerging microglia and media was collected and centrifuged to pellet the cells. Microglia were resuspended in DMEM, counted, and plated for various experiments.

3.2.2 Lipid Droplet Imaging

Cell treatments: For lipid droplet imaging experiments, cells were seeded at 60,000 cells per well on a poly-L-lysine coated 12mm glass coverslip. Cells were treated with 250uM oleic acid (OA) conjugated with BSA, 10ng lipopolysaccharide (LPS), necroptotic Neuro-2A cells (nN2A), N2A plus LPS, OA plus LPS, or an untreated control. After 24 hours, media was collected for cytokine analysis and cells were fixed in 4% paraformaldehyde. Cells were stained with BODIPY and coverslips were mounted with a DAPI nuclear staining mounting media. N2A cells were cultured and split into over thirty T-75 flasks with non-filter cap lids. Once cells grew to confluence, the caps were tightened to induce hypoxia and cell death. Cells began to detach from the flasks and all apoptotic cells and media were collected, split into 8×10^6 cells/mL aliquots and frozen for later use. Microglia were treated at a 1:10 ratio of microglia to nN2A cells during experiments.

Immunohistochemistry (IHC): Primary microglia were plated on poly-L-lysine coated glass coverslips and treated with 250uM OA for 24 hours. After PFA fixation, cells were permeabilized with 100% ice cold methanol for ten minutes at -20°C . Cells were then rinsed with 1X PBS for five minutes before blocking for 60 minutes. Primary antibody for Snx4 was added at 1:1000 and cells were incubated overnight at 4°C . Cells were washed

with 1X PBS three times for five minutes and incubated with secondary antibody for 2 hours at room temperature while covered from light exposure. Cells were rinsed again in PBS, stained with BODIPY, and mounted using DAPI nuclear stain.

Imaging took place on a Nikon A1R confocal microscope. 405nm wavelength was used to acquire microglial nuclei stained with DAPI and 488nm wavelength was used to acquire neutral lipid stained with BODIPY. 560nm wavelength was used to acquire signal for Snx4 and ApoE. Color threshold analysis was used to select high intensity regions of neutral lipid, indicating the presence of lipid droplets.

3.2.3 Cytokine Analysis

Primary microglia from E3 and E4 targeted replacement mice were plated in 96-well plates and allowed to adhere. For a 24-hour treatment, cells were treated with either a DMSO control, DGAT inhibitor (10 μ M A9250000; Millipore Sigma 252801), ACAT inhibitor (10 μ M Avisimibe; Tocris 6505/5), or both inhibitors. Six conditions were tested: control, 250 μ M OA, 10ng LPS, 1:10 ratio of nN2A cells, OA + LPS, and nN2A + LPS. Cytokines were measured using a custom V-plex assay from MesoScale Discoveries with probes for IL-1 β , IFN γ , TNF α , IL-10, and IL-6.

3.2.4 Western Blots

Human brain samples were generously bequeathed by patients and family members of patients to the University of Kentucky Brain Bank. We have 32 pieces of frozen frontal cortex from E2, E3, and E4 carriers with both no cognitive impairment and with diagnosed AD. Brains were homogenized, proteins were precipitated, and diluted in RIPA buffer with

proteinase inhibitors. BCA assays were done to determine protein concentrations of each sample to allow for normalized loading into the gel for Western blot. The sample was diluted with 10 μ l MilliQ water and 2x Laemmli Sample Buffer (Bio-Rad Laboratories, Hercules, CA, USA). The samples were heated at 96.5° Celsius for 10 minutes, after which they were chilled on ice for 5 minutes before loading into the gel. 20 μ l of the protein sample was loaded on 4-20% Criterion TGX Gels (Bio-Rad Laboratories, Hercules, CA, USA) and ran at 180V. Gels were transferred onto 0.2 μ m nitrocellulose membrane (Bio-Rad Laboratories, Hercules, CA, USA) using the Trans-Blot Turbo Transfer System (Bio-Rad Laboratories, Hercules, CA, USA). After transfer, membranes were blocked for 30 minutes in 1% casein solution while gently rocking back and forth. The membranes were incubated overnight at 4°C in 1:1000 Plin-2 primary antibody solution or 1:1000 Plin-5 primary antibody solution (Novus Biologicals, Centennial, CO, USA). After incubation, the membranes were washed with PBS-T (0.05% Tween-20), three times for five minutes each wash. The membranes were then incubated for one hour at room temperature, while protected from light, in 1:5000 Goat α -rabbit IR 700 secondary antibody solution. (Bio-Rad Laboratories, Hercules, CA, USA). They were then washed with PBS-T, three times for five minutes each, and then with PBS two times for five minutes each. Membranes were imaged using a ChemiDoc XRS Imaging System (Bio-Rad Laboratories, Hercules, CA, USA).

3.3 Results

3.3.1 E4 expressing microglia accumulate more LDs at baseline, with exogenous lipid sources, and with pro-inflammatory stimuli.

We examined LDs in E3 and E4 primary microglia to understand more about their formation, accumulation, and similarities with liver LDs. To determine the difference in LD accumulation between E3 and E4 microglia, we compared non-treated microglia to those supplemented with exogenous lipid, a pro-inflammatory stimulus (LPS), necroptotic N2A cells (nN2A), or a combination of these treatments (Figure 9a). In almost all conditions, E4 microglia showed an increase in LD accumulation (Figure 9b). E4 microglia accumulated more LDs than E3 with no treatment ($p = 0.016$), nN2A treatment ($p = 0.019$), oleic acid ($p = 0.003$), and LPS ($p = 0.028$). Other treatments had an increase in LD accumulation in E4 that was not significant: nN2a + LPS ($p = 0.337$), and oleic acid + LPS ($p = 0.079$). Analysis of individual LD area from randomly selected cells show a decrease in E4 droplet size, despite the overall increased area, similar to results seen in the liver (Figure 9c).

3.3.2 DGAT1 and ACAT1 inhibitors attenuate LD accumulation in primary microglia.

As previously described, LD inhibition improved some functional deficits in microglia like reduced phagocytosis in LDAM cells or neuronal communications in iPSCs. We hypothesized LDs may modulate cytokine release and inhibition could improve pro-inflammatory cytokine profiles. Primary microglia were treated with DMSO as a vehicle or with 10 μ M DGAT1 inhibitor (A922500) or 10 μ M ACAT1 inhibitor (Avisimibe) in DMSO. DGAT1 and ACAT1 inhibitors substantially decreased LD accumulation in both E3 and E4 primary microglia in all treatment groups and control (Figures 10 and 11,

respectively). DGAT1 and ACAT1 both decreased LD amount overall, but had different results depending on the substrate used to induce LD accumulation. The ACAT1 inhibitor reduced LDs in all conditions except those treated with OA (Figure 10a-c), while the DGAT1 inhibitor reduced LD accumulation almost completely in all conditions except nN2A treated conditions (Figure 11a-c).

3.3.3 E4 microglia secrete more TNF, IL-1 β , and IL-10.

LDs are dynamic in that their contents can be stored for cellular protection from fatty acid toxicity, used for energy production, or liberated to become lipid mediators of inflammation [64]. In aging and Alzheimer's disease, lipid droplets accumulate in microglia and cytokine production increases [62]. We sought to determine if E4 expressing microglia from non-aged and non-diseased backgrounds had a similar increase in pro-inflammatory cytokine release at baseline due to their specific expression of ApoE4. E4 microglia secreted more TNF, IL-1 β , and IL-10 than E3 at baseline and when given OA and nN2A (Figure 12a-c). Interestingly, conditions that stimulate primary microglia with LPS show a more robust cytokine secretion overall from the E3-expressing cells (Figure 12d-f). Notably, inhibition of LDs with DGATi, ACATi, or both inhibitors together did not decrease cytokine output in any condition, suggesting either an inflammatory effect of the inhibitor compounds on the cells or that the lack of ability to sequester lipids within a droplet increased cytokine output. All measured cytokines and conditions are compared in Figure 13 as a percent of E3 control of each cytokine measured.

3.3.4 Immunohistochemistry (IHC) identified proteins of interest from liver LD analyses in primary microglia and on the droplet surface in primary microglia cells.

Proteins from the incipient AD signature that showed significant results in the liver LD proteome were Sxn4 and Stat3. These proteins are of particular interest due to their contribution to AD and inflammation. We performed IHC in primary microglial cells to check for localization of these particular proteins to the LD surface. Other proteins of interest to confirm localization to LDs in microglia were ApoE and cPla2. Figure 14a shows the protein abundance of ApoE from the liver LDs between genotypes and conditions and localizes ApoE on the LD surface in primary microglia. Sxn4 localized to the droplet (Figure 14b), but Stat3 did not, though it is present in the cells as observed by IHC (Figure 14c) and implicated in at least one other LD proteome [46]. Finally, Pla2g4a, more commonly known as cPla2, had a trend toward increased abundance in E4 droplets and was found to be localized to the LD surface in primary microglia (Figure 14d).

3.3.5 Human brain tissue shows increase in Plin5 associated with dementia status in E4 carriers.

Frozen frontal cortex samples from 32 generous donors were homogenized and prepared for protein quantification. Western blot showed an increase in Plin5 with dementia status, but only in the E4 genotype, suggesting non-E4 carriers do not have as much accumulation of Plin5-LDs regardless of cognitive status (Figure 15a-b). There were no significant associations between Plin5 and Braak score or the Mini Mental State Examination (MMSE) score. Plin2 measurements showed a much more variable protein expression that was not correlated to Braak score, MMSE score, genotype, or cognitive status (Figure 15c-d).

3.4 Discussion

A characterization of LDs and their cellular contribution in an *APOE* genotype-dependent way has not been previously described. Here we show primary microglia from targeted replacement mice expressing human ApoE4 accumulate more LDs with multiple sources of exogenous lipid and stimulation compared to ApoE3 expressing cells. Additionally, droplet inhibition from two LD synthesis pathways, the incorporation of cholesterol and the incorporation of triglyceride, did not ameliorate the increased cytokine release observed in E4 microglia. Finally, immunohistochemistry showed droplet proteins of interest from the liver LD proteome to localize to LDs in microglia.

Over the course of our experiments examining LD accumulation in microglia (Chapter 3), two highly relevant papers were published using similar strategies to understand LD accumulation in the context of ApoE in microglia. First, Machlovi et al identified a distinct morphology of E4 primary microglia from the same targeted replacement mice we use in our experiments. Imaging showed a more ramified morphology that is typically indicative of homeostasis in E3 microglia, and a more amoeboid appearance of E4 cells, which is usually associated with activation. They also quantified increased cytokines from E4 microglia and a non-specific increase in phagocytosis. E4 microglia had increased phagocytic uptake of beads, myelin fragments, and apoptotic cells compared to E3 microglia. This led to an additional increase in droplet accumulation within the cells as measured by BODIPY staining and Plin3 IHC [89]. This increase of phagocytosis in cells with more LDs is in contrast to the impairment in phagocytosis observed in LDAM after exposure to myelin debris and BV2 cells treated with aged plasma and LPS [62]. Both of these conditions had reduced phagocytosis in cells with high LDs,

suggesting phagocytic impairments are formed *after* LD accumulation occurs. Droplet inhibition with Triacsin C in BV2 cells treated with LPS increased phagocytosis, suggesting LD inhibition can rescue phagocytic impairments. While together these papers infer an increased phagocytic function in E4 cells, there may be a threshold where LD accumulation within E4 cells decreases their phagocytic capacity. Perhaps the balance between LD synthesis and turnover in E4 cells is compromised, thus in turn affecting phagocytosis.

The second paper recently published was from Victor et al and used microglia-like iPSCs to assess ApoE effects on neuronal communication pathways, a relationship described in astrocytes showing deficits in E4 cells. Researchers first validated their model of microglia-like iPSCs and showed they have the capacity to communicate with neurons through soluble cues. Following previous work showing decreased oxidative phosphorylation transcripts in E4 cells from a monoculture, they showed the same in E4 iPSCs cultured with brain spheroids. Transcriptional analysis also showed a pro-inflammatory profile in E4 cells. From there they noted isogenic iPSCs expressing E4 had less fatty acid uptake from neuronal conditioned media, but more fatty acid accumulation in the form of LDs. They concluded E4 cells had deficits in the uptake, breakdown, and *de novo* synthesis of fatty acids. Using Triacsin C, an inhibitor of ACSL1, they induced a more homeostatic phenotype in E4 cells with less LDs, restored signaling, and reduced cholesterol in the media [90].

In addition to increased droplet accumulation in E4 microglia, we aimed to look at droplet markers in frozen human frontal cortex tissue from donors in the University of Kentucky Alzheimer's Disease Center (kindly provided by Dr. Peter Nelson). We received

32 samples spanning different *APOE* genotypes and various cognitive states. It is noteworthy that of the 8 E4/E4 brain samples, all were diagnosed dementia patients with severe pathology noted by their Braak score. There were no E4 homozygotes without AD, as is the case with most human study cohorts – an inherent limitation in the field due to the inability to study cognitively and pathologically normal E4/E4 brain tissue as a study control. Western blot analysis of the brain tissue showed an increase in Plin5 in E4 carriers with dementia. E3/E4 carriers that were cognitively normal had lower Plin5 levels, as did non-E4 carriers with dementia, suggesting LD accumulation specific to dementia in E4 carriers. Plin2 blots yielded confusing results and variable intensities. There were no patterns of Plin2 expression based on genotype, age, gender, Braak score, MMSE, or dementia, despite equal protein loading based on BCA protein quantification results and normalization to Ponceau S staining for total protein. While troubleshooting these results, a paper was published highlighting the expression patterns of perilipins in the brain. This paper showed highly variable Plin2 expression in gray vs. white matter with Plin2 expression higher in gray matter. However, Plin5 expression seemed ubiquitous throughout the brain. The frozen frontal cortex samples we received and did experiments on were mixtures of gray and white matter and nearly impossible to distinguish between, therefore this could explain the variance in Plin2 expression across samples [131].

It was our original hypothesis that LD proteins in E4 expressing cells drive cytokine release, contributing to the inflamed phenotype of E4 cells. However, LD inhibition through ACAT and DGAT inhibitors did not reduce cytokine output. There could be two possible explanations of this result. First, though the control conditions were also treated with DMSO as a vehicle-control, the actual inhibitors (A925000 and Avisimibe) could be

inflaming the cells and causing increased cytokine release as evidenced by an increase in cytokine output (TNF) in control primary microglia given inhibitors. Second, with no ability to form LDs to sequester fatty acids, the cells are vulnerable to fatty acid toxicity which could cause an increase in cytokine release. These results highlight the importance of LDs for homeostatic cell function and protection and remind us that inhibition of their developmental pathway is not inconsequential.

Additionally, we observed an increase in cytokine output from E4 cells in non-LPS treated conditions. However, when stimulated with LPS, E3 microglia had a more robust cytokine response. It is widely viewed in the literature that E4-individuals (both mouse and human) have an exaggerated response to inflammation [132-134], but all studies were done in multi-cell systems. A study looking at primary astrocytes from E3 and E4 targeted replacement mice also noted a reduced cytokine response in E4 cells after LPS stimulation [135]. A current limitation to our study is that we used a mixed-sex primary microglia culture. A recent paper by Jofre-Monseny et al noted significant sex-based cytokine secretion differences in primary microglia cultures from E3 and E4 targeted replacement mice, with E4 females exhibiting the most robust cytokine secretion in response to LPS [136]. It is important to understand the impact of *APOE* variants on sex and the interaction of multiple cell types to facilitate a coordinated immune response.

Taken together, our findings of increased inflammatory-related proteins on E4 LDs, a lack of robust response of E4 LDs to inflammation, and significant overlap with proteins implicated in AD, we believe LDs are modulated *APOE* genotype. Future studies may need to focus on shifting the protein profile of droplets toward a more neutral state (much like the E3 LD profile), rather than inhibiting LD synthesis, in an effort to reprogram the cell's

metabolic state to a more favorable aerobic production of energy through oxidative phosphorylation.

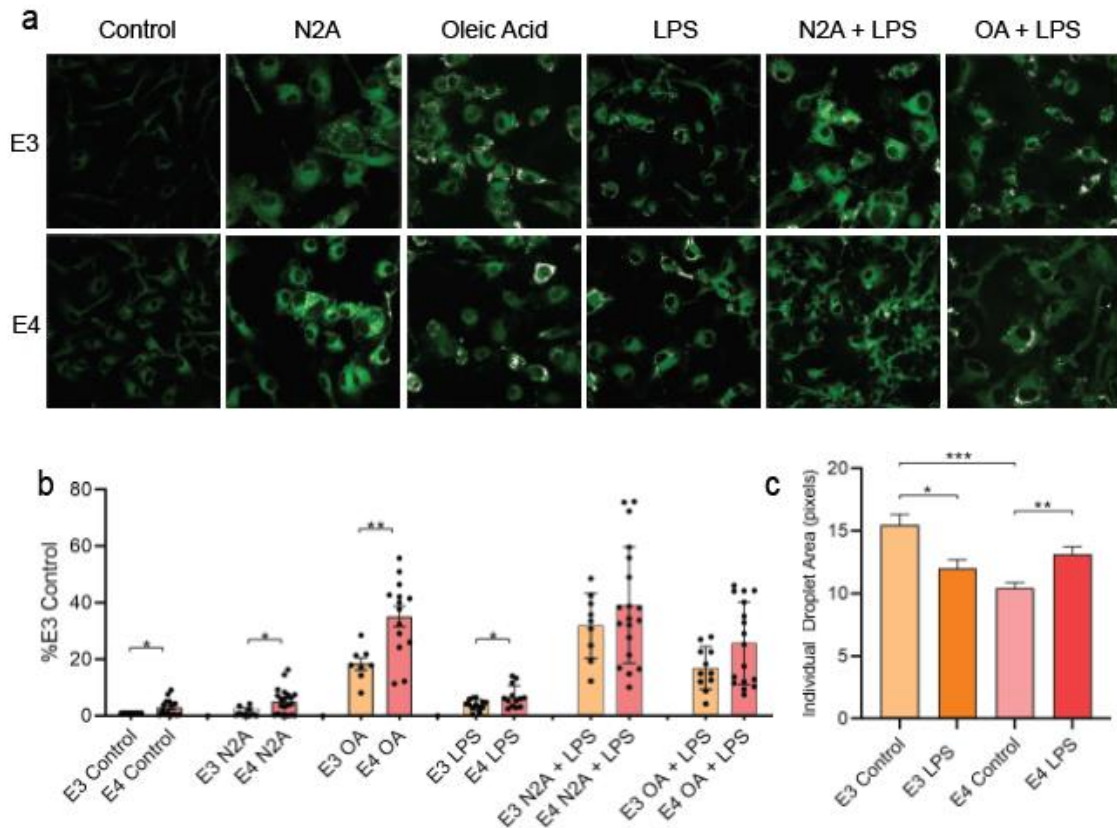


Figure 9: Primary mouse microglia expressing human E4 accumulate more LDs than E3.

A) Primary microglia from E3 and E4 post-natal P0-3 pups were plated and treated with exogenous lipid, an inflammatory stimulus, or a combination to induce LD development. E4 microglia accumulated significantly more LD than E3 in control, OA, nN2A, and LPS-treated conditions. B) Data is presented as % of E3 control due to multiple repetitions of the experiment on differing microscope platforms. However, in each experiment, the results maintained E4 yielding more LDs than E3. C) Individual measurements of LDs in control and LPS-treated microglia indicate smaller droplet formation in E4 control cells and LPS-treated cells ($p < 0.0001$ E3 to E4 control; $p < 0.001$ E4 control to LPS; $p < 0.01$ E3 control to LPS).

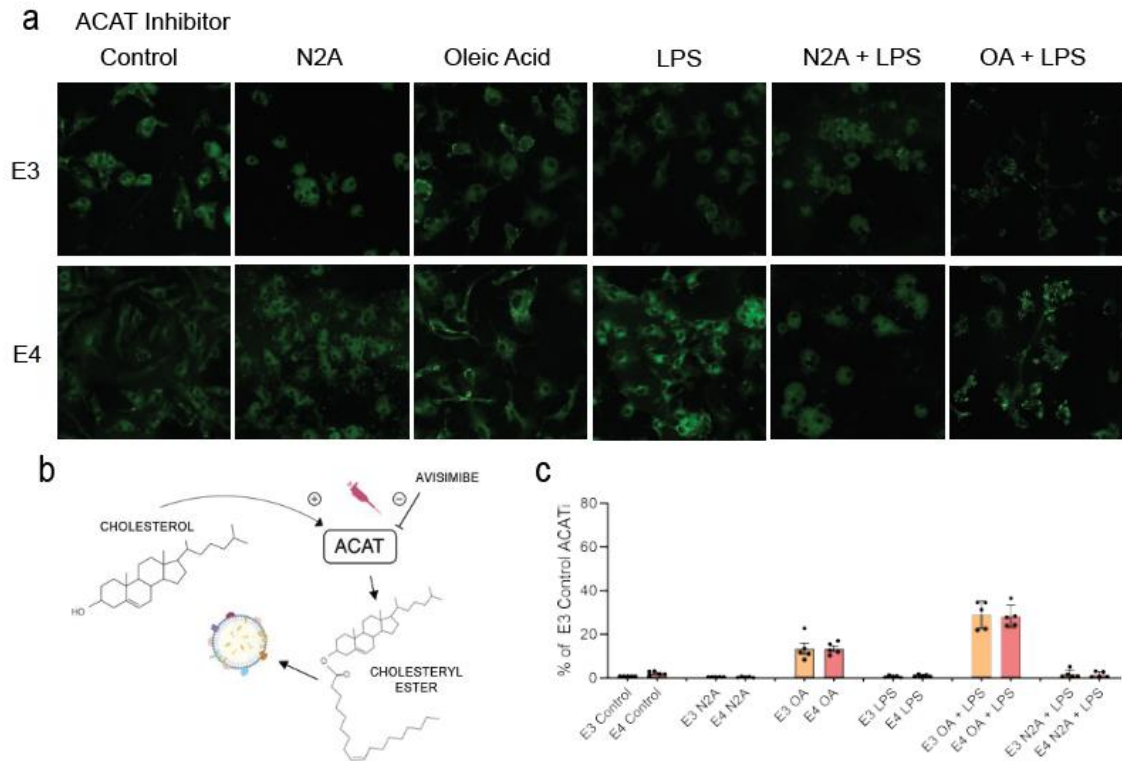


Figure 10: ACAT inhibitor reduced LD accumulation in all but OA-treated conditions.

A) Images of primary microglia stained with BODIPY for neutral lipids show relatively low droplet accumulation in all conditions except OA. B) Cholesterol is esterified by ACAT and incorporated into the LD. Avisimibe inhibits ACAT activity and reduces droplets. C) Avisimibe worked well to inhibit droplet formation in all conditions equally between E3 and E4 genotypes. Synthesis of LDs through the DGAT pathway (acylation of DAG to TAG) by substrate OA still occurred to some extent.

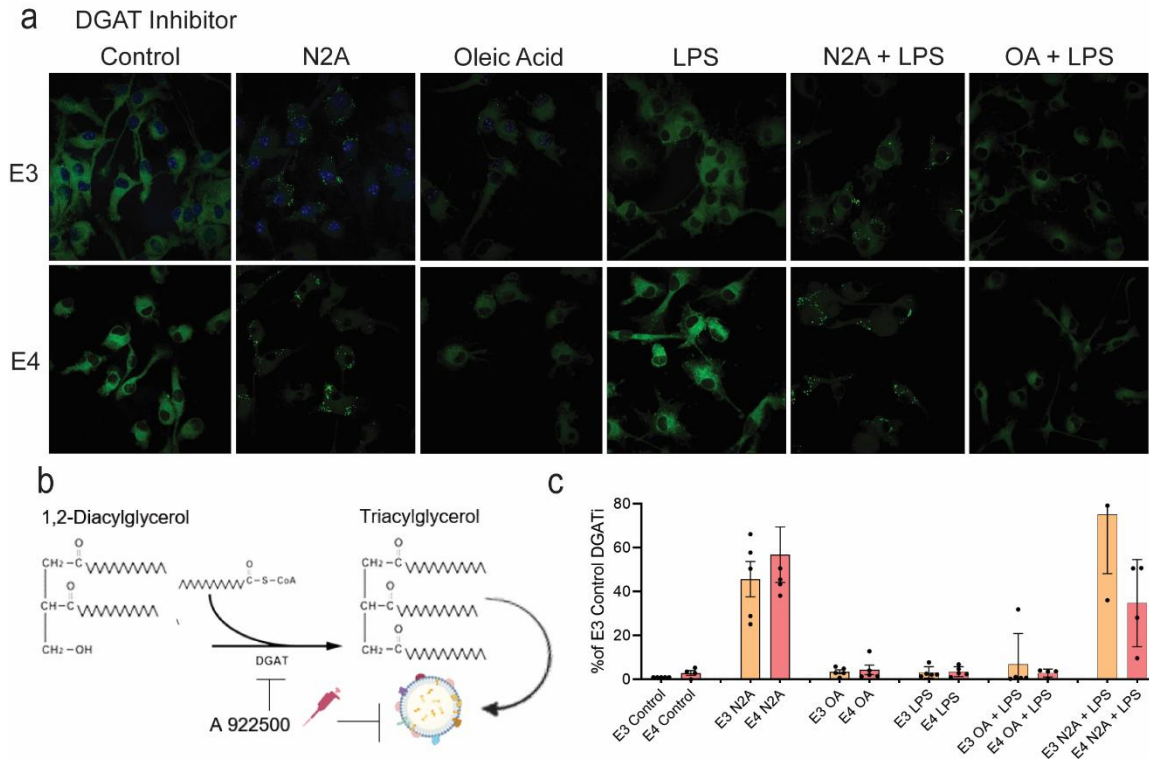


Figure 11: DGAT1 inhibitor reduced droplet formation in all conditions except nN2A treatment.

A) Images of primary microglia stained with BODIPY for neutral lipids show relatively low droplet accumulation in all conditions except those treated with nN2A. B) Diacylglycerol is acylated to become triacylglycerol and incorporated in the LD. The DGAT inhibitor prevents this process by eliminating DGAT, the rate limiting step for triacylglycerol into the droplet. C) DGATi worked to inhibit LDs in all conditions. Synthesis of LDs through the ACAT pathway still occurred with nN2A treatments.

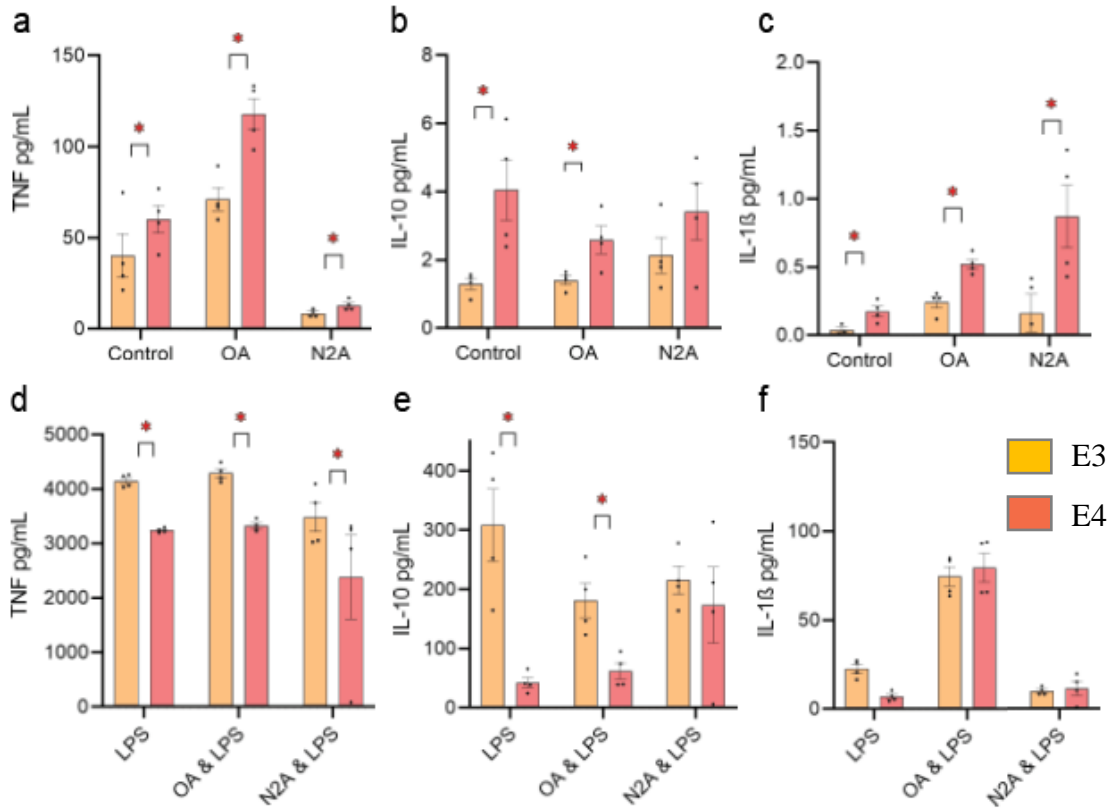


Figure 12: E4 expressing primary microglia secrete more cytokines at baseline compared to E3, but do not respond as robustly to LPS.

A-C) Primary microglia from E4 targeted replacement mice showed an increase in TNF, IL-10, and IL-1 β secretion compared to E3 cells. D-E) Cytokine measurements from plated primary microglia after 24-hour treatment with 10ng LPS show a switch in genotype-dependent cytokine secretion with E3 expressing cells responding robustly to inflammatory stimulation.

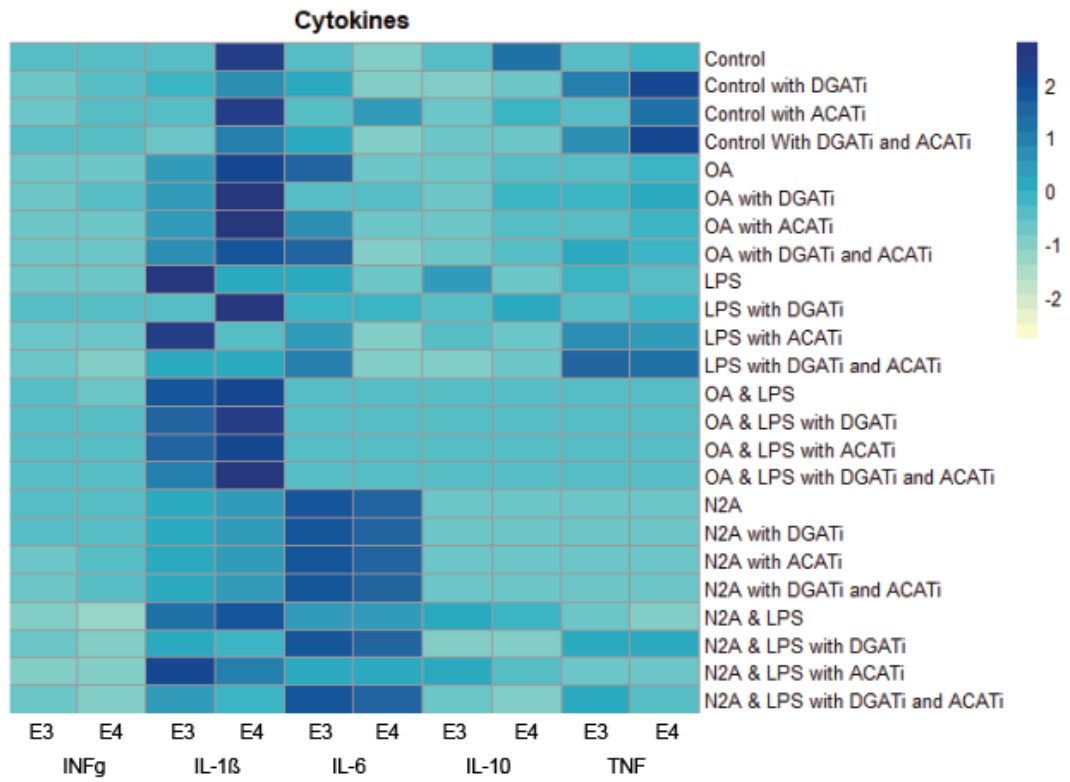


Figure 13: Heat map of cytokines show differences between genotypes in each treatment. This presentation allows viewing of various treatments on cytokine secretion. Notable differences include Control E3vE4 IL-1β and IL-10. Interesting secretion patterns occur with more IL-1β secretion after OA treatment and more IL-6 secretion after nN2A treatment.

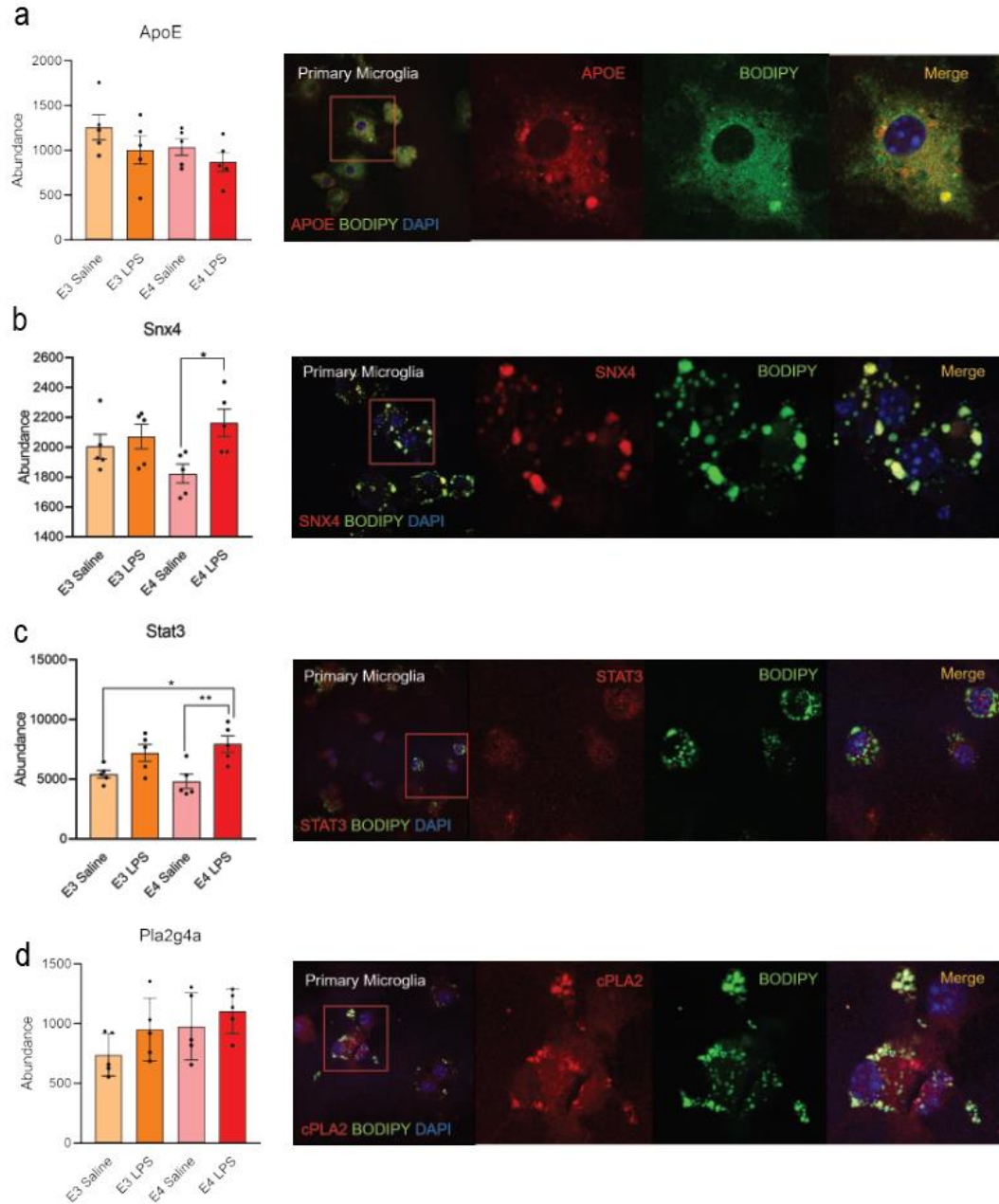


Figure 14: IHC to identify liver droplet proteins on primary microglia LDs.

A) ApoE colocalization with BODIPY verifies the presence of ApoE on the droplet surface. B) Snx4, an i-AD protein implicated in AD pathology, is located on the LD surface. C) Stat3, another i-AD protein with implications for immune function is not localized to the droplet in primary microglia, despite its presence in the cell. D) Pla2g4a, or cPLA2, is a phospholipase involved in the eicosanoid pathway, found on the LD surface in primary microglia as well as the liver.

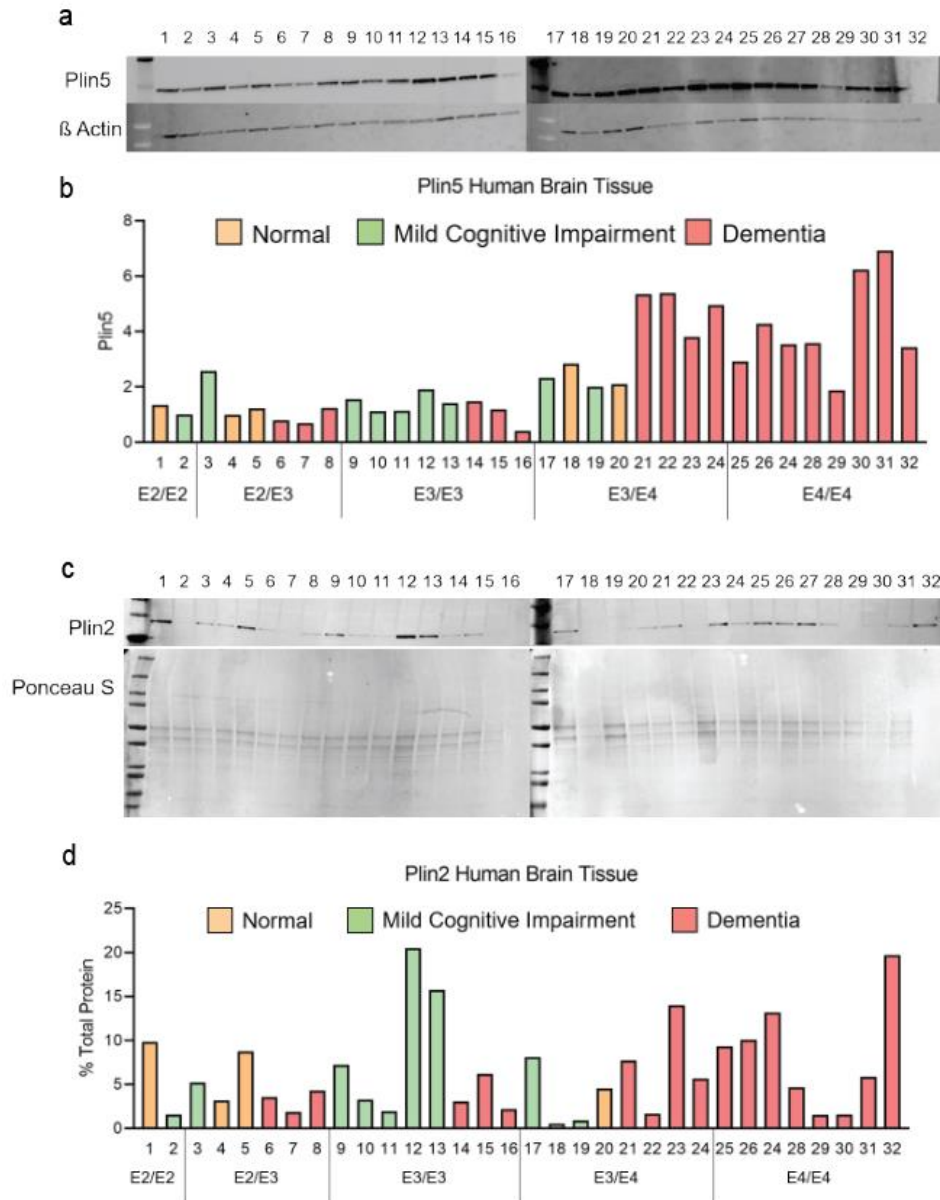


Figure 15: Western blots of human brain tissue show hypothesized increased in Plin5 with E4 genotype and dementia, but shows variable expression of Plin2.

A) Plin5 and β -actin protein levels were detected by Western blot in sections of frontal cortex from donated human brains. B) Plin5 is increased with E4 genotype in the presence of dementia. C) Plin2 and total protein were detected by Western blot in the same sections of frontal cortex. D) Plin2 levels had variance in both genotype and cognitive status. There was no correlation with Braak score or Mini Mental State Examination (MMSE) score between donor tissue, Plin2, or Plin5.

CHAPTER 4. LIPID DROPLETS IN MACROPHAGES – A STUDY INITIATION TO INVESTIGATE *APOE* MODULATION

This chapter highlights work done over the last 2.5 years to design, initiate, and optimize a human research study looking at LD dynamics in peripheral blood mononuclear cells. The study design was submitted, reviewed, and awarded independent funding as an administrative supplement through the National Institute on Aging and will be an ongoing pursuit in the laboratory as an internally-housed, *APOE*-genotyped biorepository of frozen blood cells and plasma along with a registry of volunteers for future study participation.

4.1 Introduction

The Johnson lab has recently focused on finding novel biomarkers to predict latent disease and provide new molecular targets for the prevention and treatment of AD. An NIH funded project (R01 AG062550) made use of whole-body energy expenditure measured by indirect calorimetry to investigate the underlying metabolic differences between the ApoE isoforms and how they associate with cognitive function after finding alterations in astrocyte (and microglia; under peer review [123]) metabolism in human-expressing ApoE4 mouse brains. Farmer et al performed single cell RNA sequencing and stable isotope resolved metabolomics to identify E4-associated reductions in genes and metabolites related to oxidative phosphorylation. E4 astrocytes, the most changed from the single cell data, showed increased glycolytic activity and lower oxygen consumption compared to E3 cells. To understand if this metabolic phenotype was seen in ApoE4 expressing humans, young and healthy research subjects participated in indirect calorimetry to measure energy expenditure and whole-body oxygen consumption as a way to infer systemic metabolic preference. Young and healthy E4-carrying females had

significantly lower energy expenditure and a lower rate of oxygen consumption. The plasma metabolome of E4 carriers also highlighted aerobic glycolysis-related pathways [137]. Farmer et al previously showed an increase in LDs in primary E4-expressing astrocytes with a parallel decrease in oxygen consumption [41]. Unpublished data from his work showed inhibition of LDs with DGAT improved oxygen consumption in primary E4 astrocytes, implicating LDs in the altered metabolic phenotype of E4 carriers that seems to exist from the brain to the blood. This provides the impetus for the current work, in which we aim to find meaningful peripheral biomarkers of latent disease with respect to ApoE4 carriage and LD accumulation.

The goal of this project is to elucidate ApoE LD differences in monocyte-derived-macrophages (MDMs). The choice to examine MDMs is driven by the fact that chronic inflammation is common in neurodegenerative diseases and microglia have a role that is central to neurodegeneration in AD [138-140]. Due to the limitations of directly sampling and studying microglia, given that these immune cells reside within the brain parenchyma, we proposed to investigate these cellular changes in the more easily accessible MDMs from individuals with different ApoE isoforms as a surrogate. PBMCs, including monocytes, are easy to collect from a simple and low-risk venipuncture and are easily isolated from the whole blood sample during post-processing.

The activation of microglia or macrophages requires a metabolic shift from oxidative phosphorylation toward increased glycolysis [141, 142]. Along with the identification of a shift in metabolic preference of E4 astrocytes and microglia from our laboratory, an increase in lactate was also observed. Lactate is a metabolite that can act as

an inflammatory mediator, a potential connection to link metabolic changes with inflammation – a concept known as immunometabolism [143].

The purpose of this multi-year project is to characterize LD dynamics in MDMs between different cognitively normal ApoE carriers as done in the liver tissue and microglia (Chapters 2 and 3). Next, using novel transcriptomic and metabolomics approaches, we aim to study MDMs isolated from the blood of *APOE* genotyped donors to shed light on the mechanisms by which individuals respond to inflammatory stimuli and alter metabolic preference in the presence of LDs. At a later time point, cognitively impaired adults may be recruited into the study as a comparison of preclinical genotype differences to those observed after the onset of dementia.

Due to the low frequency of heterozygous E2 expressing individuals in the population, and the even more rare homozygous E2/E2 carriers, the proposed study will have a large recruitment and genotyping phase (Phase 1). Individuals with E3/E3 and E4/x genotypes will be sex- and age-matched to the more infrequent E2/x participants identified in Phase 1. This will allow for more robust comparisons between *APOE* groups. A strength of this project is its collaboration with the University's Center for Clinical and Translational Science, which houses a well-maintained database of thousands of individuals in the region who are willing to participate in research, helping us identify participants for a mail-based campaign of saliva sample *APOE* genotyping (Phase 1, currently underway). Based on *APOE* allele frequencies and regional demographics, we expect to recruit 99 individuals for every one successfully recruited E2/E2 participant (and have scaled the study accordingly). However, a heterozygous E2 carrier is more frequently found in the population (8%) and the study will capture at least 25 E2/x participants. The

ease of access to pools of study volunteers allows us to better characterize potential immunometabolic benefits of the neuroprotective ApoE2 isoform, something that is relatively understudied due to E2 allele infrequency related challenges we plan to overcome in Phase 1.

To summarize the study goals, we first aim to determine the metabolic preference of resting and activated MDMs from ApoE variants. After recruitment and enrollment into the study, participants will receive a saliva collection kit in the mail for *APOE* genotyping (Phase I, currently in progress). Whole blood will be collected from age and gender matched *APOE* genotyped study participants in order to isolate PBMCs for analysis (Phase II, currently in progress). After a fasted blood collection, plasma will be isolated and a comprehensive metabolic panel and lipid panel will be run using standard clinical assays. The remaining blood will have PBMCs separated and frozen for batch analysis at a later date. After thawing, MDMs will be preferentially cultured based on cellular adherent properties and a protocol developed to wash away other cell types and foster growth and differentiation of monocytes. These cells will be treated with different conditions for immunometabolic experiments. Following the experimental flow in Figure 16, samples will be split to provide an intra-sample baseline, an inflammatory sample, and an anti-inflammatory sample. Cells will be stimulated with a low-dose, inflammatory LPS [144] to simulate an acute immune response or incubated with an anti-inflammatory stimulus, IL-10 [145]. The goal of these stimulations is to compare both between *APOE* genotypes as well as within each participant (baseline vs pro-inflammatory response).

Samples will undergo analysis with a Seahorse extracellular flux analyzer to measure glycolytic activity. If the hypothesis is correct and E4 cells prefer aerobic

glycolysis and E2 cells prefer oxidative phosphorylation, cells from these samples will be analyzed further with stable isotope-resolved metabolomics (SIRM). This will allow us to trace ^{13}C -labeled carbons through metabolic pathways to understand how exogenous agitations change pathway flux in the context of *APOE*. In addition, an aliquot of cells will be cultured and incubated for 6 hours with either LPS, IL-10, or normal media. Levels of ApoE, pro- and anti-inflammatory cytokines, and targeted metabolites will be analyzed using multiplex ELISA arrays. For SIRM analyses, cells will be incubated with ^{13}C -glucose and their respective conditions for thirty minutes (a time previously indicated as successful from microglia experiments within our laboratory). Metabolites will be extracted in methanol, and analyzed using GC-MS as previously described [146].

The second major aim of this endeavor is to perform single-cell sequencing analyses on *APOE* genotyped human PBMC cell populations to discern advantageous gene expression differences in E2/E2 carriers. In parallel to the metabolomics workflow described above, PBMCs from sex- and age-matched E2/E2, E3/E3 and E4/E4 individuals will be prepped for single-cell RNA sequencing (scRNA-seq) on the 10X Genomics platform. The advantage of using single-cell RNA sequencing is the elucidation of unbiased, transcriptome-wide specific cell-type changes associated with inflammation and *APOE* genotype, thereby providing novel targets for downstream analysis and future therapeutics. Preliminary data in our laboratory using targeted replacement mouse microglia indicate several sub clusters of cells with increased levels of glycolytic gene expression in E4 (Figure 17). Similar research has been done by Phongpreecha et al. to determine intracellular signaling pathways from scRNAseq of PBMCs from research participants diagnosed with various levels of cognitive decline [147], but to our knowledge

no data exists for preclinical biomarkers of emergent disease or disease risk or in the context of *APOE*.

Isolated PBMCs will be processed for scRNAseq using the established 10X Genomics library preparation workflow. scRNAseq data will be analyzed for differential gene expression, clustering (biomarkers), pathway enrichment, and gene ontology using the Seurat package in R. While proper scRNAseq analysis is a complicated and intensive undertaking, our lab has extensive experience in these bioinformatics workflows [137].

A recent study by Bosch et al observed immunometabolic shifts in hepatic cells with increased LDs, and detailed a mechanism for the role of LDs in this shift [54]. Previous research in our laboratory identified a similar increase in the number of LDs in E4 astrocytes from mice and a shift in their metabolic preference from oxidative phosphorylation to aerobic glycolysis, providing further justification to examine LDs and immunometabolism in the context of *APOE* in humans [41].

Together, the scientific literature points to LDs and their associated proteins as contributors to metabolic and immune functions within multiple cell types. Using transcriptomic and metabolomics approaches, we aim to use PBMCs isolated from the blood of young, cognitively normal study participants to shed light on the mechanisms by which E4 individuals respond to inflammatory stimuli. Eventually, we hope to compare these results to individuals with diagnosed dementia. Based on the limited knowledge in the field surrounding LDs, metabolism, and the brain, we hope to use the important findings of our lab's previous research as a translational foundation for studying the interaction and impact of LDs of individuals with varying *APOE* genotypes.

4.2 Methods

4.2.1 Recruitment

Recruitment will be split into two phases: first, a genotyping campaign by mail-in cheek saliva collection kits and second, a targeted invitation to visit the clinic for a fasted whole blood collection. The study population will be recruited primarily through the Center for Clinical and Translational Science (CCTS) and their advertisement campaigns. Interested participants will receive a consent form and DNA collection kit for genotyping directly to them for the first phase of recruitment. A health history survey will also be included as a way to identify who may be eligible for the next phase of recruitment. This form asks demographic information, date of birth, and if the participant is currently taking any medications. In addition to healthy volunteers recruited through the CCTS, recruitment will be later extended to individuals with dementia within the University of Kentucky healthcare system. A member of the study team will recruit within clinics like family medicine with the permission of healthcare providers before approaching any patients and/or families representing patients about the research study.

Based on preliminary data in mice and the observed frequency of each *APOE* allele in the population, group sizes of at least 15 should give sufficient power to quantify differences in immunometabolism between genotypes. Due to the population frequency of the E2 allele being the least at 8.4% of the general population, at least 300 individuals will be recruited for genotyping to yield a selection of ~25 E2 individuals. Of those, >15 E2 individuals are anticipated to meet the inclusion criteria for phase two of recruitment and blood draw. From these numbers there will be adequate numbers for ongoing participation of E3 and E4 individuals for the study.

Phase 1 Inclusion Criteria:

Age 18-65

- Female and male
- Any race/ethnicity
- The ability to provide informed consent

Phase 1 Exclusion Criteria:

- < 18

Phase 2 Inclusion Criteria (Healthy):

- Age 18-100+
- Female and male
- Any race/ethnicity
- The ability to provide informed consent and health history
- A successful genotype analysis for the *APOE* alleles

Phase 2 Exclusion Criteria (Healthy):

- Bleeding disorders
- Neurological disorders
- History of diabetes or metabolic syndrome
- History of alcoholism or other drug abuse
- History of chronic, major psychiatric disorders (e.g., schizophrenia, bipolar disorder, or major depression)
- Currently taking anxiolytic medication, antibiotics, anti-inflammatory medications, beta blockers, antidepressants, CNS stimulants, neuroleptics, narcotic analgesics, anti-Parkinsonian agents, sedating antihistamines, CNS-active antihypertensives

Medications listed in Table 3 are excluded while taking part in the study.

Inclusion criteria for patients:

- Over 18 years of age
- Female and male
- Any race/ethnicity
- Diagnosed cognitive impairment

Exclusion criteria for patients:

Inability to provide informed consent and no designated legal authorized representative to do so

4.2.2 Saliva Kits

Saliva collection kits (Abclonal: RK21656) were distributed to individuals interested in study participation. Participants were asked to abstain from eating or drinking for five minutes prior to providing a sample and were asked to spit at least 2mL of saliva into the tube (2mL line marked). A DNA preservative was poured into and mixed with the saliva, the sample was placed into a biohazard bag, and returned to the lab to be stored at room temperature and analyzed once there were enough samples to create a batch for genotyping.

4.2.3 DNA Extraction

Saliva tubes were placed in beads on the heat block at 50°C for at least one hour. A sampling of the saliva and preservative were placed in a new tube and combined with a cell lysate solution containing lysis buffer, EDTA, and proteinase K. After a short room temperature incubation, protein precipitation solution was added and samples chilled on ice prior to centrifugation to separate out protein from the sample. The supernatant

containing genetic material was transferred to another tube and combined with isopropanol before centrifugation. Supernatant was discarded and the DNA pellet was washed with 70% ethanol and centrifuged again. Supernatant was discarded and the pellet was left to dry for approximately 30 minutes before being resuspended in DEPC-treated water prior to PCR preparation.

4.2.4 Genotyping

Master mix was made using ApoE isoform single nucleotide polymorphisms primers rs42 (SNP rs429358 ThermoFisher) and rs74 (SNP rs7412 ThermoFisher), Taqman master mix, water, and the DNA/DEPC-treated water sample. Samples were placed in a 96-well PCR plate with human *APOE* controls for each genotype and a no DNA, non-template control. Using the BioRad PCR machine, the following thermo cycling protocol was used and results were analyzed for *APOE* genotype.

- a. Incubate at 95 degrees for 10:00
- b. Incubate at 95 degrees for 00:15
- c. Incubate at 60 degrees for 1:00
- d. Repeat b and c for 39 more cycles

4.2.5 Venipuncture

If selected to participate in the second part of the research study, volunteers will be contacted by a study coordinator and invited in for a fasted blood draw. These participants may be contacted to remind them of their scheduled appointment. Participants will be asked to fast overnight (12 hours prior to scheduled AM appointment). Participants will have blood drawn early in morning after fasting from food, drink (except water), caffeine, and alcohol for >12 hours. From a fasting blood sample, we will conduct routine blood tests

that are a normal part of a physical exam, such as immune cell counts and lipid and metabolic panels. Additionally, we will isolate cells from the blood sample and freeze them for later experiments described in Figure 16. The amount of blood taken will be no more than 50mL, or five 10mL tubes. Blood will be collected via venipuncture in EDTA coated collection tubes (purple tops) by a member of the research team and taken back to the laboratory for post-processing.

4.2.6 PBMC Isolation

SepMate tubes (StemCell, 85450), are filled below the insert with Ficoll (Lymphoprep; StemCell, 07801). Whole blood was diluted 1:1 with sterile 1xPBS + 2% FBS and quickly pipetted down the side of the SepMate tube to sit on top the insert. After centrifugation at 1200xg for 10 minutes, the red blood cells pool below the insert and the plasma and PBMC mixture is transferred into a new tube, and washed with PBS in another centrifugation to pellet PBMCs. Cells are resuspended in warmed DMEM:F12 media and counted for immediate culturing, or resuspended in warmed RPMI and counted to 20×10^6 /mL for freezing.

4.2.7 Freeze & Thaw

After PBMC isolation, the necessary volume of chilled resuspension medium (40% FBS in RPMI) to achieve a concentration of 20×10^6 cell/mL was added to the cells. The same volume of 2X freezing medium (20% DMSO in 40% FBS RPMI) was then added to dilute cells to a concentration of 10×10^6 cells/mL for freezing. The cells were gently mixed while sitting on ice and 1mL aliquots (10 million cells) were pipetted into pre-cooled cryovials. The pre-cooled cryovials were placed into a pre-cooled controlled-rate freezing

container (Mr. Frosty) and placed into the -80°C freezer to cool at a rate of $1^{\circ}\text{C}/\text{minute}$. After at least four hours, the cells were moved to be stored in liquid phase of liquid nitrogen. To thaw cells, RPMI media was warmed and cryovials were removed from the liquid nitrogen. In a 37°C water bath, each vial was swirled in the water until a single ice crystal remained. In the laminar flow hood, the cryovial's contents were poured into a large, 50mL conical tube. Warm media was used to wash the cryovial to catch any remaining cells and was gently and slowly (1 drop every 3-5 seconds) pipetted onto the cells. Four additional serial dilutions 1:1 were performed, releasing media into the tube at a controlled rate (1mL every 3-5 seconds), until the 50mL tube was full. Centrifugation at $300\times g$ for 5 minutes allowed thawed PBMCs to pellet and media was aspirated. Cells were resuspended in 10mL of warmed, complete RPMI for counting.

4.2.8 Culture

PBMCs were cultured in T-75 flasks to assess viability over time (~3 weeks). Media was changed after 1-3 days to wash away non-adherent PBMCs, leaving monocytes behind. Additional media changes were done every week. PBMCs were also cultured in 96, 24, or 12-well plates and the same washing procedures were followed to remove non-adherent cells from the culture.

4.2.9 Treatment

To date, we have not acquired enough PBMC samples from different genotypes to run a proposed experiment, though we have cultured, plated, and stained MDMs with BODIPY to ensure LD accumulation and success of the imaging protocol used in the primary microglia (Chapter 3) in blood cells. Cells plated on glass coverslips were fixed in

4% PFA and stained for CD68, a ubiquitous monocyte and macrophage marker, to verify methods were adequate for selection of monocytes. Coverslips were mounted onto slides using a DAPI-nuclear staining mounting media.

4.2.10 Imaging

Cells plated on coverslips, stained, and mounted on microscope slides were imaged on a Nikon A1R Confocal microscope.

4.3 Preliminary Results

4.3.1 Study enrollment to date includes over 250 volunteers.

Study participants vary in age from 18 to 80 and are mostly non-Hispanic Caucasians. Table 2 details the anticipated enrollment and demographic information of our local area (Lexington, Kentucky). Currently, about 2/3rd of the enrollment population is female and there is a higher percentage of volunteers with Asian ancestry (11% compared to population demographics of 1%). Due to study recruitment primarily occurring within the academic environment at the University of Kentucky, we have a bit of a skewed demographic compared to the local population and this reflects in our enrollment data. Despite differences in ethnic and gender enrollment, based on genotyping results, the *APOE* allele distribution almost perfectly falls within the reported prevalence in the literature [28] with the following results: E2/E2 = 1%; E2/E3 = 9%; E3/E3 = 59%; E2/E4 = 3%; E3/E4 = 25%; E4/E4 = 3%. Figure 18 highlights the distribution between our recruitment population and the general population.

4.3.2 Protocol optimization yields adequate cell numbers after freeze and thaw.

An imperative part of this study is the ability to freeze PBMCs from human whole blood with the successful thawing of viable cells for future experiments. As these cells are not immortal, they are more sensitive to freezing and therefore we spent a lot of time optimizing our protocol to yield the best results. Figure 19a-j details the protocol procedures utilized to isolate PBMCs, freeze, thaw, adequately recover, culture, and select for MDMs. Verification of the cell of interest (MDMs) is showed in Figure 19k with IHC of cultured cells following the isolation protocol. Cells were stained with CD68, a marker for cells in a monocyte lineage – i.e. monocytes and macrophages. In addition to staining for CD68, cells were mounted with a medium containing DAPI to stain nuclei blue. CD68 appeared in over 90% of DAPI-containing cells, verifying the isolation and culture of the correct cell type of interest.

Table 2: Enrollment and Demographics

Ethnic Category	Enrollment
Hispanic or Latino	9.2
Not Hispanic or Latino	287.2
Unknown	3.6
Ethnic Category: Total of all Subjects	300
Racial Category	
American Indian or Alaskan Native	0.8
Asian	3.6
Black or African American	25.2
Native Hawaiian or other Pacific Islander	0.4
White	2.55.2
More than one race	5.6
Unknown/Other	9.2
Racial Category: Total of all Subjects	300
Totals	300

Table 3: List of Medicines within Exclusion Criteria

Antibiotics	Penicillins, Tetracyclines, Cephalosporins, Quinolones, Lincomycins, Sulfonamides
Anti-inflammatory	Aspirin, Celebrex, Ibuprofen, Naproxen
Beta Blockers	Sectral, Tenormin, Zebeta, Lopressor, Corgard, Bystolic, Inderal LA, InnoPran XL
CNS Stimulants	Ritlan, Desoxyn, Dextrostat, Desoxyn, Adderall
Neuroleptics	Clozaril, Saphris, Zeprexa, Seroquel
Narcotic Analgesics	Codeine, Zohydro ER, Oxycodone, Methadone, Hydromorphone, Morphine, Fentanyl
Anti-Parkinsonian Agents	Sinemet, Symmetrel, Artane, Cogentin, Elderpryl, Azliect, Comtan
Sedating antihistamines	Allegra ODT, Zyrtec, Zymine, Lodrane, Phenergan, Zyzal, Allegra, Benadryl
CNS-Active antihypertensive agents	Catapres, Kapvay, Intuniv, Tenex

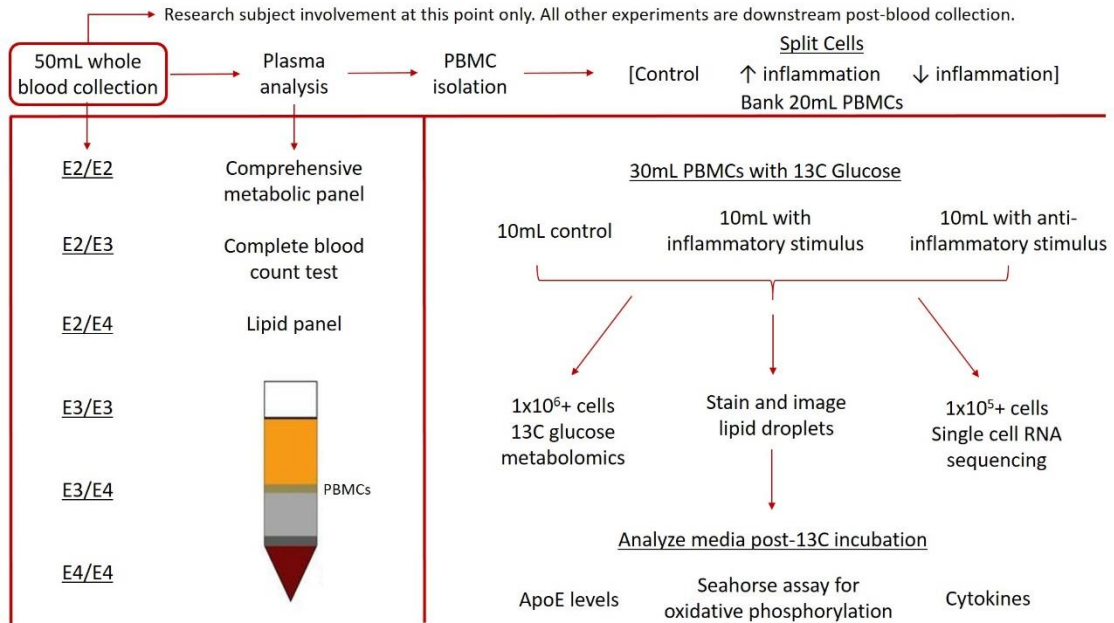


Figure 16: Study Design

APOE genotyped study volunteers will be brought into the University of Kentucky’s Center for Clinical and Translational Science for a fasted venipuncture of 50mL. Blood will be taken back to the laboratory for post-processing which will include plasma analysis and PBMC isolation. Cells will be split and experimental results can be compared against a baseline between samples and between groups.

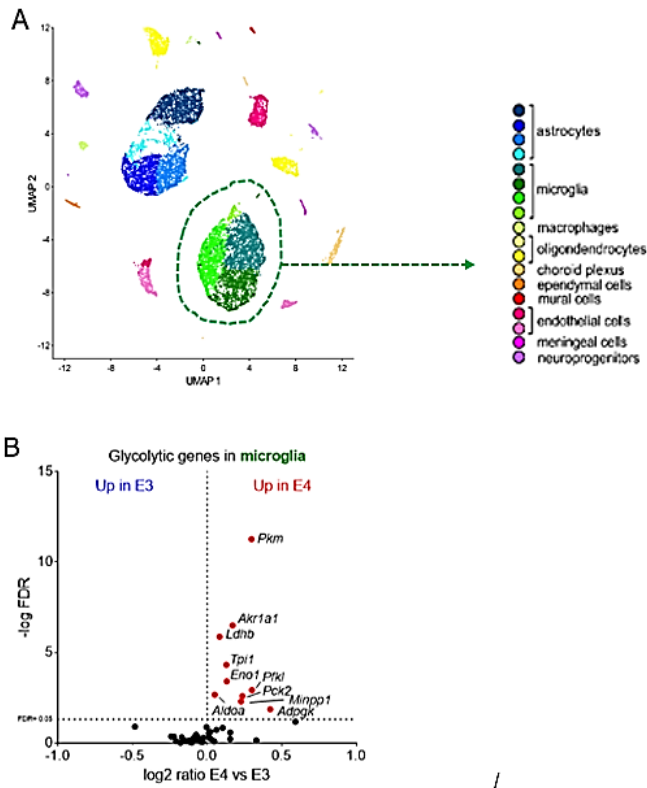


Figure 17: E4 microglia express increased levels of glycolytic genes.

A) Whole brain tissue from E3 and E4 mice underwent single-cell RNA sequencing (scRNA-seq). UMAP visualization of cells from E3 and E4 mouse brains (3 pooled hemibrains per genotype). Cells are colored by cell type (microglia colored in green). B) Volcano plot showing differentially expressed glycolytic genes for E4 vs. E3 microglia. Genes in red are upregulated in E4 microglia with false discovery rate < 0.05.

Figure adapted from previous laboratory publication by Brandon Farmer, MD, Ph.D. [137].

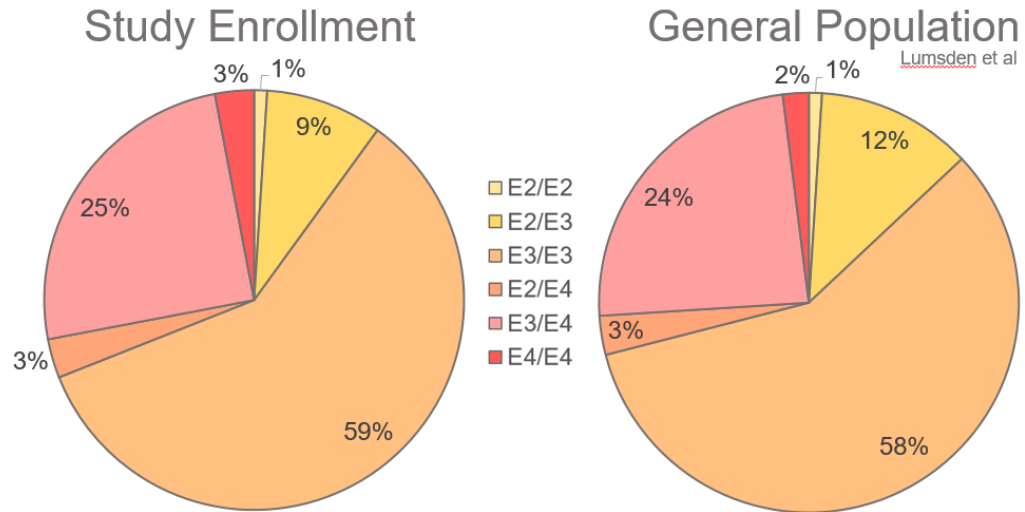


Figure 18: To date, study enrollment very closely mirrors the predicted genotype frequency of the general population.

Enrollment numbers are based on untargeted recruitment efforts through our laboratory and the Center for Clinical and Translational Sciences.

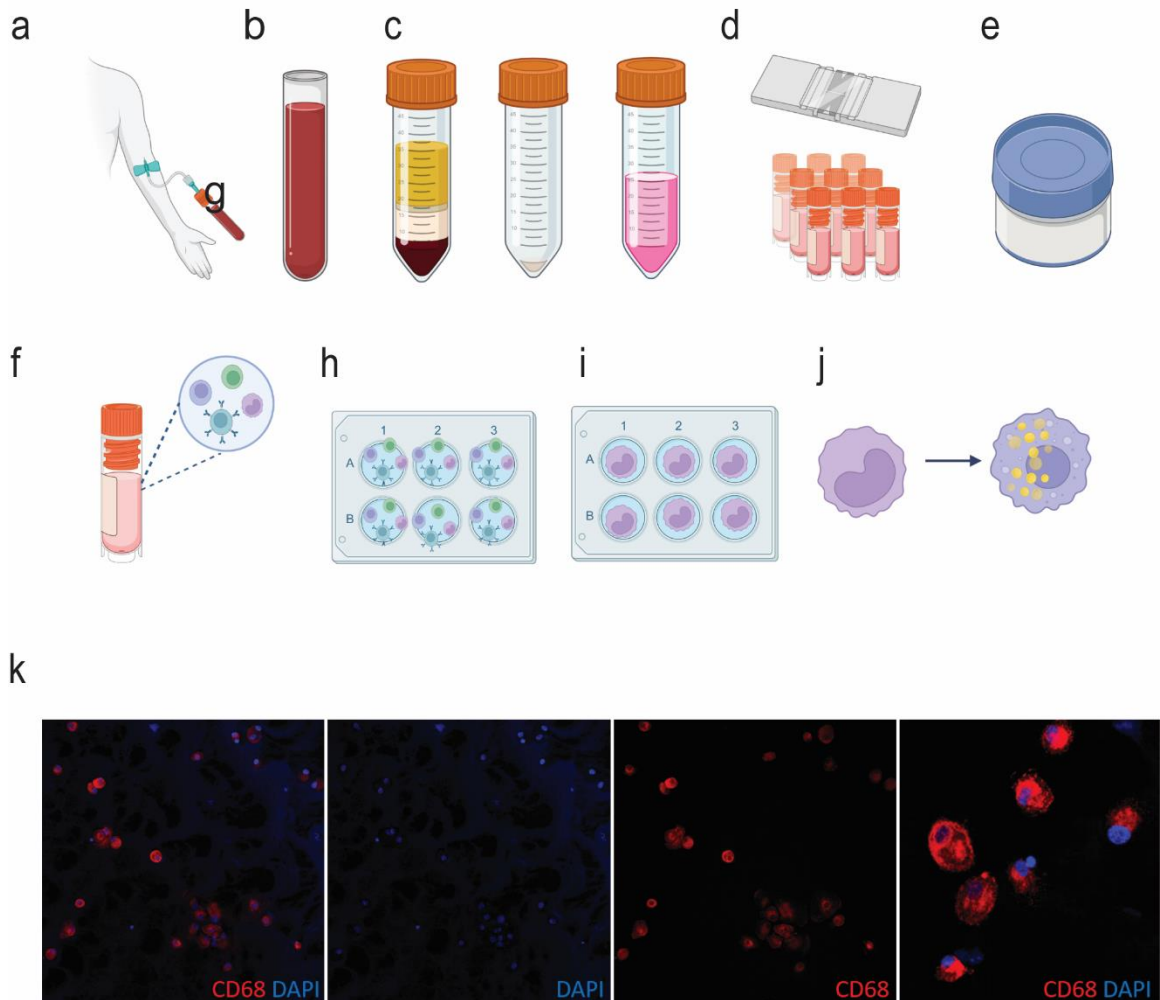


Figure 19: PBMC optimization procedures.

A) Venipuncture was performed for whole blood collection. B) Density gradient centrifugation allowed for PBMC separation and isolation. C) PBMCs were prepared in freezing media with optimized percentage of DMSO. D) Cells were counted and distributed into cryovials. E) Controlled-rate cooling of cells occurred at -80°C overnight before cells went into liquid nitrogen. F) PBMCs were thawed in 37°C . G) Cells were resuspended and counted for recovery and viability. H) A lower percentage of DMSO yielded the best cell recovery at 94%. I) PBMCs were plated and within 24 hours, media was changed to wash away all cells except adherent monocytes. J) Monocytes grew and differentiated into macrophages over a week in culture. K) Cell type of interest was confirmed ($>90\%$) using macrophage marker CD68 and analyzing colocalization with nuclei stained with DAPI.

CHAPTER 5. DISCUSSION

5.1 Summary of Dissertation

APOE4 is the strongest genetic risk factor for LOAD. The protein isoform encoded by *APOE4*, ApoE4, has deficits in lipid binding and transport, presumably contributing to its increased disease risk. Additionally, multiple studies, including our own, have shown that cells expressing ApoE4 accumulate more lipid droplets than those expressing the ‘neutral’ E3 allele. While a handful of studies have characterized LDs in models of disease/inflammation, to our knowledge no studies have examined LD dynamics in the context of *APOE* – an important endeavor given the substantial percentage of the population carrying ApoE4 and the rapidly-increasing numbers of AD cases. Such investigations are key in determining if there are implications for *APOE* genotype in LD biology, and if so, the impact on cellular function and disease.

The versatile nature of LDs has led to the investigation of their circumstantial neutral lipid content and protein profile on the outer LD monolayer and their respective consequences for cellular function. For example, proteomic analyses show differing protein composition around cholesteryl ester (CE)-enriched vs. triacylglycerol (TAG)-enriched LDs, suggest that the inner lipid content may influence the assembly of proteins on the LD monolayer [148]. Further, the outer protein arrangement may also direct the function and location of the LD within the cell. Finally, LDs are traditionally formed as a compensatory mechanism to protect cells from fatty acid toxicity, but they can also liberate fatty acids as lipid mediators of inflammation [64] or supply fatty acids for metabolism in the mitochondria [149]. Given that i) LD protein and lipid composition can influence the function of their host cell, ii) *APOE* is the strongest genetic risk factor for AD and is a

resident LD protein, iii) LDs have been implicated in AD pathogenesis, and iv) E4-expressing glia accumulate more LDs, our main goal was to contrast and compare the lipid and protein composition of E3 vs E4 lipid droplets.

To work toward this characterization, we first targeted LDs in the liver of ApoE3 and ApoE4 expressing mice. The liver is the largest producer of ApoE in the periphery of the body, it accumulates LDs in an amount large enough to isolate for quantitative proteomics (unlike the cells of the brain), and there are many established connections between the liver and the brain, including ones related specifically to ApoE4 and AD. Before analyzing samples for LD proteomics and lipidome analysis, we needed to first ensure we had indeed isolated LDs successfully. Chapter 2 describes the methodology and validation of LD isolation from liver tissue, verified by the presence of Plin2, a ubiquitous LD protein, in only the top-most buoyant fraction from the LD isolation. We also performed oil red o staining on liver tissue from the same mice to 1) ensure hepatic lipid content was within a normal distribution among groups and 2) quantify total LD area and individual droplet size. In terms of total lipid area, E4 liver tissue had significantly more positive oil red o staining than E3 livers, and both E3 and E4 tissue had significant increases in droplet accumulation after a 24-hour LPS treatment. In addition to having more droplets, the droplets found in E4 livers were smaller in size compared to E3, but were similar in size to the E3 and E4 LPS-droplets.

Lipidome analysis verified the largely glycerolipid content of the droplets with about 90% of the droplet fraction consisting of TAG. However, the remaining lipid content differed greatly between E3 and E4 droplets at baseline, with E4 droplets showing a larger distribution of PC in the droplet membrane compared to E3 which had more DAG.

Interestingly, the E4 lipidome was very similar to the E3 and E4 LPS lipidomes in terms of glycerophospholipid distribution with a high ratio of PC to other phospholipid species. The proportion of glycerophospholipid species along with the size of the droplets reveal important inferences about E4 and LPS-droplets and the relationship between LD size, metabolic contribution, and lipid content that are further discussed in this chapter.

The droplet proteome revealed 2,092 proteins implicated on LDs in other proteomes and another 2,175 that were unique to our model. Analyses were completed on both the overlapping LD-resident proteins and the full proteome from our liver tissues. All analyses revealed a distinct contribution of E4-droplet proteins to innate immunity-related pathways and E3-droplet proteins to oxidation of fatty acids. Droplet proteins that were significantly increased on E4 compared to E3 and vice versa revealed this distinctive pattern of proteins related to inflammatory vs metabolic pathways. WGCNA analysis echoed this pattern of E3 droplets enriched with metabolic pathways for fatty acid oxidation. These findings fit a larger theory where E4 hepatocytes, astrocytes, and microglia have all been observed to be at an increased inflammatory state with a glycolytic phenotype compared to their E3 expressing counterparts with less inflammation and a more homeostatic oxidative metabolic states [41, 84, 123]. It is our hypothesis that LDs play a major contribution to the metabolic fate of a cell based on their lipid and protein composition.

When looking at the proteins enriched on E4 vs E3 droplets, there were several familiar proteins recognized from the AD literature. A recently published paper describing an incipient AD protein signature in young E4 carriers had a 60% overlap with LD proteins. This observation is exciting as it links LD proteins from the liver to known proteins

expressed in the brain which may contribute to AD pathogenesis. Looking further at AD-related brain and cerebrospinal fluid proteomes, we found substantial overlap in E3 vs E4 brain proteomes of AD patients that implicated increased inflammation in E4 AD brains through gene ontology of biological processes. E3 AD brains also had immune-related pathways enriched, however the E4 AD brains enrichment of immune pathways was much larger, suggesting a higher contribution of inflammation-related proteins [114]. A recent AD brain proteome from the same laboratory pinpointed a protein module implicated in glial metabolism within AD (non ApoE isoform specific). The 30 proteins in this distinct microglia-AD network overlapped 90% with proteins from our liver LD proteome. This exciting finding underscores the connection between the liver LD proteome and the brain, particularly microglia, the immune cell of the brain.

Characterization of LDs in microglia was also a main goal of this dissertation work and was performed in primary microglia from targeted replacement mice expressing human ApoE3 or ApoE4. At the beginning of our research, there were no studies or observations of LD accumulation in microglia with ApoE3 or ApoE4, representing a knowledge gap we sought to fill. We used a variety of conditions to characterize LD formation in microglia that included no treatment, the addition of exogenous lipids in the form of oleic acid or dying N2A cells, inflammation with LPS, and combinations of exogenous lipid and LPS. In all conditions, E4 primary microglia accumulated more LDs compared to E3 cells. We also report smaller LD area in E4 primary cells at baseline and with LPS treatment. This falls in line with results from Machlovi et al (one of two papers published at the same time of our findings) who observed E4 primary microglia to have increased phagocytosis and LD accumulation [89]. Although this research was not the first to describe an increase of

LDs in E4 microglia, it is reassuring to be in the good company of two other high-caliber research laboratories that found the same results. Their interest in these questions bolsters the need to fill the gaps in knowledge surrounding LDs and ApoE, and drive this research forward in our own unique way.

LD inhibition in primary microglia was accomplished through the DGAT and ACAT pathways and successfully diminished LDs in almost all conditions. When primary cells were treated with a DGAT inhibitor, the only condition in which LDs were not inhibited were treatment with nN2A cells. The cholesterol content in nN2A cells was still esterified and incorporated into LDs via the ACAT pathway in the presence of the DGAT inhibitor. Alternatively, treatment with an ACAT inhibitor reduced LDs in all conditions except those given oleic acid where the substrate was incorporated into LDs through the DGAT pathway.

One of the other critical knowledge gaps concerning LDs and microglia was their relationship with cytokine production based on which ApoE isoform they carry. We found E4 expressing primary microglia to secrete more TNF α , IL-6, and IL-1 β at baseline and after the addition of oleic acid and nN2As. Treatment with LPS caused a greater spike in cytokine release from E3 cells – an unexpected result given the documentation of a hyper-robust inflammatory response from E4 cells reported previously. Nevertheless, we hypothesized LD inhibition could dampen the cytokine response by removing the inflammation-related proteins and the lipid mediators stored within LDs to contribute to cytokine production. However, LD inhibition with DGATi, ACATi, or a combination of the two actually increased cytokine production in all conditions. We believe this is due to the introduction of a pharmacologic into an immune cell – a foreign substance that should

trigger an immune response, and possibly fatty acid and free cholesterol toxicity within the cell. As substrates were added to induce LD formation in the presence of the inhibitors, there was no mechanism for the cells to neutralize and store the lipids, therefore leaving them susceptible to toxicity and the observed inflammation response. These results emphasize the importance of LDs to cell homeostasis and provides a cautionary guidance for the application of LD inhibitors.

5.2 Lipid Droplet Inhibition

Triacsin C has been used as a droplet inhibitor in two papers reviewed in Chapter 3 related to microglia [62, 90], however, our experiments used ACAT1 and DGAT1 inhibitors instead. The choice to do so was intentional, in order to increase the translatability of our findings to potential future therapeutics and to minimize impact on fatty acid oxidation. Triacsin C inhibits long-chain acyl-CoA synthetase (ACSL). ACSL is essential for esterification of fatty acids into a neutral lipid for storage within a droplet and for fatty acid activation to form an acyl-coA for its metabolic contribution. Inhibition of these pathways with Triacsin C inhibits the esterification of fatty acids and cholesterol, preventing the *de novo* synthesis of LDs, but it also reduces oxidation of fatty acids. We had concerns that due to the inherently pro-glycolytic phenotype of E4 cells [41, 123, 137], preventing the capability to oxidize fatty acids that cannot be sequestered into a LD could potentially drive further pathology in E4 cells. Also, Triacsin C has not been tested as a therapeutic in humans and shows cellular toxicity at IC₅₀ [150, 151].

LD synthesis through the DGAT1 and ACAT1 pathways can be targeted with A 922500 and Avisimibe, respectively. A brief review of current literature provides many

points for discussion and sets the stage for LD-related therapeutics for AD. DGAT1 is the final step in triglyceride synthesis with the formation of an ester linkage between fatty acyl CoA and diacylglycerol. DGAT1 knockout mice are resistant to diet-induced obesity yet still form triglyceride through alternative pathways. As promising as this solution to obesity and LD accumulation sounds, a knockout of DGAT1 renders a female mouse unable to lactate [152]. DGAT2 knockout mice do not live long and have severe lipopenia and skin barrier anomalies [153]. Similar to the knockout model of DGAT1, inhibition of DGAT1 with A 922500 protects mice fed a high fat diet from diet-induced obesity and depletes their plasma triglycerides after a lipid challenge [154], however there are not adverse effects on lactation in females, making DGAT1 inhibition a promising approach to LD-related issues. DGAT2 inhibition also showed promising results in mice, but little effect in non-human primates [155]. Curiously, DGAT1 inhibitors have not fared well in clinical trials with several study withdrawals due to gastrointestinal upset and intolerability with multiple compounds and doses (a result which has led to repurposing of DGAT1 inhibitors for functional constipation and IBS-C clinical trials, currently ongoing), but DGAT2 inhibitors continue to be tested in trials to reduce hepatic steatosis with little adverse effects [156, 157].

ACAT2 was not targeted for inhibition in our study due to its selective expression in the liver and intestines, compared to ubiquitous expression of ACAT1. ACAT1 is responsible for the esterification of cholesterol to a cholesteryl ester capable of being incorporated into the neutral LD core. A disease where ACAT inhibition is highly relevant is atherosclerosis where increased cholesterol incorporation into LDs create lipid-laden ‘foam cells’ from macrophages or smooth muscle cells that become hallmark features of

atherosclerotic plaques. ACAT1 inhibition, in a way similar to DGAT1 inhibition, creates a free pool of cholesterol within the cell that can become cytotoxic. However, smooth muscle cells are resistant to free cholesterol toxicity and macrophages are susceptible. Nonselective ACAT1 inhibition, therefore, could yield mixed results with positive effects in plaque burden consisting of mostly smooth muscle cells, but negative effects on macrophages [158]. An area of potential concern is the similarity between macrophages and microglia, immune cells of myeloid origins. ACAT1 inhibition in microglia could be intolerable due to free cholesterol toxicity. A recent study in Trem2^{-/-} and ApoE^{-/-} mice shows dysregulated cholesterol transport and metabolism in microglia when challenged with myelin cholesterol. Microglia accumulate cholesteryl ester in LDs and cholesteryl esters throughout the brain (forebrain, glial cells, and cerebrospinal fluid). Cholesteryl ester accumulation in Trem^{-/-} bone marrow-derived macrophages treated with an ACAT inhibitor *in vitro* prevented LD accumulation. To ensure clearance of cholesteryl esters, cells were also treated with an LXR agonist to increase expression of cholesterol transporters ABCA1 and ABCG1. The pairing of ACAT1 inhibitors and an LXR agonist worked to reduce accumulation and storage of cholesteryl esters in LDs and prevent cell toxicity by promoting cholesterol efflux [159]. Perhaps, this combination is essential to ameliorate the cellular deficits observed in both macrophage-foam cells and lipid droplet accumulating microglia without the toxicity of ACAT1 inhibitors alone.

It is important to note the above studies detailing the efficacy of DGAT and ACAT inhibition were all performed in models of obesity, liver disease, or cholesterol abnormalities, while we are focused on LDs in the context of ApoE and AD in the brain. As shown in Figures 12 and 13, LD inhibition with both DGAT and ACAT did not improve

cytokine profiles of microglia in any condition, despite dramatic reduction in LD formation. This gives important verification of the effectiveness of LDs in protecting cells from fatty acid toxicity, further validated (a bit paradoxically) by a recently described use of DGAT1 inhibitors in glioblastoma cancer. DGAT1 inhibitor was used to prevent LD formation in glioblastoma cells (expression levels of DGAT1 were significantly higher than DGAT2, leading to their target preference) with the hypothesis that tumor cells are using LDs as an energy reservoir that could be leveraged for proliferation. Treatment with A 922500 significantly reduced LD accumulation and TG levels in glioblastoma cell lines and patient-derived glioblastoma cells. The strategy to free lipids from storage with the cell appeared successful, as the cells showed increased fatty acid oxidation, reactive oxygen species, mitochondrial damage, and apoptosis through synthesis of acylcarnitines. To test in an animal model, tumor cells were grafted in mice (flanks) and DGAT inhibitor was given to mice after the tumor had substantially grown. The inhibitor significantly suppressed tumor growth in the xenograft model with similar results as the cell lines in terms of reduced LD formation, increased acylcarnitine levels, and apoptosis [160]. There was no reported toxicity in peripheral mouse organs, but of course this crucial proof of concept study was not performed within the brain. Currently, no marketed DGAT1 inhibitors cross the BBB, but targeting DGAT1 for brain cancer is a great future therapeutic option, as non-cancer cells express lower levels of DGAT1 and therefore should not be affected by treatment. It was noted in the glioblastoma paper that inhibition of triglyceride synthesis significantly increased PC and phosphatidylethanolamine (PE), as DAGs entered the Kennedy pathway for phospholipid synthesis instead. Another DGAT1 inhibitor study focused on this principle to successfully promote the phospholipid synthesis necessary for

axon regeneration after neuronal injury by routing triglyceride synthesis via DGAT1 inhibition *in vitro* [161]. These studies begin to string together the important connection between LDs, their size, their phospholipid content, and their function within the cell as described below.

5.3 The role of phosphatidylcholine (and other molecules) in LD biophysics

The primary job of LDs is to store neutral lipids within their core. Most think of LDs and their lipid composition as only triacylglycerol or cholesteryl ester. However, these neutral lipids are sheathed in a monolayer composed of glycerophospholipids, fatty acids, sphingolipids, and proteins. Studies of LDs in other systems have revealed purposeful distribution of membrane lipids and implications for when ratios of certain membrane components change. In our data, PC was the phospholipid most altered within the total ratio of membrane components of E4, E3-LPS, and E4-LPS droplets with PC contributing to the abundance of substrate in the membrane by 50% or greater compared to PC contribution in E3 LDs at 30%. In 2008, the lab of LD enthusiasts Tobias Walter and Robert Farese found that shutting down phospholipid synthesis enzymes like CCT (rate-limiting enzyme of PC synthesis) causes the fusion of LDs into giant organelles [162]. In 2011, a member of their laboratory, Natallie Krahmer, described the importance of CCT activation and PC incorporation into the expanding LD membrane [121]. Inhibition of CCT1 and choline kinase both led to giant LDs. Additionally, culturing cells in choline-deficient media induced the same giant-LD phenotype. Adding PC back to the cells reversed the effect and prevented the coalescence of droplets. From these experiments, it was determined that PC acts as a surfactant to prevent LD fusion. The higher the surface to

volume ratio (i.e. the higher the ratio of PC to neutral lipids), the smaller the LD. With less PC, droplets have a smaller surface to volume ratio and therefore are larger.

Based on principles of emulsion physics, the size of LDs can indicate their stability. In simplistic terms, the neutral core of a large LD provides ‘safety in numbers’ – there is more neutral lipid that adheres together in their respective oil phase and the bulk of that lipid is farther in distance from the aqueous phase outside the LD monolayer and therefore has a lower Laplace pressure within its core (the pressure equivalent to the surface tension at the LD surface) – all factors working to provide stability to the droplet. However, a smaller LD has less neutral lipid within, therefore its oil phase adhesion is not as strong. Smaller droplets have a higher surface-to-volume ratio and a larger Laplace pressure within their core. There is evidence smaller emulsions are less stable due to these features and may have leakage into the aqueous phase around them, a phenomena known as Ostwald ripening [163]. Sometimes, Ostwald ripening can contribute to larger LDs as lipids diffused from small droplets are picked up and incorporated into larger droplets [53]. However, there is no anecdotal evidence of this type of exchange based on the universally small LD sizes found in our E4 and LPS data. Rather, it is possible this type of ripening from small LDs could be releasing lipids which are utilized as lipid mediators of inflammation, contributing to the increased inflammatory profiles of E4-cells harboring small-sized droplets.

5.4 Droplet size, content, and droplet proteins

In addition to the contribution of PC to size and stability of LDs, we are also interested in the contribution of surface proteins to their stability and function within the

cell. Many think of LDs as simple reservoirs for lipid storage, however droplets can also act as protein storage organelles. A set of ubiquitous LD proteins known as perilipins (Plin), provide clues about LD function based on their expression within the cell and their incorporation on the droplet surface. For example, Plin5 is associated with oxidative phosphorylation and colocalization of LDs to the mitochondria [50, 56, 57, 164], whereas Plin2 expression is associated with immunologic and inflammatory function within the cell [54, 122]. Plin2 has also been shown to block lipases from hydrolyzing fatty acids within LDs and its downregulation allows liberation of lipids from droplets for metabolism. In our liver LD data, there is an increased amount of Plin2 in E4 droplet fractions. This observation makes sense because E4 cells had an overall higher abundance of LDs and therefore more LD proteins. However, when stimulated with LPS, the LD abundance increased equally in both E3 and E4 mice, but the abundance of Plin proteins did not increase in parallel with the increase in LD area. At baseline, E3 liver tissue had significantly less Plin2 and Plin5 compared to E4. LPS treatment caused a 400% increase in E3-LPS Plin2 abundance and an 85% increase in Plin5. E4-LPS treatment caused a more modest 85% increase in Plin2 (to an abundance matching E3 LPS) and a 71% increase in Plin5. Overall, LPS treatment disproportionately increased Plin2 compared to Plin5. This validates the previous associations of Plin2 with inflammation [58, 59].

Taken together, we propose the increased PC distribution in the E4 and LPS-treated LDs serves as a surfactant to increase the surface-to-volume ratio of LDs, keeping their size small and preventing them from contributions toward metabolism. The additional increase of Plin2 on the smaller E4 and LPS LD surfaces acts to shield inner contents from lipases, therefore trying to stabilize the droplets and further prevent their contribution to

energy production. With this information in mind, it is reasonable to believe the lipid and protein makeup of LDs is dynamic, and that their now recognized multitude of functions are likely driven by changes in this composition and should be carefully considered when studying LD-related pathological processes. As described earlier, LDs not only harbor lipids, but also house a variety of proteins on their outer surface. This protein composition consists of a set of core, LD-resident proteins, but also includes transiently interacting proteins that differ based on cell type and condition (as observed in our droplet proteome between E3-E4 and baseline-LPS). Along with the size of the LDs (which could also be partially driven by surface proteins like CCT directing more PC to the droplet monolayer), their function can be driven by the type and amount of surface proteins they express. The next section works to explain the links between LDs, metabolic, and immune function in the context of *APOE*.

5.5 Lipid Droplets and Immunometabolism

Traditionally, immunometabolism describes the changes that occur in metabolic pathways within immune cells upon their activation with an inflammatory challenge. However, we believe this concept of immunometabolism can be broadened to also encompass the links between energy and inflammation provided by LDs. The basic principle of immunometabolism is that the activation of immune cells to elicit a pro-inflammatory response requires a shift in metabolism to provide rapid energy for proliferation, chemotaxis, etc. Activated immune cells show an increase in glycolysis and a decrease in oxidative phosphorylation, despite the presence of oxygen, a phenomenon often termed “aerobic glycolysis” [165]. A resting immune cell typically lacks a large accumulation of LDs, but within hours after insult, LDs rapidly develop and can be

considered a sign of inflammation within the cell. LD biogenesis can serve different roles in different stages of inflammation. For example, a pro-inflammatory activation of immune cells shifts metabolism to aerobic glycolysis and LDs also are believed to shift to act as hubs to support host immunity through the release of lipids for signaling, rather than release lipids for oxidation. Conversely, in pro-resolving stages of a cell's immune response, the cell shifts primarily to fatty acid oxidation. It is thought during this 'anti-inflammatory' stage that LDs provide a majority of the lipid substrates for beta-oxidation through their turnover and release of fatty acids [165-167].

Our lab previously found that compared to E3, E4 expressing astrocytes have increased numbers of smaller-sized LDs, decreased oxidation of fatty acids, and increased glycolysis [41]. In the whole brains of E4 mice using stable isotope resolved metabolomics (SIRM) and single-cell RNA sequencing, some of these findings were recapitulated. Our lab found decreased expression of genes related to oxidative phosphorylation in E4 brains, particularly in astrocytes. Isotopic tracing of ^{13}C -glucose in E4 mice and astrocytes also showed decreased pyruvate entering the TCA cycle for oxidative phosphorylation and increased lactate [137]. The overall metabolic phenotype of E4 cells was patterned as aerobic glycolysis, or the use of glucose through glycolysis in the presence of oxygen.

In addition to this data, ongoing studies in the lab show similar findings in E4 expressing microglia [123]. Microglia, the immune cells of the brain, provide clear links between E4 expression and alterations in immunometabolism. Brain tissue from aging E4 mice revealed a distinct cluster of microglia enriched for DAM genes, innate immunity, and glycolytic pathways. E4 mice injected with LPS (the same conditions used for the current dissertation research), showed an exaggerated metabolic response to inflammation

compared to E3 mice receiving the same treatment. Metabolic phenotyping of primary microglia revealed increased aerobic glycolysis in E4 and increased glycolytic ATP production in response to an inflammatory stimulus. E3 cells had higher rates of mitochondrial respiration, and upon inflammatory stimulation had increased ATP production via the mitochondria. Spatial transcriptomics and lipid content analysis through a method called matrix assisted laser desorption/ionization mass spectrometry imaging (MALDI MSI) reveal distinct changes in the lipidomes of E3 and E4 mice.

When crossed with a model of AD (5xFAD), E4 mice had increased PCs containing PUFAs arachidonic acid (AA) and linoleic acid in them [123]. This is important to note, as these PUFAs are precursors of eicosanoid production. Additionally, their oxidation exacerbates inflammation and has been associated with impaired electron transport chain activity [168, 169]. Dysregulation of AA metabolism and an increase in the eicosanoid lipidome is a feature of AD and is increased in E4 carriers [170]. Recently, an AA positron emission tomography (PET) tracer was developed and tested in the ApoE targeted replacement mice due to the interest in monitoring dysregulations in AA metabolism in the brains of E4 carriers, much like amyloid and tau pathology can be monitored via PET imaging [171].

Our data also shows a significant increase in lysophosphatidylcholine (LPC), a lipid species recognized for its inflammatory contribution to atherosclerosis and within demyelination and neurodegeneration [172]. The proposed mechanism by which LPC triggers inflammation is through its action as a ‘find me-eat me’ signal, or damage-associated molecular pattern (DAMP). Ismaeel et al found LPC not only serves as a DAMP, but also increases other DAMPs while reducing the threshold by which receptors

respond to them and initiate inflammation, cytokine release, and/or cell death [173]. LPC is a product of PC synthesis within the Lands cycle, the alternative PC production mechanism to the Kennedy Pathway. LPC in circulation is carried by oxidized LDL molecules or is transported back to the liver by albumin and re-acylated by lysophosphatidylcholine acyltransferase (LPCAT). LPCAT is remarkably a LD surface protein and its presence is associated with the increased synthesis of PC for the LD membrane [174]. A downregulation of LPCAT results in larger LDs, and conversely, an upregulation yields smaller LDs via increased incorporation of PCs to the droplet membrane [175]. Our proteomic data highlights LPCATs 1, 2 and 3 and all show an increase (non-significant) in E4 abundance compared to E3. As predicted by the action of LPCAT, LPS treatment increased its abundance. E4 saline LD fractions had 22% more LPCAT1-3 than E3 LDs; LPS treatment increased E3 LPCAT abundance by 41% and increased E4 LPCAT abundance by a mere 8%. The original increased LPCAT abundance of E4 likely prevented a more robust response to LPS as seen in E3 droplets. Looking back at single-cell RNA sequencing data in E4 microglia, LPCAT1 was significantly increased compared to E3 microglia, an important observation to further draw the line between liver LD characterization and glial cells.

Both AA and LPC are liberated by cytosolic phospholipase A2 (cPLA2), encoded for by the gene *PLA2G4A*. Greater phosphorylated cPLA2 (i.e. increased activity) and downstream leukotriene B4 levels were found in E4 expressing primary astrocytes, targeted replacement E4 mouse brains, and human brain homogenates of E4 carriers with AD [176]. In our proteomics data, *PLA2G4A* showed a trend (not statistically significant) toward increased expression in E4 saline LD fractions. Further, single-cell analysis of E3

versus E4 microglia show a significant increase in *PLA2G4A* expression in E4 cells of targeted replacement mice. We also were able to localize cPla2 on the surface of LDs in primary microglia using IHC. The observation of increased cPla2 in AD, specifically in E4 carriers, along with the knowledge of its identification as a LD protein acting on lipid mediators of inflammation harbored within LDs, makes it another meaningful target for therapeutics in AD.

5.6 E4 lipid droplets may drive changes in immunometabolism, increase risk for AD onset, and exacerbate existing AD pathology

To summarize the critical patterns observed between ApoE3 and ApoE4 across multiple peripheral and cerebral cell types: E3 cells are more oxidative, more pro-resolving, have fewer but larger LDs, and are associated with a neutral risk of AD. On the other hand, E4 cells are more glycolytic, more pro-inflammatory, have more LDs that are smaller in size, and are associated with an increased risk to develop AD. Based upon my own dissertation research and a synthesis of the existing literature, I propose LDs in E4 carriers are a primary driver of E4-related AD risk through the above-mentioned pathologies.

The increased distribution of PC in the LD membrane of E4 cells is likely responsible for their small size. In combination with the increase in Plin2 (which could help shield the LD from lipolysis), and the increase in LPCAT on E4 droplets (to provide additional PCs), E4 droplets are smaller, less susceptible to hydrolysis of fatty acids, and more amenable to lipophagy and leakage of fatty acids. The increase in PUFA species and cPla2 on E4 droplets may also add to their contribution toward inflammation, increased release of cytokines, glycolytic metabolic profile, and proteome that is attributed to innate

immunity. Conversely, the decreased proportion of PCs within E3 droplets lead to coalescence of droplets and a larger overall size, despite lower total droplet area. With decreased Plin2, E3 droplets are more susceptible to lipolysis and liberation of fatty acids to beta oxidation. In my proposed model, alterations in lipid binding, transport and metabolism (potentially a direct result of the structural differences in the E4 isoform) are the upstream source of inflammation and/or LD accumulation. This presents a chicken v egg paradigm, as it is still unclear if inflammation or LD accumulation is the initial driver for this feed-forward scenario. However, the specific nature of E4 droplets further contribute to the abnormal metabolic profile and inflammatory status of the cell.

The quantitative characterization of E3 versus E4 LDs reveals stark differences in the lipid and protein content which mirrors a larger cellular pattern: E3 = oxidative and homeostatic; E4 = glycolytic and inflammatory. These observations have held true while studying LDs in the liver, astrocytes, and microglia. Importantly, LDs have exciting overlap with protein signatures found in E4 carriers and AD brains. We believe LDs provide detail on the status of the cell, as their dynamic nature allow them to rapidly change size, content, and protein adornment based on their contribution. Finally, LD inhibitor experiments emphasize the importance of LDs within the cell and tell us their inhibition is not without consequence.

5.7 What do we do about it?

Based on the findings of this dissertation, I believe LDs both drive and intensify the aberrant metabolic and inflammatory phenotypes observed in E4 cells. This includes decreased glucose uptake, decreased LD turnover, increased inflammation, increased

glycolysis, and mitochondrial dysfunction. Given this, the use of LD inhibitors in E4 cells would be a prudent approach. However, from our data we see this causes an increase in cytokine release, presumably due to an increase in fatty acid buildup within the cell and subsequent toxicity. The use of a cholesterol efflux drug alongside a droplet inhibitor may ameliorate this specific problem, however, this must be balanced with the fact that LD presence can still be favorable to the cells in which they reside. We can conclude LDs are an essential component to the normal function of a cell (liver, brain, or blood), but when their profile is unfavorable, it is reflected in the cell's function. Rather than eliminating the harmful LDs in E4 cells, we should focus on leveraging their dynamic nature to change their configuration to a resemblance of E3 droplets.

The natural progression of this work should focus on manipulating droplets in E4 glia to shift their metabolic contribution to a more favorable mitochondrial respiration and eliminate their pro-inflammatory predisposition. Several approaches can be used to achieve this shift. Since the size of the droplets are distinctly connected to E3 (large) and E4 (& LPS, small), the size of the droplet is a promising target to manipulate. For example, this could be done by culturing cells in choline deficient media to decrease the amount of PC substrate available for LD membrane incorporation. This has been shown to create larger LDs, but there is no evidence of how this functionally changes them. This also could theoretically be achieved by blocking CCT or LPCAT enzymatic activity, reducing the number of PCs synthesized. Experiments to look at the baseline LD size and metabolic phenotype in E3 and E4 cells followed by PC reduction or choline supplementation (addition of choline to media or overexpression of synthesis pathway enzymes) are necessary to see if changing droplet size effects its metabolic contribution within the cell.

Additional targets can be found in the eicosanoid production pathway. E4 cells have more AA which is used as mediators of inflammation through the synthesis of eicosanoids. Decreasing the activation of cPla2, reducing the abundance of AA or linoleic acid as inflammatory substrates, or increasing anti-inflammatory mediators like DHA and EPA within the LD membrane may help alleviate inflammation driven by LDs. Notably, these targets are all E4-cell specific. In our data, even E3 LPS LDs maintained a set of proteins that were specifically upregulated and resembled a pro-resolving phenotype through increased oxidation of fatty acids for energy, while E4 LPS LDs had a protein profile indicative of an increased immune response and cellular stress. Despite a large inflammatory insult to E3 cells, they still responded with typical activation, represented by their LD profile, compared to E4 cells. To simplify this point, inflamed E3 cells have LDs that seem to respond appropriately and allow the cell to leverage their energy stores to respond to inflammation in a functional way. However, E4 LDs have more baseline inflammation-related pathways. This pattern holds true more broadly in the AD literature as E4 carriers have an earlier and more severe pathology compared to E3 carriers.

The future of AD research is accelerating to meet the upcoming demand of patients, and new technology allows us to better understand the natural progression of this disease. Even more exciting, technical advances are allowing for better precision in care for different ethnic groups, patients in different geographical regions, and patients with comorbidities. In my opinion, the most important and relevant focus should be on stratification through *APOE* genotype. As the largest genetic risk factor for LOAD, E4 should be a central component of AD research and clinical trials. In looking at the etiology of AD in E4 carriers (which begins much earlier than non-carriers), we find decreased

glucose uptake, increased energy expenditure, increased neuroinflammation, decreased cholesterol metabolism, decreased amyloid beta clearance, and increased LD accumulation. Our findings here that E4 LDs are characteristically and functionally different from E3 LDs leads me to believe they are central in the above-mentioned symptoms.

In conclusion, to support our hypotheses, LD dynamics seem to be significantly modulated by *APOE* genotype in multiple systems. Further, prior knowledge of the metabolic differences in cells with different ApoE isoforms and their association with distinct droplet phenotypes, gives credence to the hypothesis that LDs are major contributors to the metabolic profiles of the cells in which they accumulate. Although future studies are necessary to leverage the dynamic nature of LDs to manipulate their contribution within the cell towards favorable outcomes, I believe this dissertation work and review of the relevant literature gives justification and direction to this pursuit.

APPENDIX

ABCA1	ATP binding cassette subfamily A member 1
ACAT	acyl-CoA cholesterol acyltransferase
ACSL	acyl-CoA synthetase
AD	Alzheimer's disease
ApoE	Apolipoprotein E
ApoER2	ApoE receptor 2
APP	amyloid precursor protein
ATGL	adipose triglyceride lipase
BACE1	beta-amyloid precursor protein cleaving enzyme 1
BBB	blood brain barrier
CCTS	Center for Clinical and Translational Science
CNS	central nervous system
DAG	diacylglycerol
DAM	disease associated microglia
DAMP	danger associated molecular pattern
DGAT	diglyceride acyltransferase
FBS	fetal bovine serum
GPCR	G protein-coupled receptors
GWAS	genome-wide association study
HBSS	Hanks Balanced Salt Solution
HDL	high density lipoprotein
iAD	incipient Alzheimer's disease
IHC	immunohistochemistry
iPSC	induce pluripotent stem cell
LD	lipid droplet

LDAM	lipid droplet accumulating microglia
LDL	low density lipoprotein
LDLR	low density lipoprotein receptor
LOAD	late-onset Alzheimer's disease
LPC	lysophosphatidylcholine
LPCAT	lysophosphatidylcholine acyltransferase
LPL	lipoprotein lipase
LPS	lipopolysaccharide
LRP1	LDLR-related protein 1
LXR	liver X receptors
MDM	monocyte-derived macrophages
MGnD	neurodegenerative microglia
MMSE	mini mental state examination
MS	multiple sclerosis
NF κ B	nuclear factor κ B
nN2A	necroptotic N2A cells
OA	oleic acid
PBMC	peripheral blood mononuclear cells
PBS	phosphate buffered saline
PC	phosphatidylcholine
PCR	polymerase chain reaction
PET	positron emission tomography
PLIN	perilipin
PPAR	peroxisome proliferator-activated receptors
PUFA	poly unsaturated fatty acid
ROS	reactive oxygen species
RXR	retinoid X receptors
scRNAseq	single-cell RNA sequencing

SIRM	stable isotope resolved metabolomics
SNP	single nucleotide polymorphism
SREBPs	sterol regulatory element-binding proteins
TAG	triacylglycerol
TLR	toll-like receptor
VLDL	very low density lipoprotein
VLDLR	very-low-density lipoprotein receptor
WGCNA	weighted gene co-expression network analysis

REFERENCES

1. Cahill, S., *WHO's global action plan on the public health response to dementia: some challenges and opportunities*. Aging Ment Health, 2020. **24**(2): p. 197-199.
2. *2021 Alzheimer's disease facts and figures*. Alzheimers Dement, 2021. **17**(3): p. 327-406.
3. Wong, W., *Economic burden of Alzheimer disease and managed care considerations*. Am J Manag Care, 2020. **26**(8 Suppl): p. S177-S183.
4. Gendron, T.F. and L. Petrucelli, *The role of tau in neurodegeneration*. Mol Neurodegener, 2009. **4**: p. 13.
5. Hansen, D.V., J.E. Hanson, and M. Sheng, *Microglia in Alzheimer's disease*. J Cell Biol, 2018. **217**(2): p. 459-472.
6. Aging, N.I.o., *What Happens to the Brain in Alzheimer's Disease?* 2017.
7. Karch, C.M. and A.M. Goate, *Alzheimer's disease risk genes and mechanisms of disease pathogenesis*. Biol Psychiatry, 2015. **77**(1): p. 43-51.
8. Guerreiro, R., J. Bras, and J. Hardy, *SnapShot: genetics of Alzheimer's disease*. Cell, 2013. **155**(4): p. 968-968 e1.
9. Liu, C.C., et al., *Apolipoprotein E and Alzheimer disease: risk, mechanisms and therapy*. Nat Rev Neurol, 2013. **9**(2): p. 106-18.
10. Phillips, M.C., *Apolipoprotein E isoforms and lipoprotein metabolism*. IUBMB Life, 2014. **66**(9): p. 616-23.
11. Zhang, J. and Q. Liu, *Cholesterol metabolism and homeostasis in the brain*. Protein Cell, 2015. **6**(4): p. 254-64.
12. Huang, Y. and R.W. Mahley, *Apolipoprotein E: structure and function in lipid metabolism, neurobiology, and Alzheimer's diseases*. Neurobiol Dis, 2014. **72 Pt A**: p. 3-12.
13. Chernick, D., et al., *Peripheral versus central nervous system APOE in Alzheimer's disease: Interplay across the blood-brain barrier*. Neurosci Lett, 2019. **708**: p. 134306.
14. Zhao, N., et al., *Apolipoprotein E, Receptors, and Modulation of Alzheimer's Disease*. Biol Psychiatry, 2018. **83**(4): p. 347-357.
15. Rebeck, G.W., et al., *The generation and function of soluble apoE receptors in the CNS*. Mol Neurodegener, 2006. **1**: p. 15.
16. Frieden, C., H. Wang, and C.M.W. Ho, *A mechanism for lipid binding to apoE and the role of intrinsically disordered regions coupled to domain-domain interactions*. Proc Natl Acad Sci U S A, 2017. **114**(24): p. 6292-6297.
17. Krimbou, L., et al., *Molecular interactions between apoE and ABCA1: impact on apoE lipidation*. J Lipid Res, 2004. **45**(5): p. 839-48.
18. Koldamova, R., N.F. Fitz, and I. Lefterov, *ATP-binding cassette transporter A1: from metabolism to neurodegeneration*. Neurobiol Dis, 2014. **72 Pt A**: p. 13-21.
19. Chen, J., Q. Li, and J. Wang, *Topology of human apolipoprotein E3 uniquely regulates its diverse biological functions*. Proc Natl Acad Sci U S A, 2011. **108**(36): p. 14813-8.
20. Steinmetz, A., et al., *Differential distribution of apolipoprotein E isoforms in human plasma lipoproteins*. Arteriosclerosis, 1989. **9**(3): p. 405-11.

21. Lanfranco, M.F., C.A. Ng, and G.W. Rebeck, *ApoE Lipidation as a Therapeutic Target in Alzheimer's Disease*. Int J Mol Sci, 2020. **21**(17).
22. Heinsinger, N.M., M.A. Gachechiladze, and G.W. Rebeck, *Apolipoprotein E Genotype Affects Size of ApoE Complexes in Cerebrospinal Fluid*. J Neuropathol Exp Neurol, 2016. **75**(10): p. 918-924.
23. Hu, J., et al., *Opposing effects of viral mediated brain expression of apolipoprotein E2 (apoE2) and apoE4 on apoE lipidation and Abeta metabolism in apoE4-targeted replacement mice*. Mol Neurodegener, 2015. **10**: p. 6.
24. Morikawa, M., et al., *Production and characterization of astrocyte-derived human apolipoprotein E isoforms from immortalized astrocytes and their interactions with amyloid-beta*. Neurobiol Dis, 2005. **19**(1-2): p. 66-76.
25. Zhao, J., et al., *APOE epsilon4/epsilon4 diminishes neurotrophic function of human iPSC-derived astrocytes*. Hum Mol Genet, 2017. **26**(14): p. 2690-2700.
26. Wang, C., et al., *Gain of toxic apolipoprotein E4 effects in human iPSC-derived neurons is ameliorated by a small-molecule structure corrector*. Nat Med, 2018. **24**(5): p. 647-657.
27. Liao, F., et al., *Targeting of nonlipidated, aggregated apoE with antibodies inhibits amyloid accumulation*. J Clin Invest, 2018. **128**(5): p. 2144-2155.
28. Lumsden, A.L., et al., *Apolipoprotein E (APOE) genotype-associated disease risks: a phenome-wide, registry-based, case-control study utilising the UK Biobank*. EBioMedicine, 2020. **59**: p. 102954.
29. Association, A.s. *Genetic Testing*. 2022 [cited 2022; Available from: <https://www.alz.org/media/documents/alzheimers-dementia-genetic-testing-ts.pdf>].
30. Farrer, L.A., et al., *Effects of age, sex, and ethnicity on the association between apolipoprotein E genotype and Alzheimer disease. A meta-analysis. APOE and Alzheimer Disease Meta Analysis Consortium*. JAMA, 1997. **278**(16): p. 1349-56.
31. Corbo, R.M. and R. Scacchi, *Apolipoprotein E (APOE) allele distribution in the world. Is APOE*4 a 'thrifty' allele?* Ann Hum Genet, 1999. **63**(Pt 4): p. 301-10.
32. Jia, L., et al., *The APOE epsilon4 exerts differential effects on familial and other subtypes of Alzheimer's disease*. Alzheimers Dement, 2020. **16**(12): p. 1613-1623.
33. Rajabli, F., et al., *A locus at 19q13.31 significantly reduces the ApoE epsilon4 risk for Alzheimer's Disease in African Ancestry*. PLoS Genet, 2022. **18**(7): p. e1009977.
34. Wardell, M.R., et al., *Apolipoprotein E2-Christchurch (136 Arg----Ser). New variant of human apolipoprotein E in a patient with type III hyperlipoproteinemia*. J Clin Invest, 1987. **80**(2): p. 483-90.
35. Sepulveda-Falla, D., et al., *Distinct tau neuropathology and cellular profiles of an APOE3 Christchurch homozygote protected against autosomal dominant Alzheimer's dementia*. Acta Neuropathol, 2022. **144**(3): p. 589-601.
36. Le Guen, Y., et al., *Association of Rare APOE Missense Variants V236E and R251G With Risk of Alzheimer Disease*. JAMA Neurol, 2022. **79**(7): p. 652-663.
37. Rasmussen, K.L., et al., *Plasma levels of apolipoprotein E and risk of dementia in the general population*. Ann Neurol, 2015. **77**(2): p. 301-11.
38. Blanchard, V., et al., *Kinetics of plasma apolipoprotein E isoforms by LC-MS/MS: a pilot study*. J Lipid Res, 2018. **59**(5): p. 892-900.

39. Garcia, A.R., et al., *APOE4 is associated with elevated blood lipids and lower levels of innate immune biomarkers in a tropical Amerindian subsistence population*. *Elife*, 2021. **10**.
40. Javadifar, A., et al., *Foam Cells as Therapeutic Targets in Atherosclerosis with a Focus on the Regulatory Roles of Non-Coding RNAs*. *Int J Mol Sci*, 2021. **22**(5).
41. Farmer, B.C., J. Klumper, and L.A. Johnson, *Apolipoprotein E4 Alters Astrocyte Fatty Acid Metabolism and Lipid Droplet Formation*. *Cells*, 2019. **8**(2).
42. Bersuker, K. and J.A. Olzmann, *Establishing the lipid droplet proteome: Mechanisms of lipid droplet protein targeting and degradation*. *Biochim Biophys Acta Mol Cell Biol Lipids*, 2017. **1862**(10 Pt B): p. 1166-1177.
43. Casey, C.A., et al., *Lipid droplet membrane proteome remodeling parallels ethanol-induced hepatic steatosis and its resolution*. *J Lipid Res*, 2021. **62**: p. 100049.
44. Krahmer, N., et al., *Organellar Proteomics and Phospho-Proteomics Reveal Subcellular Reorganization in Diet-Induced Hepatic Steatosis*. *Dev Cell*, 2018. **47**(2): p. 205-221 e7.
45. Khan, S.A., et al., *Quantitative analysis of the murine lipid droplet-associated proteome during diet-induced hepatic steatosis*. *J Lipid Res*, 2015. **56**(12): p. 2260-72.
46. Mejhert, N., et al., *Partitioning of MLX-Family Transcription Factors to Lipid Droplets Regulates Metabolic Gene Expression*. *Mol Cell*, 2020. **77**(6): p. 1251-1264 e9.
47. Alzheimer, A., et al., *An English translation of Alzheimer's 1907 paper, "Uber eine eigenartige Erkankung der Hirnrinde"*. *Clin Anat*, 1995. **8**(6): p. 429-31.
48. Guo, Y., et al., *Lipid droplets at a glance*. *J Cell Sci*, 2009. **122**(Pt 6): p. 749-52.
49. Olzmann, J.A. and P. Carvalho, *Dynamics and functions of lipid droplets*. *Nat Rev Mol Cell Biol*, 2019. **20**(3): p. 137-155.
50. Bosch, M. and A. Pol, *Eukaryotic lipid droplets: metabolic hubs, and immune first responders*. *Trends Endocrinol Metab*, 2022. **33**(3): p. 218-229.
51. Dalhaimer, P., *Lipid Droplets in Disease*. *Cells*, 2019. **8**(9).
52. Onal, G., et al., *Lipid Droplets in Health and Disease*. *Lipids Health Dis*, 2017. **16**(1): p. 128.
53. Walther, T.C., J. Chung, and R.V. Farese, Jr., *Lipid Droplet Biogenesis*. *Annu Rev Cell Dev Biol*, 2017. **33**: p. 491-510.
54. Bosch, M., et al., *Mammalian lipid droplets are innate immune hubs integrating cell metabolism and host defense*. *Science*, 2020. **370**(6514).
55. Bersuker, K., et al., *A Proximity Labeling Strategy Provides Insights into the Composition and Dynamics of Lipid Droplet Proteomes*. *Dev Cell*, 2018. **44**(1): p. 97-112 e7.
56. Wang, H., et al., *Perilipin 5, a lipid droplet-associated protein, provides physical and metabolic linkage to mitochondria*. *J Lipid Res*, 2011. **52**(12): p. 2159-2168.
57. Kien, B., et al., *Lipid droplet-mitochondria coupling via perilipin 5 augments respiratory capacity but is dispensable for FA oxidation*. *J Lipid Res*, 2022. **63**(3): p. 100172.
58. Feingold, K.R., et al., *ADRP/ADFP and Mall expression are increased in macrophages treated with TLR agonists*. *Atherosclerosis*, 2010. **209**(1): p. 81-8.

59. Huang, Y.L., et al., *Toll-like receptor agonists promote prolonged triglyceride storage in macrophages*. J Biol Chem, 2014. **289**(5): p. 3001-12.
60. Gao, J. and G. Serrero, *Adipose differentiation related protein (ADRP) expressed in transfected COS-7 cells selectively stimulates long chain fatty acid uptake*. J Biol Chem, 1999. **274**(24): p. 16825-30.
61. Shang, C., J. Qiao, and H. Guo, *The dynamic behavior of lipid droplets in the pre-metastatic niche*. Cell Death Dis, 2020. **11**(11): p. 990.
62. Marschallinger, J., et al., *Lipid-droplet-accumulating microglia represent a dysfunctional and proinflammatory state in the aging brain*. Nat Neurosci, 2020. **23**(2): p. 194-208.
63. Lalancette-Hebert, M., et al., *Lipopolysaccharide-QD micelles induce marked induction of TLR2 and lipid droplet accumulation in olfactory bulb microglia*. Mol Pharm, 2010. **7**(4): p. 1183-94.
64. Jarc, E. and T. Petan, *A twist of FATE: Lipid droplets and inflammatory lipid mediators*. Biochimie, 2020. **169**: p. 69-87.
65. Hourieux, C., et al., *The genotype 3-specific hepatitis C virus core protein residue phenylalanine 164 increases steatosis in an in vitro cellular model*. Gut, 2007. **56**(9): p. 1302-8.
66. Samsa, M.M., et al., *Dengue virus capsid protein usurps lipid droplets for viral particle formation*. PLoS Pathog, 2009. **5**(10): p. e1000632.
67. Melo, R.C., et al., *Lipid bodies in inflammatory cells: structure, function, and current imaging techniques*. J Histochem Cytochem, 2011. **59**(5): p. 540-56.
68. Bozza, P.T., K.G. Magalhaes, and P.F. Weller, *Leukocyte lipid bodies - Biogenesis and functions in inflammation*. Biochim Biophys Acta, 2009. **1791**(6): p. 540-51.
69. den Brok, M.H., et al., *Lipid Droplets as Immune Modulators in Myeloid Cells*. Trends Immunol, 2018. **39**(5): p. 380-392.
70. Libbing, C.L., et al., *Lipid Droplets: A Significant but Understudied Contributor of Host(-)Bacterial Interactions*. Cells, 2019. **8**(4).
71. Papackova, Z. and M. Cahova, *Fatty acid signaling: the new function of intracellular lipases*. Int J Mol Sci, 2015. **16**(2): p. 3831-55.
72. Zechner, R., et al., *FAT SIGNALS--lipases and lipolysis in lipid metabolism and signaling*. Cell Metab, 2012. **15**(3): p. 279-91.
73. Dichlberger, A., et al., *Adipose triglyceride lipase regulates eicosanoid production in activated human mast cells*. J Lipid Res, 2014. **55**(12): p. 2471-8.
74. Schlager, S., et al., *Adipose triglyceride lipase acts on neutrophil lipid droplets to regulate substrate availability for lipid mediator synthesis*. J Leukoc Biol, 2015. **98**(5): p. 837-50.
75. Ost, A., et al., *Attenuated mTOR signaling and enhanced autophagy in adipocytes from obese patients with type 2 diabetes*. Mol Med, 2010. **16**(7-8): p. 235-46.
76. Madrigal-Matute, J. and A.M. Cuervo, *Regulation of Liver Metabolism by Autophagy*. Gastroenterology, 2016. **150**(2): p. 328-39.
77. Moore, K.J. and I. Tabas, *Macrophages in the pathogenesis of atherosclerosis*. Cell, 2011. **145**(3): p. 341-55.
78. Goldberg, I.J., et al., *Deciphering the Role of Lipid Droplets in Cardiovascular Disease: A Report From the 2017 National Heart, Lung, and Blood Institute Workshop*. Circulation, 2018. **138**(3): p. 305-315.

79. Cole, N.B., et al., *Lipid droplet binding and oligomerization properties of the Parkinson's disease protein alpha-synuclein*. J Biol Chem, 2002. **277**(8): p. 6344-52.
80. Girard, V., et al., *Abnormal accumulation of lipid droplets in neurons induces the conversion of alpha-Synuclein to proteolytic resistant forms in a Drosophila model of Parkinson's disease*. PLoS Genet, 2021. **17**(11): p. e1009921.
81. Martinez-Vicente, M., et al., *Cargo recognition failure is responsible for inefficient autophagy in Huntington's disease*. Nat Neurosci, 2010. **13**(5): p. 567-76.
82. Voss, E.V., et al., *Characterisation of microglia during de- and remyelination: can they create a repair promoting environment?* Neurobiol Dis, 2012. **45**(1): p. 519-28.
83. Faustino, A.F., et al., *Understanding Dengue Virus Capsid Protein Interaction with Key Biological Targets*. Sci Rep, 2015. **5**: p. 10592.
84. Johnson, L.A., et al., *Apolipoprotein E4 exaggerates diabetic dyslipidemia and atherosclerosis in mice lacking the LDL receptor*. Diabetes, 2011. **60**(9): p. 2285-94.
85. Qi, G., et al., *ApoE4 Impairs Neuron-Astrocyte Coupling of Fatty Acid Metabolism*. Cell Rep, 2021. **34**(1): p. 108572.
86. Liu, L., et al., *The Glia-Neuron Lactate Shuttle and Elevated ROS Promote Lipid Synthesis in Neurons and Lipid Droplet Accumulation in Glia via APOE/D*. Cell Metab, 2017. **26**(5): p. 719-737 e6.
87. Liu, L., et al., *Glial lipid droplets and ROS induced by mitochondrial defects promote neurodegeneration*. Cell, 2015. **160**(1-2): p. 177-90.
88. Sienski, G., et al., *APOE4 disrupts intracellular lipid homeostasis in human iPSC-derived glia*. Sci Transl Med, 2021. **13**(583).
89. Machlovi, S.I., et al., *APOE4 confers transcriptomic and functional alterations to primary mouse microglia*. Neurobiol Dis, 2022. **164**: p. 105615.
90. Victor, M.B., et al., *Lipid accumulation induced by APOE4 impairs microglial surveillance of neuronal-network activity*. Cell Stem Cell, 2022. **29**(8): p. 1197-1212 e8.
91. Lin, Y.T., et al., *APOE4 Causes Widespread Molecular and Cellular Alterations Associated with Alzheimer's Disease Phenotypes in Human iPSC-Derived Brain Cell Types*. Neuron, 2018. **98**(6): p. 1141-1154 e7.
92. Gale, S.C., et al., *APOepsilon4 is associated with enhanced in vivo innate immune responses in human subjects*. J Allergy Clin Immunol, 2014. **134**(1): p. 127-34.
93. Gaudreault, N., et al., *ApoE suppresses atherosclerosis by reducing lipid accumulation in circulating monocytes and the expression of inflammatory molecules on monocytes and vascular endothelium*. Arterioscler Thromb Vasc Biol, 2012. **32**(2): p. 264-72.
94. Mighiu, P.I., B.M. Filippi, and T.K. Lam, *Linking inflammation to the brain-liver axis*. Diabetes, 2012. **61**(6): p. 1350-2.
95. Bassendine, M.F., et al., *Is Alzheimer's Disease a Liver Disease of the Brain?* J Alzheimers Dis, 2020. **75**(1): p. 1-14.
96. Husain, M.A., et al., *Investigating the plasma-liver-brain axis of omega-3 fatty acid metabolism in mouse knock-in for the human apolipoprotein E epsilon 4 allele*. J Nutr Biochem, 2022: p. 109181.

97. Mahley, R.W. and S.C. Rall, Jr., *Apolipoprotein E: far more than a lipid transport protein*. *Annu Rev Genomics Hum Genet*, 2000. **1**: p. 507-37.
98. Goldberg, I.J., *Lipoprotein lipase and lipolysis: central roles in lipoprotein metabolism and atherogenesis*. *J Lipid Res*, 1996. **37**(4): p. 693-707.
99. Trent, C.M., et al., *Lipoprotein lipase activity is required for cardiac lipid droplet production*. *J Lipid Res*, 2014. **55**(4): p. 645-58.
100. Loving, B.A., et al., *Lipoprotein Lipase Regulates Microglial Lipid Droplet Accumulation*. *Cells*, 2021. **10**(2).
101. Shimizu, K., et al., *Liver-specific overexpression of lipoprotein lipase improves glucose metabolism in high-fat diet-fed mice*. *PLoS One*, 2022. **17**(9): p. e0274297.
102. Deng, L., et al., *Macrophages take up VLDL-sized emulsion particles through caveolae-mediated endocytosis and excrete part of the internalized triglycerides as fatty acids*. *PLoS Biol*, 2022. **20**(8): p. e3001516.
103. Wu, J.W., et al., *Deficiency of liver adipose triglyceride lipase in mice causes progressive hepatic steatosis*. *Hepatology*, 2011. **54**(1): p. 122-32.
104. Ong, K.T., et al., *Adipose triglyceride lipase is a major hepatic lipase that regulates triacylglycerol turnover and fatty acid signaling and partitioning*. *Hepatology*, 2011. **53**(1): p. 116-26.
105. Singh, R., et al., *Autophagy regulates lipid metabolism*. *Nature*, 2009. **458**(7242): p. 1131-5.
106. Schott, M.B., et al., *Lipid droplet size directs lipolysis and lipophagy catabolism in hepatocytes*. *J Cell Biol*, 2019. **218**(10): p. 3320-3335.
107. Rensen, P.C. and T.J. van Berkel, *Apolipoprotein E effectively inhibits lipoprotein lipase-mediated lipolysis of chylomicron-like triglyceride-rich lipid emulsions in vitro and in vivo*. *J Biol Chem*, 1996. **271**(25): p. 14791-9.
108. Huang, Y., et al., *Overexpression of apolipoprotein E3 in transgenic rabbits causes combined hyperlipidemia by stimulating hepatic VLDL production and impairing VLDL lipolysis*. *Arterioscler Thromb Vasc Biol*, 1999. **19**(12): p. 2952-9.
109. Mensenkamp, A.R., et al., *Hepatic steatosis and very low density lipoprotein secretion: the involvement of apolipoprotein E*. *J Hepatol*, 2001. **35**(6): p. 816-22.
110. Liu, C.C., et al., *Peripheral apoE4 enhances Alzheimer's pathology and impairs cognition by compromising cerebrovascular function*. *Nat Neurosci*, 2022. **25**(8): p. 1020-1033.
111. Sullivan, P.M., et al., *Targeted replacement of the mouse apolipoprotein E gene with the common human APOE3 allele enhances diet-induced hypercholesterolemia and atherosclerosis*. *J Biol Chem*, 1997. **272**(29): p. 17972-80.
112. Plubell, D.L., et al., *Extended Multiplexing of Tandem Mass Tags (TMT) Labeling Reveals Age and High Fat Diet Specific Proteome Changes in Mouse Epididymal Adipose Tissue*. *Mol Cell Proteomics*, 2017. **16**(5): p. 873-890.
113. Johnson, E.C.B., et al., *Large-scale proteomic analysis of Alzheimer's disease brain and cerebrospinal fluid reveals early changes in energy metabolism associated with microglia and astrocyte activation*. *Nat Med*, 2020. **26**(5): p. 769-780.
114. Dai, J., et al., *Effects of APOE Genotype on Brain Proteomic Network and Cell Type Changes in Alzheimer's Disease*. *Front Mol Neurosci*, 2018. **11**: p. 454.

115. Krasemann, S., et al., *The TREM2-APOE Pathway Drives the Transcriptional Phenotype of Dysfunctional Microglia in Neurodegenerative Diseases*. *Immunity*, 2017. **47**(3): p. 566-581 e9.
116. Langfelder, P. and S. Horvath, *WGCNA: an R package for weighted correlation network analysis*. *BMC Bioinformatics*, 2008. **9**: p. 559.
117. Roberts, J.A., et al., *A brain proteomic signature of incipient Alzheimer's disease in young APOE epsilon4 carriers identifies novel drug targets*. *Sci Adv*, 2021. **7**(46): p. eabi8178.
118. Choi, M., et al., *Inhibition of STAT3 phosphorylation attenuates impairments in learning and memory in 5XFAD mice, an animal model of Alzheimer's disease*. *J Pharmacol Sci*, 2020. **143**(4): p. 290-299.
119. Millot, P., et al., *STAT3 inhibition protects against neuroinflammation and BACE1 upregulation induced by systemic inflammation*. *Immunol Lett*, 2020. **228**: p. 129-134.
120. Kim, N.Y., et al., *Sorting nexin-4 regulates beta-amyloid production by modulating beta-site-activating cleavage enzyme-1*. *Alzheimers Res Ther*, 2017. **9**(1): p. 4.
121. Krahmer, N., et al., *Phosphatidylcholine synthesis for lipid droplet expansion is mediated by localized activation of CTP:phosphocholine cytidyltransferase*. *Cell Metab*, 2011. **14**(4): p. 504-15.
122. He, Y., et al., *Lipid Droplet-Related PLIN2 in CD68(+) Tumor-Associated Macrophage of Oral Squamous Cell Carcinoma: Implications for Cancer Prognosis and Immunotherapy*. *Front Oncol*, 2022. **12**: p. 824235.
123. Sangderk Lee, N.D., Lesley Golden, Cathryn Smith, James Schwarz, Adeline Walsh, Harrison Clarke, Danielle Goulding, Elizabeth Allenger, Gabriella Morillo-Segovia, Cassi Friday, Amy Gorman, Tara Hawkinson, Steven MacLean, Holden Williams, Ramon Sun, Josh Morganti, Lance Johnson, *APOE modulates microglial immunometabolism in response to age, amyloid pathology, and inflammatory challenge*. 2022.
124. Griciuc, A. and R.E. Tanzi, *The role of innate immune genes in Alzheimer's disease*. *Curr Opin Neurol*, 2021. **34**(2): p. 228-236.
125. Podlesny-Drabiniok, A., E. Marcora, and A.M. Goate, *Microglial Phagocytosis: A Disease-Associated Process Emerging from Alzheimer's Disease Genetics*. *Trends Neurosci*, 2020. **43**(12): p. 965-979.
126. Keren-Shaul, H., et al., *A Unique Microglia Type Associated with Restricting Development of Alzheimer's Disease*. *Cell*, 2017. **169**(7): p. 1276-1290 e17.
127. Henningfield, C.M., et al., *Microglia-specific ApoE knock-out does not alter Alzheimer's disease plaque pathogenesis or gene expression*. *Glia*, 2022. **70**(2): p. 287-302.
128. Duro, M.V., B. Ebright, and H.N. Yassine, *Lipids and brain inflammation in APOE4-associated dementia*. *Curr Opin Lipidol*, 2022. **33**(1): p. 16-24.
129. Farmer, B.C., et al., *Lipid Droplets in Neurodegenerative Disorders*. *Front Neurosci*, 2020. **14**: p. 742.
130. Ioannou, M.S., et al., *Neuron-Astrocyte Metabolic Coupling Protects against Activity-Induced Fatty Acid Toxicity*. *Cell*, 2019. **177**(6): p. 1522-1535 e14.
131. Conte, M., et al., *Expression pattern of perilipins in human brain during aging and in Alzheimer's disease*. *Neuropathol Appl Neurobiol*, 2021.

132. Shi, Y., et al., *ApoE4 markedly exacerbates tau-mediated neurodegeneration in a mouse model of tauopathy*. *Nature*, 2017. **549**(7673): p. 523-527.
133. Vitek, M.P., C.M. Brown, and C.A. Colton, *APOE genotype-specific differences in the innate immune response*. *Neurobiol Aging*, 2009. **30**(9): p. 1350-60.
134. Zhu, Y., et al., *APOE genotype alters glial activation and loss of synaptic markers in mice*. *Glia*, 2012. **60**(4): p. 559-69.
135. Maezawa, I., et al., *Apolipoprotein E-specific innate immune response in astrocytes from targeted replacement mice*. *J Neuroinflammation*, 2006. **3**: p. 10.
136. Mhatre-Winters, I., et al., *Sex and APOE Genotype Alter the Basal and Induced Inflammatory States of Primary Microglia from APOE Targeted Replacement Mice*. *Int J Mol Sci*, 2022. **23**(17).
137. Farmer, B.C., et al., *APOE4 Lowers Energy Expenditure and Impairs Glucose Oxidation by Increasing Flux through Aerobic Glycolysis*. *bioRxiv*, 2020: p. 2020.10.19.345991.
138. Calsolaro, V. and P. Edison, *Neuroinflammation in Alzheimer's disease: Current evidence and future directions*. *Alzheimers Dement*, 2016. **12**(6): p. 719-32.
139. Mosher, K.I. and T. Wyss-Coray, *Microglial dysfunction in brain aging and Alzheimer's disease*. *Biochem Pharmacol*, 2014. **88**(4): p. 594-604.
140. Simpson, D.S.A. and P.L. Oliver, *ROS Generation in Microglia: Understanding Oxidative Stress and Inflammation in Neurodegenerative Disease*. *Antioxidants (Basel)*, 2020. **9**(8).
141. Yang, S., et al., *Microglia reprogram metabolic profiles for phenotype and function changes in central nervous system*. *Neurobiol Dis*, 2021. **152**: p. 105290.
142. Liu, Y., et al., *Metabolic reprogramming in macrophage responses*. *Biomark Res*, 2021. **9**(1): p. 1.
143. Manosalva, C., et al., *Role of Lactate in Inflammatory Processes: Friend or Foe*. *Front Immunol*, 2021. **12**: p. 808799.
144. Jansky, L., P. Reymanova, and J. Kopecky, *Dynamics of cytokine production in human peripheral blood mononuclear cells stimulated by LPS or infected by Borrelia*. *Physiol Res*, 2003. **52**(5): p. 593-8.
145. Asadullah, K., W. Sterry, and H.D. Volk, *Interleukin-10 therapy--review of a new approach*. *Pharmacol Rev*, 2003. **55**(2): p. 241-69.
146. Williams, H.C., et al., *APOE alters glucose flux through central carbon pathways in astrocytes*. *Neurobiol Dis*, 2020. **136**: p. 104742.
147. Phongprecha, T., et al., *Single-cell peripheral immunoprofiling of Alzheimer's and Parkinson's diseases*. *Sci Adv*, 2020. **6**(48).
148. Khor, V.K., et al., *The proteome of cholesteryl-ester-enriched versus triacylglycerol-enriched lipid droplets*. *PLoS One*, 2014. **9**(8): p. e105047.
149. Walther, T.C. and R.V. Farese, Jr., *Lipid droplets and cellular lipid metabolism*. *Annu Rev Biochem*, 2012. **81**: p. 687-714.
150. Dechandt, C.R.P., et al., *Triacsin C reduces lipid droplet formation and induces mitochondrial biogenesis in primary rat hepatocytes*. *J Bioenerg Biomembr*, 2017. **49**(5): p. 399-411.
151. Zou, J., et al., *Potent inhibitors of lipid droplet formation*, in *Probe Reports from the NIH Molecular Libraries Program*. 2010: Bethesda (MD).

152. Smith, S.J., et al., *Obesity resistance and multiple mechanisms of triglyceride synthesis in mice lacking Dgat*. Nat Genet, 2000. **25**(1): p. 87-90.
153. Stone, S.J., et al., *Lipopenia and skin barrier abnormalities in DGAT2-deficient mice*. J Biol Chem, 2004. **279**(12): p. 11767-76.
154. Zhao, G., et al., *Validation of diacyl glycerol acyltransferase I as a novel target for the treatment of obesity and dyslipidemia using a potent and selective small molecule inhibitor*. J Med Chem, 2008. **51**(3): p. 380-3.
155. McLaren, D.G., et al., *DGAT2 Inhibition Alters Aspects of Triglyceride Metabolism in Rodents but Not in Non-human Primates*. Cell Metab, 2018. **27**(6): p. 1236-1248 e6.
156. Calle, R.A., et al., *ACC inhibitor alone or co-administered with a DGAT2 inhibitor in patients with non-alcoholic fatty liver disease: two parallel, placebo-controlled, randomized phase 2a trials*. Nat Med, 2021. **27**(10): p. 1836-1848.
157. Amin, N.B., et al., *Targeting diacylglycerol acyltransferase 2 for the treatment of nonalcoholic steatohepatitis*. Sci Transl Med, 2019. **11**(520).
158. Fazio, S., D.E. Dove, and M.F. Linton, *ACAT inhibition: bad for macrophages, good for smooth muscle cells?* Arterioscler Thromb Vasc Biol, 2005. **25**(1): p. 7-9.
159. Nugent, A.A., et al., *TREM2 Regulates Microglial Cholesterol Metabolism upon Chronic Phagocytic Challenge*. Neuron, 2020. **105**(5): p. 837-854 e9.
160. Cheng, X., et al., *Targeting DGAT1 Ameliorates Glioblastoma by Increasing Fat Catabolism and Oxidative Stress*. Cell Metab, 2020. **32**(2): p. 229-242 e8.
161. Yang, C., et al., *Rewiring Neuronal Glycerolipid Metabolism Determines the Extent of Axon Regeneration*. Neuron, 2020. **105**(2): p. 276-292 e5.
162. Guo, Y., et al., *Functional genomic screen reveals genes involved in lipid-droplet formation and utilization*. Nature, 2008. **453**(7195): p. 657-61.
163. Thiam, A.R., R.V. Farese, Jr., and T.C. Walther, *The biophysics and cell biology of lipid droplets*. Nat Rev Mol Cell Biol, 2013. **14**(12): p. 775-86.
164. Gallardo-Montejano, V.I., et al., *Perilipin 5 links mitochondrial uncoupled respiration in brown fat to healthy white fat remodeling and systemic glucose tolerance*. Nat Commun, 2021. **12**(1): p. 3320.
165. Viola, A., et al., *The Metabolic Signature of Macrophage Responses*. Front Immunol, 2019. **10**: p. 1462.
166. Russell, D.G., L. Huang, and B.C. VanderVen, *Immunometabolism at the interface between macrophages and pathogens*. Nat Rev Immunol, 2019. **19**(5): p. 291-304.
167. Batista-Gonzalez, A., et al., *New Insights on the Role of Lipid Metabolism in the Metabolic Reprogramming of Macrophages*. Front Immunol, 2019. **10**: p. 2993.
168. Hazen, S.L., *Oxidized phospholipids as endogenous pattern recognition ligands in innate immunity*. J Biol Chem, 2008. **283**(23): p. 15527-31.
169. Chen, R., A.E. Feldstein, and T.M. McIntyre, *Suppression of mitochondrial function by oxidatively truncated phospholipids is reversible, aided by bid, and suppressed by Bcl-XL*. J Biol Chem, 2009. **284**(39): p. 26297-308.
170. Ebright, B., et al., *Eicosanoid lipidome activation in post-mortem brain tissues of individuals with APOE4 and Alzheimer's dementia*. Alzheimers Res Ther, 2022. **14**(1): p. 152.

171. Van Valkenburgh, J., et al., *Radiosynthesis of 20-[(18)F]fluoroarachidonic acid for PET-MR imaging: Biological evaluation in ApoE4-TR mice*. Prostaglandins Leukot Essent Fatty Acids, 2022. **186**: p. 102510.
172. Freeman, L.C. and J.P. Ting, *The pathogenic role of the inflammasome in neurodegenerative diseases*. J Neurochem, 2016. **136 Suppl 1**: p. 29-38.
173. Ismaeel, S. and A. Qadri, *ATP Release Drives Inflammation with Lysophosphatidylcholine*. Immunohorizons, 2021. **5**(4): p. 219-233.
174. Moessinger, C., et al., *Human lysophosphatidylcholine acyltransferases 1 and 2 are located in lipid droplets where they catalyze the formation of phosphatidylcholine*. J Biol Chem, 2011. **286**(24): p. 21330-9.
175. Moessinger, C., et al., *Two different pathways of phosphatidylcholine synthesis, the Kennedy Pathway and the Lands Cycle, differentially regulate cellular triacylglycerol storage*. BMC Cell Biol, 2014. **15**: p. 43.
176. Wang, S., et al., *Calcium-dependent cytosolic phospholipase A2 activation is implicated in neuroinflammation and oxidative stress associated with ApoE4*. Mol Neurodegener, 2021. **16**(1): p. 26.

VITA

Cassi M (Binkley) Friday

Education

- 2020- PhD Physiology, University of Kentucky College of Medicine, Lexington, KY
- 2012-2015 PhD Physiology, University of Kentucky College of Medicine, Lexington, KY
- 2011-2012 M.S. Medical Science, University of Kentucky College of Medicine, Lexington, KY
- 2007-2011 B.A. Biology, Hanover College, Hanover, IN
- 2004-2007 Academic Honors Diploma, Crawford County Jr/Sr High School, Marengo, IN

Employment

- 09/2020- Graduate Research Assistant, University of Kentucky Department of Physiology
- 05/2013-07/2015 Research Assistant, Cardiac Imaging Research Lab, Geisinger Medical Center, Danville, PA and Kentucky Children's Hospital, Lexington, KyY

Awards and Honors

- 2022 Brian Hardin Award, Department of Physiology
- 2022 **Best poster award**, Department of Physiology Research Retreat
- 2021 American Physiological Society **Early Career Advocacy Fellow**
- One of 3 graduate and early career professors awarded 2-yr fellowship
- 2021 **McCullers Scholar 2021**, Sanders-Brown Center on Aging
- 2021 **Honorable Mention Poster Award**, Physiology Department
- 2014 3rd Place Poster Award, Gill Heart Cardiovascular Research Day
- 2014 **Best poster award**, Department of Physiology Research Retreat

Manuscripts

- 2017 Jing L, Nevius CD, **Friday CM**, Suever JD, Pulenthiran A, Mejia-Spiegeler A, Kirchner HL, Cochran WJ, Wehner GJ, Chishti AS, Haggerty CM, Fornwalt BK. Ambulatory systolic blood pressure and obesity are independently associated with left ventricular hypertrophic remodeling in children. *J. Cardiovascular Magnetic Resonance*. 2017.

- 2016 *Jing L, ***Binkley CM**, Suever, JD, Umasankar N, Haggerty CM, Rich J, Wehner GJ, Hamlet SM, Powell DK, Radulescu A, Kirchner HL, Epstein FH, Fornwalt BK. Cardiac remodeling and dysfunction in childhood obesity: a cardiovascular magnetic resonance study. *J Cardiovascular Magnetic Resonance*. 2016.
- 2015 Haggerty CM, Mattingly AC, Kramer SP, **Binkley CM**, Jing L, Suever JD, Powell DK, Charnigo RJ, Epstein FH, Fornwalt BK. Left ventricular mechanical dysfunction in diet-induced obese mice is exacerbated during inotropic stress: a cine DENSE cardiovascular magnetic resonance study. *J Cardiovascular Magnetic Resonance*. 2015.
- 2014 Suever JD, Wehner GJ, Haggerty CM, Jing L, Hamlet SM, **Binkley CM**, Kramer SP, Mattingly AC, Powell DK, Bilchick KC, Epstein FH, Fornwalt BK. Simplified post processing of cine DENSE cardiovascular magnetic resonance for quantification of cardiac mechanics. *J Cardiovascular Magnetic Resonance*. 2014
- 2014 Haggerty CM, Kramer SP, Skrinjar O, **Binkley CM**, Powell DK, Mattingly AC, Epstein FH, Fornwalt BK. Quantification of left ventricular volumes, mass, and ejection fraction using cine displacement encoding with stimulated echoes (DENSE) MRI. *J Cardiovascular Magnetic Resonance*. 2014.
- 2014 Qing H, Liu Y, Zhao Y, Aono J, Jones KL, Heywood EB, Howatt D, **Binkley CM**, Daugherty A, Liang Y, Bruemmer D. Deficiency of the NR4A orphan nuclear receptor NOR1 in hematopoietic stem cells accelerates atherosclerosis. *Stem Cells*. 2014.
- 2013 Kramer SP, Powell DK, Haggerty CM, **Binkley CM**, Mattingly AC, Cassis LA, Epstein FH, Fornwalt BK. Obesity reduces left ventricular strains, torsion, and synchrony in mouse models: a cine displacement encoding with stimulated echoes (DENSE) cardiovascular magnetic resonance study. *J Cardiovascular Magnetic Resonance*. 2013.
- 2013 Haggerty CM, Kramer SP, **Binkley CM**, Powell DK, Mattingly AC, Charnigo R, Epstein FH, Fornwalt BK. Reproducibility of cine displacement encoding with stimulated echoes (DENSE) cardiovascular magnetic resonance for measuring left ventricular strains, torsion, and synchrony in mice. *J Cardiovascular Magnetic Resonance*. 2013

* co-first author

Published Abstracts

- 2022 **Cassi Friday**, Cathryn Smith, Sangderk Lee, Gaby Morillo-Segovia, Diksha Satish, Nick A. Devanney, Josh Morganti, Scott Gordon, and Lance A. Johnson. *APOE4* alters the lipid droplet proteome and modulates droplet dynamics. Frederickson Lipid Research Conference, Durham, North Carolina
- 2022 **Cassi Friday**, Nicholas Devanney, Katy Smith, Elizabeth Allenger, Ana Maria Cornea, Scott Gordon, Lance Johnson. The Effect of *APOE* on Lipid Droplet Dynamics in Microglia. AAIC. San Diego, California
- 2022 **Cassi Friday**, Nicholas Devanney, Katy Smith, Elizabeth Allenger, Ana Maria Cornea, Scott Gordon, Lance Johnson. The Effect of *APOE* on Lipid Droplet Dynamics in Microglia. American Society for Neurochemistry 2022
- 2022 Devanney N, Lee S, Williams H, Allenger E, Smith C, Schwartz J, Goulding D, Gorman A, **Friday C**, Morganti J, and Johnson L. *Apolipoprotein E modulates microglial immunometabolism*. Poster presented at: Department of Physiology Research Retreat. 2022 May 20. Lexington, KY.
- 2021 **Cassi Friday**, Nicholas Devanney, Katy Smith, Elizabeth Allenger, Ana Maria Cornea, Scott Gordon, Lance Johnson. The Effect of *APOE* on Lipid Droplet Dynamics in Microglia. University of Kentucky Physiology Department Research Retreat. **Honorable Mention Poster Award**
- 2021 **Cassi Friday**, Nicholas Devanney, Katy Smith, Elizabeth Allenger, Ana Maria Cornea, Scott Gordon, Lance Johnson. The Effect of *APOE* on Lipid Droplet Dynamics in Microglia. Markesbery Symposium, Lexington, KY. **Invited Talk**
- 2017 **Cassi M. Friday**, Sarah L. Stuebing, Jennifer R. Peterson, Brynn Critcher, Ian R. Davis, Pallie Koehn, and Kimberly Kirkpatrick. Fading in and out of time: Interventions to promote self-control: *Society for the Quantitative Analyses of Behavior* 2017
- 2015 **Cassi M Friday**, Linyuan Jing, Jonathan D Suever, Nivedita Umasankar, Gregory J Wehner, Sean M Hamlet, David K Powell, Aurelia Radulescu, Frederick H Epstein, Brandon K Fornwalt. Children with obesity have cardiac remodeling and dysfunction: a magnetic resonance imaging study. Society for Cardiovascular Magnetic Resonance, Nice, France. February 2015.

- 2014 **Cassi M Binkley**, Linyuan Jing, Jonathan D Suever, Nivedita Umasankar, Sean M Hamlet, Gregory J Wehner, David K Powell, Aurelia Radulescu, Frederick H Epstein, Brandon K Fornwalt. Children with obesity have cardiac remodeling and dysfunction: a cine DENSE magnetic resonance imaging study. University of Kentucky Physiology Department Research Retreat 2014 **Best Overall Poster Prize**
- 2014 **Cassi M Binkley**, Linyuan Jing, Jonathan D Suever, Nivedita Umasankar, Sean M Hamlet, Gregory J Wehner, David K Powell, Aurelia Radulescu, Frederick H Epstein, Brandon K Fornwalt. Children with obesity have cardiac remodeling and dysfunction: a cine DENSE magnetic resonance imaging study. Gill Heart Cardiovascular Research Day, Lexington, Kentucky, October 2014 **Invited Talk, Third Place Poster Prize**
- 2014 **Cassi M Binkley**, Christopher M. Haggerty, PhD, Jonathan D. Suever, Phd, Linyuan Jing, PhD, Sean Hamlet, MS, Greg Wehner, BS, Sage P. Kramer, BS, David Powell, PhD, Aurelia Radulescu, MD, Frederick H. Epstein, PhD, Brandon K. Fornwalt, MD, PhD, “Children with Obesity have cardiac remodeling and dysfunction: a magnetic resonance imaging study”, Barnstable Brown Diabetes and Obesity Research Day, Lexington, KY, May 2014.
- 2014 **Cassi M Binkley**, Christopher M Haggerty, Jonathan D Suever, Gregory J Wehner, Sage P Kramer, David K Powell, Frederick H Epstein, Brandon K Fornwalt. Quantifying the Effects of Pediatric Obesity on Cardiovascular Function Using Magnetic Resonance Imaging. Center for Clinical and Translational Science Symposium, Lexington, Kentucky, March 2014. **Invited Talk**
- 2013 **Cassi M Binkley**, Christopher M. Haggerty, PhD, Jonathan D. Suever, PhD, Greg Wehner, BS, Sage P. Kramer, BS, David K. Powell, PhD, Frederick H. Epstein, PhD, Brandon K. Fornwalt, MD, PhD. Quantifying the Effects of Pediatric Obesity on Cardiovascular Function Using Magnetic Resonance Imaging. Center for Muscle Biology Retreat, Lexington, Kentucky November 2013
- 2011 **Cassi M Binkley**. A Limnological Study and Bioassessment of Fish Populations on the Ohio River near Zimmer Power Plant, Moscow Ohio. Butler Undergraduate Research Conference, Indianapolis, Indiana, 2011 **Invited Talk**

Invited Talks

- 2022 Cure HHT International Scientific Conference, Cure HHT Research Network: Building the Roadmap to Cure HHT; Lisbon, Portugal
- 2021 Markesbery Symposium on Aging and Dementia; The Effect of *APOE* on Lipid Droplet Dynamics in Microglia; Lexington, Kentucky

- 2014 Gill Heart Cardiovascular Research Day; The Effect of Pediatric Obesity on Cardiovascular Disease: An MRI Study; Lexington, Kentucky
- 2013 Center for Clinical and Translational Sciences Symposium, The Effect of Pediatric Obesity on Cardiovascular Disease: An MRI Study; Lexington, Kentucky
- 2007 Butler Undergraduate Research Conference; A Limnological Study and Bioassessment of Fish Populations on the Ohio River Near Zimmer Power Plan, Moscow, OH; Butler University

Extracurricular Activities and Memberships

- 2021- American Physiological Society; Science Policy Committee; Early-Career Advocacy Fellowship
- 2021- Kentucky Academy of Science
- 2021- American Society of Neurochemistry
- 2021- Military Spouses in STEM
- 2021- Trainees in Research Advisory Committee, University of Kentucky College of Medicine
- 2021- Women in Medicine and Science, University of Kentucky College of Medicine

Certificates

- 2022 Kentucky Science Advocate, Kentucky Academy of Science
- 2022 Project Management Professional, Project Management Institute
- 2015 Certificate in Teaching Physiology, University of Kentucky
- 2014 Clinical Research Coordinating 101, University of Kentucky
- 2014 Phlebotomy 101, University of Kentucky

Reviewed Manuscripts

- 2020 Aging Cell
- 2020 Frontiers

Mentored Students

- 2014 Nivedita Umasankar – Rotating Medical Student; 6 months
- 2015 Chris Nieves – Geisinger Medical Center; 6 months
- 2017 Pallie Swartz – Kansas State University; 1 year
- 2020 Ana Maria Cornea – High School Research Program Participant; 1.5 years
- 2021 Diksha Satish – Undergraduate Student and USTiCR fellow; 1 year